USGS-OFR-84-792

UNITED STATES
DEPARTMENT OF THE INTERIOR
GEOLOGICAL SURVEY

A SUMMARY OF GEOLOGIC STUDIES THROUGH JANUARY 1, 1983, OF A POTENTIAL HIGH-LEVEL RADIOACTIVE WASTE REPOSITORY SITE AT YUCCA MOUNTAIN, SOUTHERN NYE COUNTY, NEVADA

compiled by the
U.S. Geological Survey

Open-File Report 84-792

Prepared in cooperation with the
Nevada Operations Office
U.S. Department of Energy
(Interagency Agreement DE-AI08-78ET44802)

Menlo Park, California

1984

PREFACE

Yucca Mountain in southern Nye County, Nevada has been under investigation since late 1977 to determine its suitability as the site for an underground repository for the permanent isolation of high-level radioactive waste. It has been the principle responsibility of the U.S. Geological Survey, under agreement with the U.S. Department of Energy, to characterize the geology and hydrology of the potential site and the surrounding region.

The present report covers the geologic factors of concern in evaluating the potential repository site. It is preliminary because most of the investigations are still in progress. The discussion generally includes data acquired before January 1, 1983. As investigations are concluded, additional reports will complete the description of specific aspects of the geology of Yucca Mountain.

The technical data discussed in this report largely result from investigations by members of the U.S. Geological Survey, with a contribution by Los Alamos National Laboratory to the discussion of volcanism and volcanic hazards. The principal contributers of technical drafts for this report include Michael D. Carr, Wilfred J. Carr, David L. Hoover, Howard W. Oliver, Albert M. Rogers, Robert B. Scott, Richard W. Spengler, Joann M. Stock, W C Swadley, all of the Geological Survey, and Bruce M. Crowe of Los Alamos National Laboratory. Gary L. Dixon, Edward J. Helley, Gershon D. Robinson, John W. Whitney, and James C. Yount, all of the U. S. Geological Survey contributed to editing of the report. The manuscript benifited from technical reviews by Warren B. Hamilton, George E. Ulrich, Carl M. Wentworth, and Robert L. Wesson.

CONTENTS

LIST OF FIGURES

LIST OF TABLES

ABSTRACT

Yucca Mountain, located at the southwest corner of the Nevada Test Site in southern Nevada, is being investigated as a potential site for the storage of high-level radioactive waste. Sequences of ash-flow tuff like those at Yucca Mountain potentially could provide multiple geologic barriers against the release of nuclear waste, assuming that the geologic and hydrogeologic setting of the site are favorable. This report describes the geology of the Yucca Mountain site and presents preliminary conclusions on the basis of work in progress.

Yucca Mountain occupies roughly 54 km^2 within the southern part of the Great Basin subprovince of the Basin and Range, an arid region of generally linear mountain ranges and topographically and hydrologically closed basins. The mountain consists of several north-trending linear ridges, which are underlain by blocks of resistant bedrock tilted eastward along steeply dipping normal faults. These faults commonly are concealed in the narrow valleys that separate the ridges. Yucca Mountain is flanked on the east and west by broad alluvial basins.

Erosion has been slow in modifying the morphology of Yucca Mountain due mainly to the arid climate and the relatively high erosional resistance of the welded tuffs that make up the mountain. Considering past erosion rates, it is likely that even under wetter climatic conditions erosion at Yucca Mountain will continue to be relatively slow. Maximum stream incision rates of less than 10 cm per 1,000 years for the past 300,000 years have been estimated for Forty Mile Wash, the principal drainage along the east side of Yucca Mountain.

Rocks in the Yucca Mountain region range in age from Proterozoic to Quaternary. The older rocks are largely marine, deposited without significant interruption during late Proterozoic and Paleozoic time on the western continental shelf of ancient North America. These rocks comprise the major hydrogeologic units of the deep groundwater system. Mesozoic plutonic rocks crop out in the region west of Yucca Mountain, and to a lesser extent to the northeast. No pre-Cenozoic rocks crop out at Yucca Mountain. The Cenozoic rocks of the region mainly consist of nonmarine volcanic and sedimentary rocks, predominantly ash-flow tuffs of Miocene age. Tertiary plutonic rocks occur in the Death Valley area southwest of Yucca Mountain. Extensive and commonly thick Pliocene and Quaternary alluvial, eolian, and lacustrine sediments fill

the valleys. Pliocene and Quaternary basaltic rocks crop out in a weakly defined belt of volcanic centers passing west of Yucca Mountain. The nearest basaltic volcanoes are in Crater Flat approximately 7 km from Yucca Mountain.

The documented geologic history of the Yucca Mountain region extends back nearly 2 b.y. to the formation of the gneissic crystalline rocks that are the stratigraphic basement for the Upper Proterozoic and Paleozoic sedimentary rocks in the region. Mississippian rocks in much of the region are flysch deposited in response to compressive tectonism during the Late Devonian and Early Mississippian, but no faults or folds clearly related to this orogeny are recognized in the vicinity of Yucca Mountain.

During Mesozoic time, a series of major mountain building events affected the entire western margin of ancient North America. In the vicinity of Yucca Mountain, this orogeny resulted in major thrust faults and folds. The Mesozoic tectonism was important in establishing the distribution of the rocks that control the present flow patterns of deep groundwater.

Silicic volcanism accompanied by extensional tectonism began in the region north of Yucca Mountain about 40 m.y. ago and was widespread in the southern Great Basin throughout Miocene time (24 to 5 m.y. ago.) The silicic tuffs and minor lava flows that make up Yucca Mountain were erupted between about 14 and 11 m.y. ago. Volcanism has diminished during the past 8 m.y., and only limited basaltic volcanism has occurred in the region since about 5 m.y. ago. Several small basaltic centers were active during the Quaternary.

The stratigraphy and structure of Yucca Mountain have been explored in three dimensions from geologic mapping and drilling. The mountain is underlain by a thick sequence of ash-flow and ash-fall tuff, lava, and volcanic breccia that range in composition from rhyolite to dacite. Most of the subsurface volcanic units are continuous under Yucca Mountain. Major ash-flow units, ranging from approximately 70 to 370 m thick, generally are separated by reworked tuff or bedded-tuff units as much as several tens of meters thick. Ash-flow units vary laterally and vertically in thickness, welding characteristics, mineral composition, content of incorporated rock fragments, and in degree and products of secondary alteration.

Paleozoic stratified rocks underlie the volcanic sequence at Yucca Mountain, but granitic intrusive rocks also could occur locally. Estimates of the depth to the subvolcanic basement surface on the basis of geophysical data range from less than 1 km beneath the southeast part of the Site to more than 3.5 km beneath the northwest part.

Yucca Mountain is in a region of complex Cenozoic structures characterized by normal faults, volcano-tectonic features, and major zones of strike-slip faulting. The normal faults occur on many scales; a few range-bounding faults have dip slip on the order of thousands of meters. In some areas, normal faulting could have begun before volcanism, but much of the faulting occurred at the same time as silicic volcanism. Faulting continued during the Pliocene and Quaternary after silicic volcanism ceased.

A broad northwest-striking zone of right-lateral strike-slip faulting called the Walker Lane occurs in the southwest part of the Basin and Range province. The inception of faulting in this belt is not well dated, but some faults were active from approximately 17 to 11 m.y. ago. Faults in the vicinity of Yucca Mountain that could be related to the Walker Lane include northwest-striking, right-lateral faults that parallel the Walker Lane trend and complementary northeast-striking, left-lateral faults.

Tectonism and volcanism in the Great Basin continued during Pliocene and Quaternary time. This activity is expressed by both normal and strike-slip extensional faults and by localized basaltic volcanoes. The basalts are of two types: (1) older basalt spatially related to waning silicic volcanic centers, and (2) younger basalts that postdate silicic volcanism and occur along a belt between Death Valley and the Pancake Range in central Nevada. The younger basalts are the only type present near Yucca Mountain. The last volcanic eruptions in the vicinity of Yucca Mountain were 200,000 to 300,000 years ago.

Quaternary faults occur in the vicinity of Yucca Mountain, but dating of their youngest movements is difficult. No unequivocal Holocene faulting has been recognized at the Yucca Mountain site. Two areas having unequivical Holocene faults, Death Valley and Yucca Flat, are recognized in the region. Faults with possible early Holocene displacement occur both west and east of Yucca Mountain.

Yucca Mountain itself consists of gently eastward-tilted fault blocks of volcanic rocks. The potential site is in the largest of these blocks. Three sets of steeply dipping Cenozoic faults and fractures cut Yucca Mountain. Most of the displacement on the principal set of block-bounding faults occurred between 12.5 and 11.3 m.y. ago.

The subsurface structure above about 1 km depth at Yucca Mountain is similiar in style and complexity to surface structure. Subsurface data indi-

cates that fracturing, which is of fundamental concern in understanding hydrology and evaluating mining conditions at the site, is most extensive in brittle rock types such as densely welded tuff.

Stress measurements and modeling indicate a stress field with minimum principal stress in a northwest direction in the vicinity of Yucca Mountain. Hydrofracture experiments in one drill hole at Yucca Mountain show that the magnitude of the least principal stress is only one third of the effective confining pressure and effective vertical load. The state of stress warrants careful evaluation with respect to the possibility of future normal faulting at Yucca Mountain.

Much of the current seismicity in the southern Great Basin is associated with north- to northeast-trending faults. Although Yucca Mountain appears to lie within a zone of relative seismic quiescence, two small earthquakes have been located several kilometers below the Site. Examination of the most likely magnitudes on active faults in the Yucca Mountain region indicates that the largest magnitude is M 7 to 8. The largest value of the most probable peak accelerations at the Site, due to occurrence of these potential earthquakes, is 0.4 g and is produced by a M 6.8 earthquake on a nearby fault. This result assumes that faults at Yucca Mountain are inactive. A probability of less than four percent was calculated that a peak acceleration of 0.4 g would be exceeded in a 30-year period at any given location in the region.

Rates of basaltic volcanism during the past 8 m.y. have been uniformly low in the region. Basaltic eruptions were of small volume and short duration, resulting in monogenetic scoria cones or clusters of scoria cones. Erupted magmas have been predominantly of hawaiite compositions. These magmas were formed repeatedly throughout the region for the last 6 to 8 m.y., with no recognizable changes or trends in composition or volumes through time. The calculated values for the probability of disruption of a repository site at Yucca Mountain by basaltic volcanism for a one year period range from 10^{-8} to 10^{-10}. The likelihood of renewed silicic volcanism is considered very low.

The radiological consequences of repository disruption are interpreted to be limited, based on calculated release values. The consequences reflect the small subsurface area of basalt disruption zones and the limited dispersal of eruptive material by the predominant eruptive mechanisms. The combination of volcanic hazard studies and risk assessment consistantly suggest a low hazard of future volcanism at Yucca Mountain.

INTRODUCTION

Geologic studies in the area of the Nevada Test Site, mostly by the U.S. Geological Survey, date back to 1907. Concentrated research in the area began in the late 1950's in connection with underground testing of nuclear weapons (see Eckel, 1968, for a summary of earlier work). Geologic mapping of the Nevada Test Site at 1:24,000 scale was largely completed during the 1960's. Numerous geologic, geophysical, and hydrologic investigations at and near the Test Site have provided the data necessary to construct the general geologic framework and history of the area, and many detailed studies concerned with nuclear testing have also been completed. However, efforts directed specifically toward locating a nuclear waste repository at the Nevada Test Site are relatively recent. Most of the specialized geologic investigations related to waste disposal are still in progress and data are incomplete. Much of the information already collected has yet to be completely analyzed, and much work remains to be done, especially with regard to site-specific exploration, tectonic framework, seismicity, and Quaternary history. Consequently, it is not possible at this stage to provide a complete evaluation of many of the geologic characteristics of the proposed site as related to waste storage. Studies in progress will be presented in future publications.

The Nevada Test Site began to attract interest as a possible nuclear waste storage site in the late 1970's. Initially, attention was focused on low-permeability shale and granitic plutons. General studies were made of areas underlain by shale and granitic rocks in southern Nevada (Simpson and others, 1979; Spengler and others, 1979a), and detailed studies were made of the argillite-rich Eleana Formation (Hoover and Morrison, 1980) and of known or suspected plutons (Maldonado, 1977a, 1981; Maldonado and others, 1979; Ponce, 1981) within the Nevada Test Site. More recently, emphasis has shifted to consideration of ash-flow tuff as a host rock.

Subsurface exploration at Yucca Mountain began in late 1978 (Spengler and others, 1979b) and has demonstrated the presence of a thick sequence of ash-flow tuff units having reasonable lateral continuity. Important problems are still posed, however, by the complex tectonic setting, variation in the physical characteristics of the tuff units, fracturing, and complex hydrologic conditions.

The geologic setting of the Yucca Mountain site is discussed herein at three scales as outlined in Figure 1. These are referred to as the Candidate Area, Site Vicinity, and Site.

The Candidate Area, which provides a frame of reference for discussing the regional setting of Yucca Mountain, includes the area within a 100-km radius of the proposed site as specified in Nuclear Regulatory Commission guidelines (10CFR60). It contains the surface and subsurface hydrologic systems that include Yucca Mountain, except for a small part of the surface drainage along the Amargosa River in the southern parts of the Amargosa Desert and Death Valley. The limits of the surface hydrologic flow system are the principal technical base for definition of a Candidate Area. Although the Candidate Area provides a useful base for discussion of the regional geologic framework, it does not strictly conform to the limits of the area that might be directly affected by waste storage at Yucca Mountain.

The geology of the Candidate Area is shown on the 1:500,000-scale geologic map of Nevada (Stewart and Carlson, 1978) and the 1:750,000-scale geologic map of California (Jennings, 1977). An index to larger scale geologic mapping in the Candidate Area was compiled by Fouty (1984). Regional isostatic residual gravity data for the Candidate Area are shown at 1:500,000-scale on figure 2 (in pocket). Aeromagnetic data are not available for the entire Candidate Area, however a 1:1,000,000 scale aeromagnetic map of Nevada has been compiled by Zietz and others (1978).

The Site Vicinity, depicted at a scale of 1:48,000 on figures 3 and 4 (in pocket), was arbitrarily defined to include features thought to be of greatest significance in evaluating the local geologic setting of Yucca Mountain. A 1:48,000 scale aeromagnetic map is available for the Site Vicinity (Kane and Bracken, 1983).

The Site, which is the specific area under consideration as a potential nuclear waste repository, is in the central part of Yucca Mountain. The geology of the Site is generalized on figures 5 and 6 from 1:12,000 scale mapping by Scott and Bonk (1984). Geologic mapping is currently being supplemented by analysis of remote sensing imagery, electrical resistivity studies, low-altitude aeromagnetic studies and seismic refraction and reflection studies. These studies are aiding in the location of concealed faults, the assessment of fault and fracture patterns, and the mapping and interpretation of pre-Cenozoic rocks.

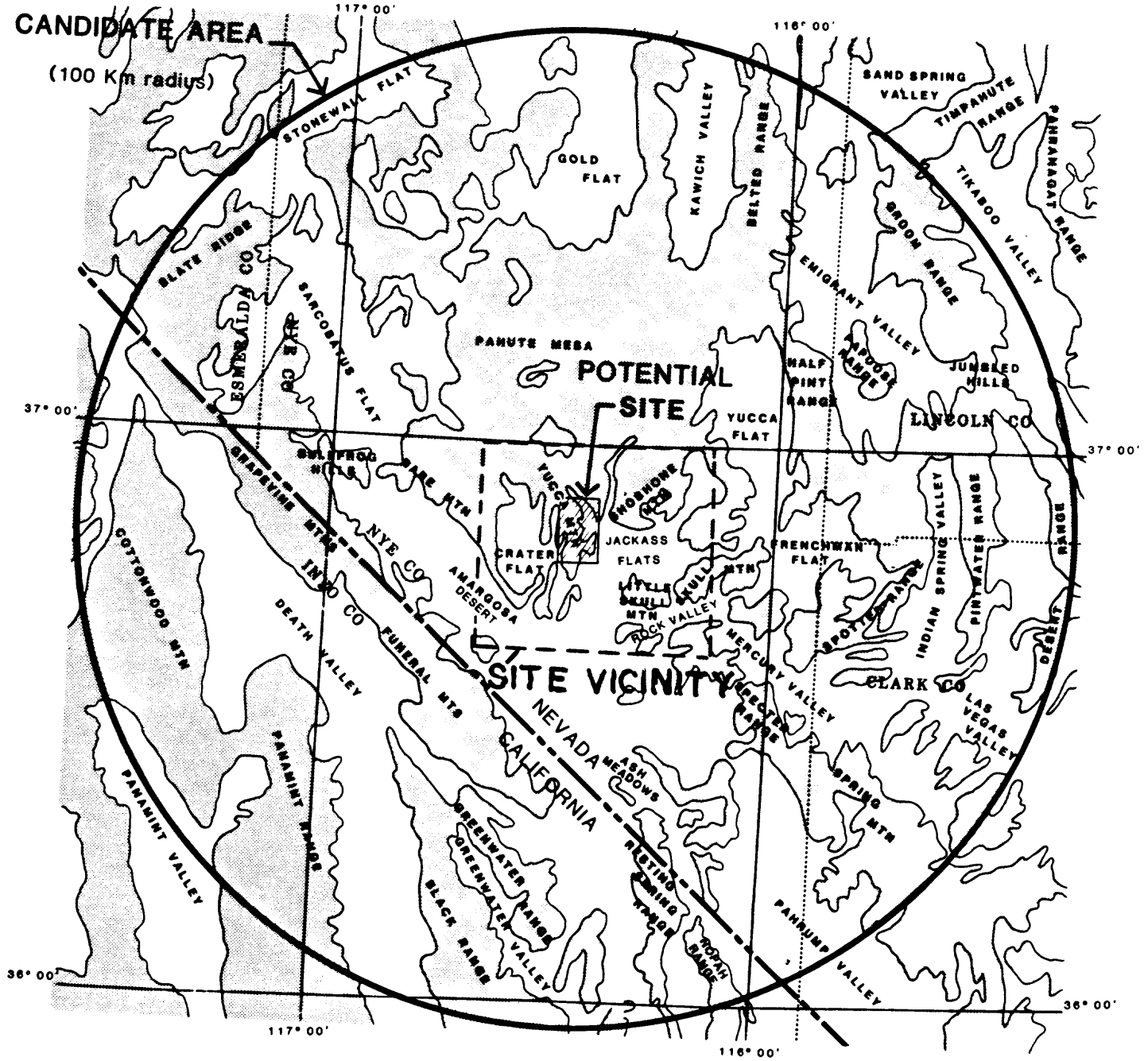

FIGURE -1 LOCATION OF CANDIDATE AREA AND POTENTIAL SITE

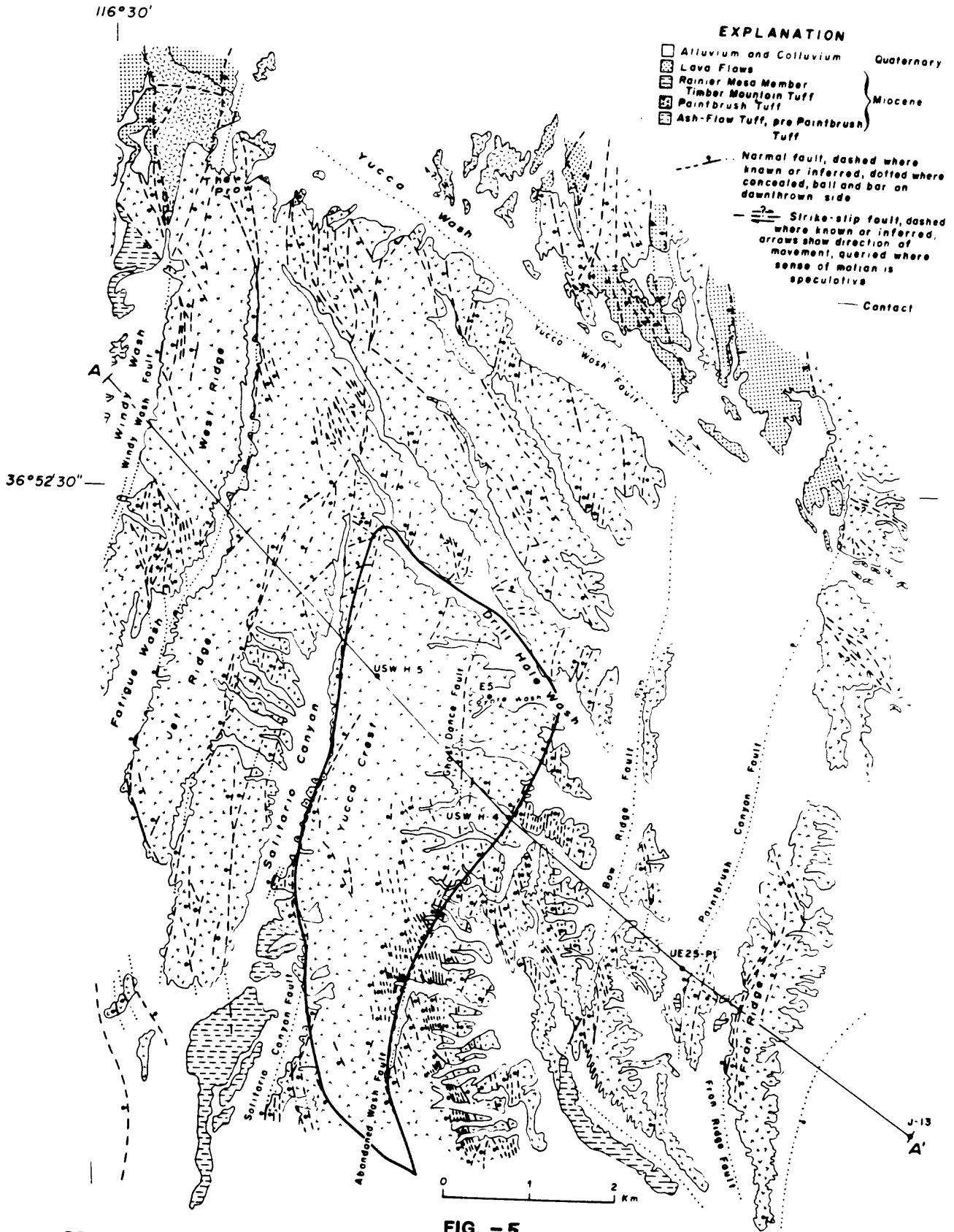

FIG. – 5
GEOLOGIC MAP OF YUCCA MOUNTAIN (generalized from Scott and Bonk, 1984). Heavy line encloses the potential repository.

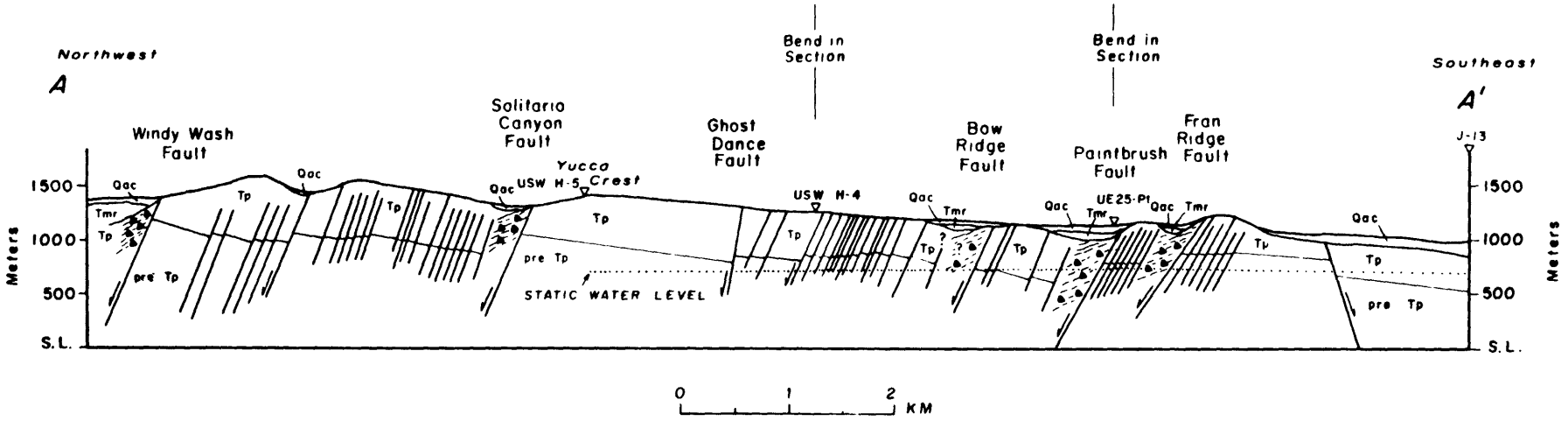

FIG. 6

GEOLOGIC CROSS SECTION A-A' (generalized from Scott and Bonk, 1984).

Qac=Quaternary alluvium and colluvium; Tm=Ranier Mesa Member; Tp=Paintbrush Tuff; pre-Tp=pre-Paintbrush Tuff; ∴ =abundant breccia, SL=sea level; ▨ =west-dipping strata; arrows on faults indicate relative motion.

GEOMORPHOLOGY

Geomorphic processes acting in conjunction with tectonism are responsible for the present topography of the Site. These processes continue to affect the landscape, and future tectonism and (or) changes in climate could alter present patterns and rates of erosion and deposition. Changes in erosion and deposition could in turn affect topography, drainage patterns, and groundwater recharge and flow patterns. To estimate the nature and magnitude of future surficial changes and to appraise their effect on waste isolation at the Site, it is necessary to characterize the landforms in the Candidate Area and to understand the processes that have shaped them.

Physiography and Topography

The Candidate Area lies within the southern Great Basin, the northern subprovince of the Basin and Range physiographic province (Figure 7). The Basin and Range physiographic province in the western United States corresponds to a region of Cenozoic extensional tectonism, which includes the Mojave and Sonoran Deserts in addition to the Great Basin. The Great Basin is generally characterized by linear, fault-bounded ranges separated by alluviated basins filled with sediment eroded from adjacent ranges. Throughgoing streams rarely connect adjacent basins. Most drainages are internal within individual basins. The topography of the region is closely related to late Cenozoic tectonism. Range fronts typically are steep and Quaternary basin-fill deposits that border the ranges are broken by fault scarps in many areas (Slemmons, 1967).

The Great Basin is bordered on the south by the Mojave Desert and the northwesternmost part of the Sonoran Desert. This physiographic boundary coincides with a major structural boundary, the Garlock Fault, and with a zone of abrupt transition in seismicity and principal geophysical characteristics (Eaton and others, 1978). The Mojave and Sonoran Deserts are typically lower in topographic relief than the Great Basin, mountain fronts are less well defined than in the Great Basin, and highlands are surrounded by wide complexes of pediments and alluvial fans. Christiansen and McKee (1978) suggest that the higher average elevation and greater topographic relief of the Great Basin reflect active extensional tectonism, in contrast to the

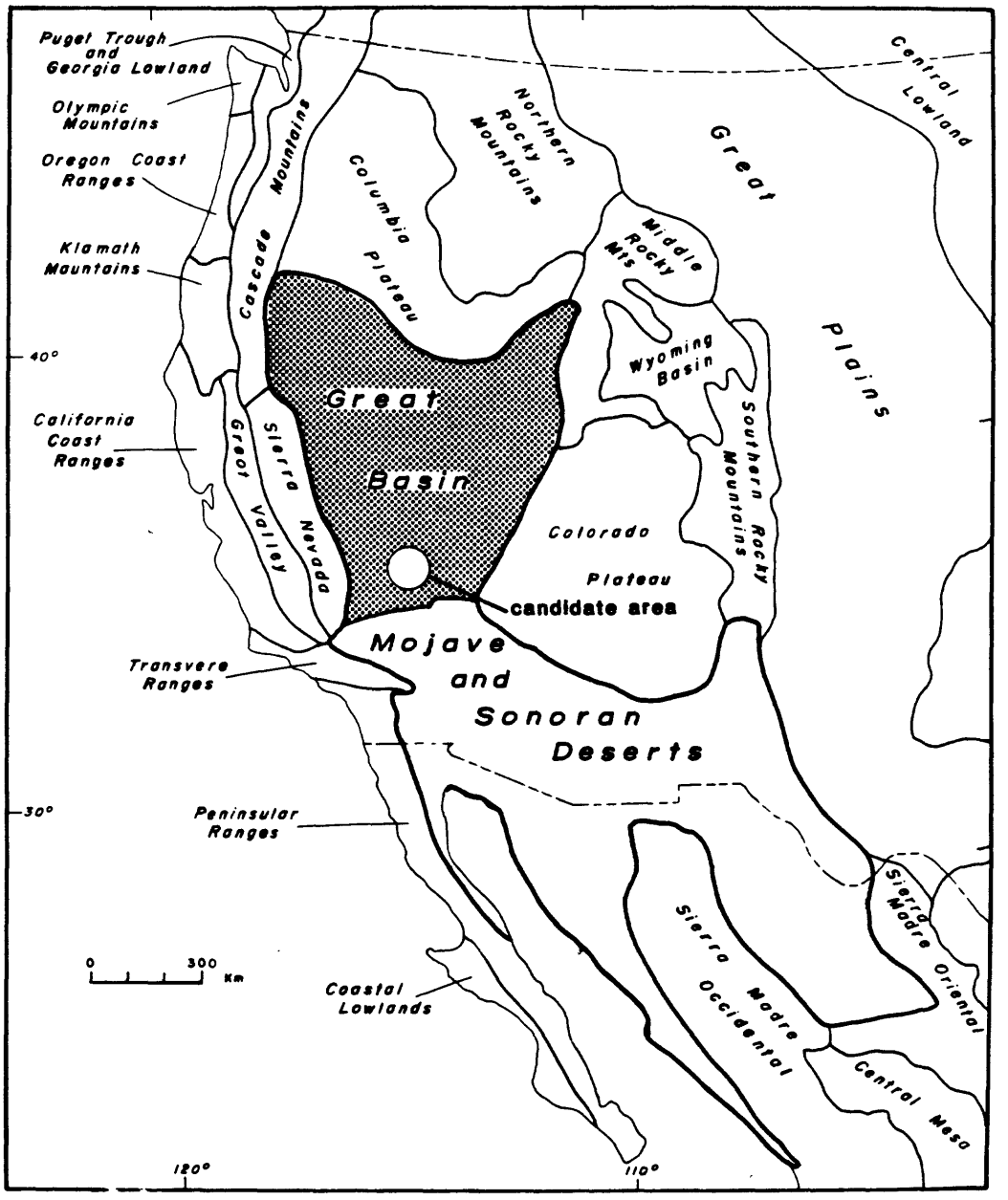

FIG. 7 MAP OF THE BASIN AND RANGE PROVINCE (outlined by heavy line) AND SURROUNDING PHYSIOGRAPHIC PROVINCES IN WESTERN NORTH AMER

Mojave and Sonoran desert areas to the south that are nearly stabilized areas of former extension.

The eastern and western physiographic boundaries of the southern Great Basin are sharp and coincide with structural and geophysical boundaries. The high Colorado Plateau on the east is a tectonically stable area underlain by relatively undeformed Paleozoic, Mesozoic and Cenozoic strata that unconformably overlie Precambrian crystalline basement rock (Stewart, 1978). The boundary between the Colorado Plateau and Great Basin is a complex series of bold escarpments that coincides with the easternmost of the Basin and Range extensional faults. The Sierra Nevada on the west is primarily underlain by Mesozoic granitic rocks. The boundary between the Sierra Nevada and the Great Basin is also a steep, fault-controlled mountain front. The northern Great Basin is bounded on the east, west, and north by the middle Rocky Mountains, Cascade Mountains, and Columbia Plateau, respectively (Figure 7). These provinces are not discussed here because of their great distance from the Candidate Area.

Mountain ranges make up approximately 35% of the landscape in the Great Basin (Figure 8); intermontane sedimentary basins, several erosional desert stream valleys and a few dissected plateaus make up the remainder (Peterson, 1981). The mountain ranges characteristically are 50 to 150 km long and 5 to 25 km wide. They are fairly linear and rise steeply 2 to 3 km above sealevel, and as much as 3.6 km locally (Stewart, 1978). Ridgecrests are continuous and many are jagged. The largest ranges, especially in central Nevada, are roughly parallel and trend northward. The mountain ranges are mostly fault-bounded blocks modified by erosion. Commonly, both sides of a range are faulted, giving rise to steep range fronts cut by deep canyons and ravines (Peterson, 1981). Deep V-shaped canyons and ravines are incised into bedrock, their channels are perpendicular to range fronts; alluvial fill commonly forms flat or terraced canyon floors, particulary in large canyons. Other ranges are only faulted along one flank, i.e. tilted, such that the faulted range front is steep and the opposite front slopes more gently. The ridges at Yucca Mountain are small examples of such a landform. Isolated small elongate mountains surrounded by wide alluvial slopes are common in the basins. These mountains are the highest parts of nearly buried, fault-bounded blocks.

The broad intermontane basins of the Great Basin are deep sediment-filled structural depressions (grabens or half grabens) between the high-standing,

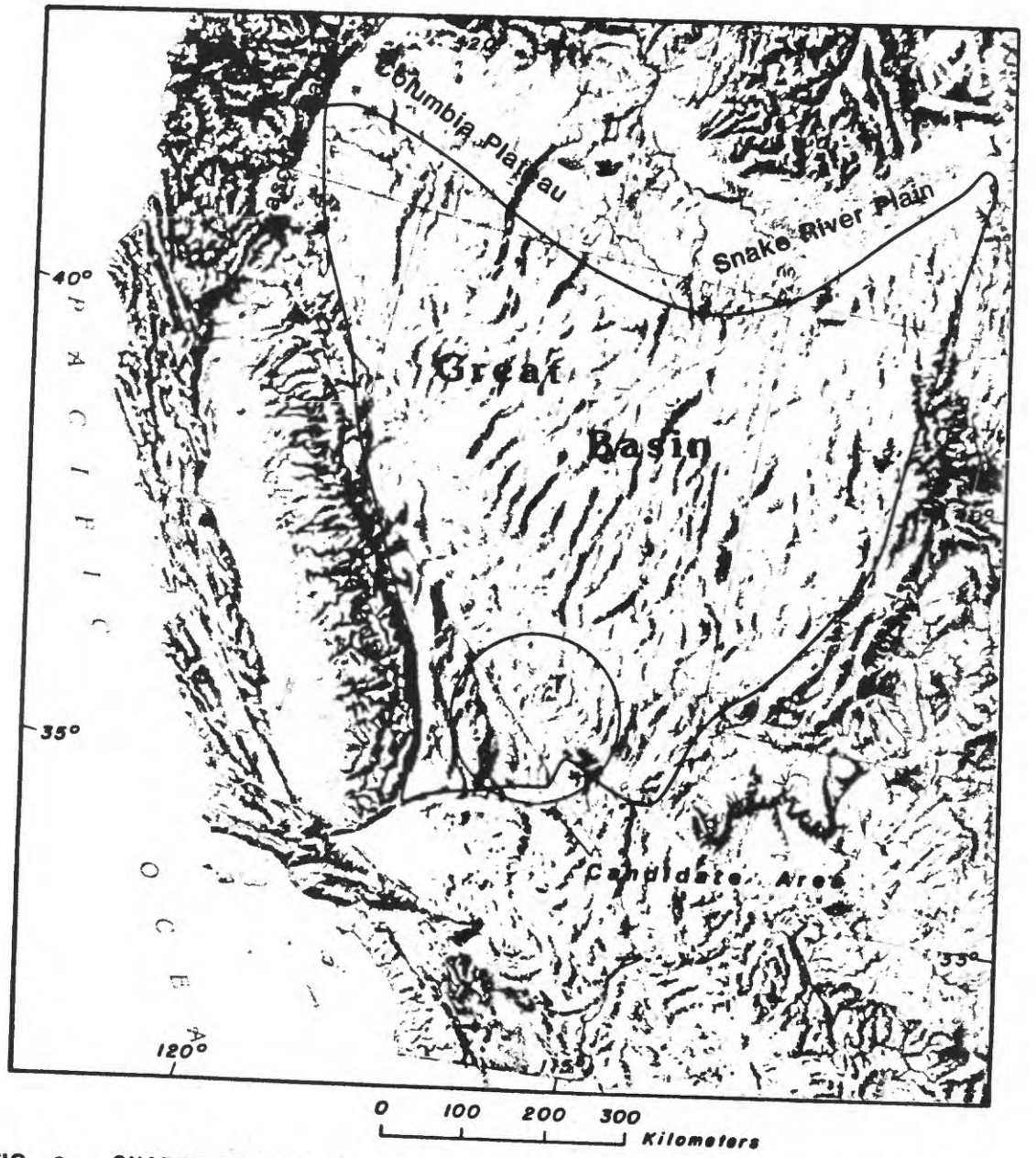

FIG. 8 SHADED RELIEF MAP OF THE GREAT BASIN AND SURROUNDING REGION

fault-bounded blocks (horsts) that make up the ranges (Peterson, 1981). Structural relief across the range-bounding faults between bedrock units under the valleys and equivalent units in adjacent ranges is commonly 2 to 5 km, and the typical thickness of sedimentary fill determined from drill holes in the basins is between a few hundred meters and more than 3 km (Stewart, 1978). Most surface drainage systems in the Great Basin are closed either within a single intermontane basin or within several adjacent basins that are connected across low bedrock divides. Only the Colorado River system in the southeast part of the Great Basin and the Snake River system in its northern part discharge into the sea.

The depositional topography of the intermontane basins, created through alluvial filling of the broad structural depressions, contains two distinctive geomorphic elements, piedmont slopes and nearly level basin floors (Figure 9, A); mountain ranges can be considered a third major element (Peterson, 1981). Piedmont slopes include all of the terrain between the steep mountain fronts and the level basin floors. Slopes on the piedmonts are generally less than 15% (8.5°), whereas slopes in the mountain ranges are greater. The piedmont slopes consist of complex systems of coalescing alluvial fans and dissected alluvial fans that flare out downslope onto the basin floors (Figure 9, B). Pediment surfaces are cut across all or part of some piedmont slopes. The flat basin floors are typically covered by fine-grained sedimentary deposits that accumulate in and around ephemeral lakes (playas). Some intermontane basins lack flat floors, but have axial ephemeral streams flowing along the intersection of opposing piedmont slopes near the centers of the basins.

Erosional stream valleys occur throughout the Great Basin ranges. However, perennial streams are few, and erosion is generally accomplished by flash flooding. Most streams in the Great Basin are graded to the baselevels of closed internal basins. Consequently, streams cut down only where base-level changes have occurred in response to local controls such as tectonism and stream capture. External factors such as climate change can also affect stream equilibrium. Intermittently downcutting streams typically form steep-walled, flat-bottomed or terraced dry washes with relatively straight courses, like Fortymile Wash near Yucca Mountain.

Dissected volcanic plateaus within the Great Basin commonly are underlain by thick sequences of flat lying ash-flow tuff. These plateaus generally are

FIG. 9 MAJOR PHYSIOGRAPHIC ELEMENTS AND LANDFORMS OF AN INTERNALLY DRAINED INTERMONTANE BASIN

A. PHYSIOGRAPHIC ELEMENTS

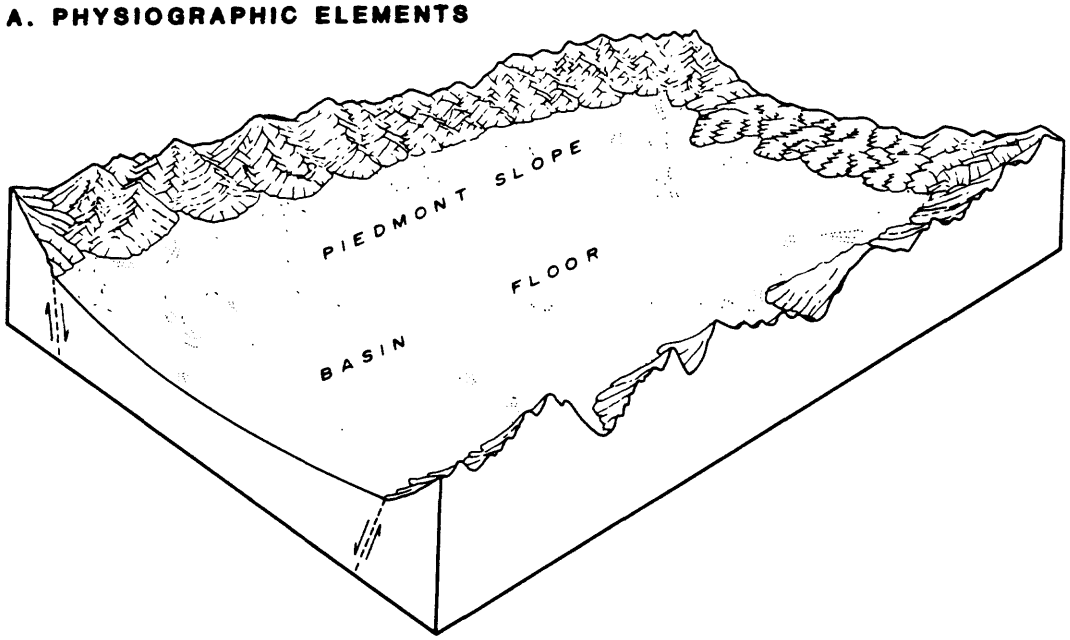

B. LANDFORMS

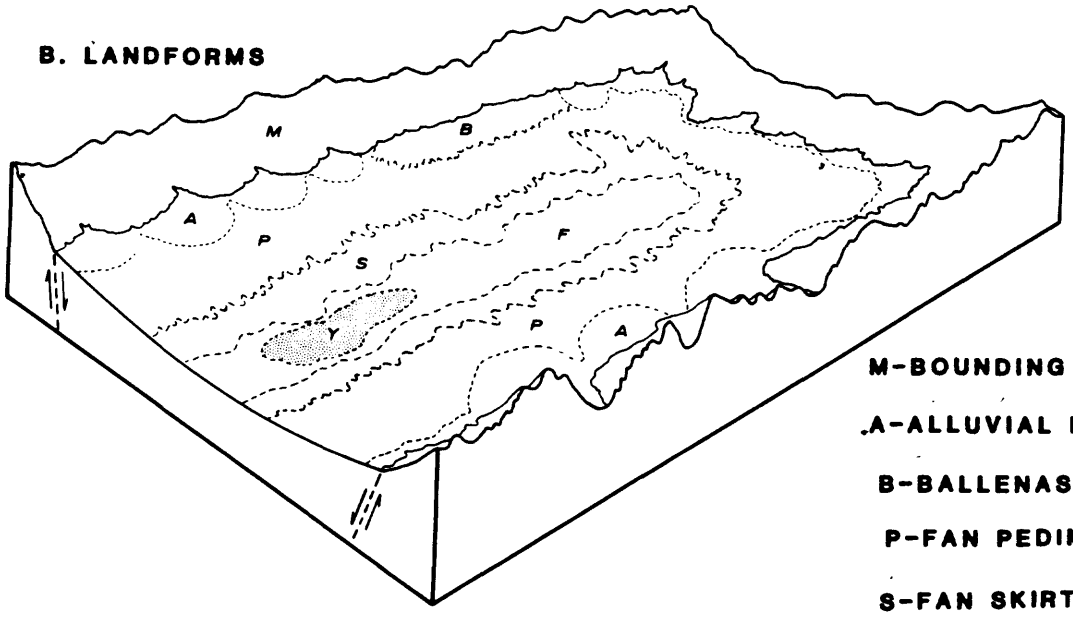

M-BOUNDING MOUNTAINS

A-ALLUVIAL FANS

B-BALLENAS

P-FAN PEDIMENTS

S-FAN SKIRT

F-ALLUVIAL FLAT

Y-PLAYA

modified from Peterson (1981)

areas that were not strongly faulted. The degree to which such plateaus are dissected largely is influenced by the amount of relative subsidence in surrounding areas, as well as the amount of rainfall and the competence of bedrock.

Physiographic Elements

Candidate Area

The Candidate Area can be subdivided physiographically into five grossly defined elements or areas that have characteristic suites of landforms formed by a common set of geomorphic processes and geologic conditions. The physiography of each of these areas reflects regional variations in surficial processes and bounding geologic conditions, such as bedrock type and structure. The major physiographic areas recognized within the Candidate Area are: 1) the north-trending basins and ranges in the eastern and far northern parts, 2) the dissected volcanic plateaus in the north-central part, 3) the irregularly shaped mountains and broad alluvial valleys along the Nevada-California border, 4) the north- and northwest-trending basins and ranges in the south and southwest parts, and 5) the Spring Mountains in the southeast (Figure 10, in pocket).

1) North-trending basins and ranges such as the Belted Range and Kawich Valley and the Halfpint, Pintwater, and Desert Ranges and adjacent valleys are typical of the smaller (50 km long and 5 to 10 km wide) basins and ranges of the Great Basin (See Figure 10 for place names). Mountain range, piedmont slope, and basin plain landforms similar to those listed above are typical of the northernmost and eastern parts of the Candidate Area. The ranges are underlain by Proterozoic and Paleozoic sedimentary rocks and Tertiary volcanic rocks in fault-bounded blocks.

2) Prominent dissected volcanic plateaus include Pahute Mesa, Timber Mountain, Shoshone Mountain and northern Yucca Mountain. The typical features of such plateaus in the Great Basin are relatively flat summit surfaces with minor relief, and steep side slopes covered with rubble. Many have patterned ground like stone stripes. The plateaus are underlain by relatively undeformed Tertiary volcanic rocks.

3) A 50- to 100-km-wide belt of broad alluvial basins and irregularly shaped low ranges roughly parallels the California-Nevada border. This belt, called the Walker belt (Stewart, 1980), includes such basins as Sarcobatus Flat, the Amargosa Desert, Crater Flat, and Jackass Flats. Highland areas include the Gold Mountain area, Bullfrog Hills, Bare Mountain, and Yucca Mountain. Additionally, the belt includes the irregularly trending hills, ridges, and basins north of Pahrump Valley and the Spring Mountains, and south of the Shoshone and Timber Mountains, between the Amargosa Desert and the north end of Las Vegas Valley. The belt coincides generally with the drainage basin of the Amargosa River south of Beatty, Nevada. The irregular pattern of highlands and basins is largely a result of structural complexity as well as variability in erosion rates. The belt also coincides with part of the Walker Lane, a complex zone of normal and strike-slip faults.

4) The major basins and ranges in the southern and southwestern part of the Candidate Area include Death Valley, Panamint Valley, northern Pahrump Valley, the Panamint, Grapevine, Funeral, and Black Mountains, and the Nopah, Resting Spring, and Greenwater Ranges. These basins and ranges are typical of landforms in much of the Great Basin, as are those in the eastern and northernmost part of the Candidate Area. However, recent tectonic activity in the southwestern part of the Candidate Area, particularly in Death Valley, has created a landscape having some of the greatest topographic relief in North America.

5) The Spring Mountains are a dissected, relatively high standing structural block underlain by stratified Upper Proterozoic and Paleozoic sedimentary rocks. The Spring Mountain block was relatively undeformed during the Cenozoic as compared to the surrounding area, and much of the topography is controlled by the pre-Cenozoic structure and relative resistance of the rocks to erosion. Deep canyons are cut essentially at right angles to the trend of the range.

Elevations in the Candidate Area range from 86 m below sea level in Death Valley to 3,633 m on Charleston Peak in the Spring Mountains, 100 km to the southeast. Typically, the topographic relief varies between about 300 and 1000 m over distances of 50 km, except in the Death Valley area where elevation differences are more than 3400 m over similar distances.

There are no perennial streams within the Candidate Area, except for the uppermost reaches of a few streams in the highest parts of the Spring Moun-

tains. The largest river is the intermittent Amargosa River, 250 km long, which flows southward through the Amargosa Desert, draining the Site Vicinity, and eventually discharging into an ephemeral lake in southern Death Valley. The course of the Amargosa River appears structurally controlled. It heads on Timber Mountain and would naturally drain to Sarcobatus Flat except for interception of its drainage through the Bullfrog Hills by a canyon controlled by the Beatty Fault. The Colorado River and its tributaries to the east and southeast of the Candidate Area are the only through-going streams near the Candidate Area. The Las Vegas Valley in the southeastern part of the Candidate Area is part of the Colorado River drainage but contains no perennial streams.

Site Vicinity and Site

Physiographic elements in and near the Site can be divided as follows: (1) the ridges and valleys that make up Yucca Mountain, (2) the irregular rugged topography north of Yucca Wash, (3) the piedmont slopes surrounding Yucca Mountain on the south and east, (4) Fortymile Wash east of Yucca Mountain, (5) Jackass Flats east of Fortymile Wash, and (6) Crater Flat west of Yucca Mountain.

1) Yucca Mountain is made up of a prominent group of north-trending, en echelon, fault-block ridges and valleys stretching southward from Beatty Wash on the north to U.S. Highway 95 in the Amargosa Valley (Figure 11). The Site is located near the middle of this group of ridges and valleys. Topography at the site is controlled by the high-angle faults, which tilt the resistant volcanic strata eastward. Slopes are locally steep on the west-facing escarpments eroded along the faults and in some of the valleys that cut into the more gentle eastward-facing dip slopes. Narrow valleys and ravines are cut in bedrock; wider valleys are floored by alluvial deposits into which terraces have been cut by intermittent streams. Locally, small sandy fans extend up the lower slopes of Yucca Mountain and spread out on the valley floors. East of the crest of Yucca Mountain, drainage is into Fortymile Wash; west of the crest, streams flow southwestward down fault-controlled canyons and discharge in Crater Flat.

2) Yucca Mountain terminates abruptly on the northeast at Yucca Wash, an erosional valley which drains southeastward to Fortymile Wash. Intermittent

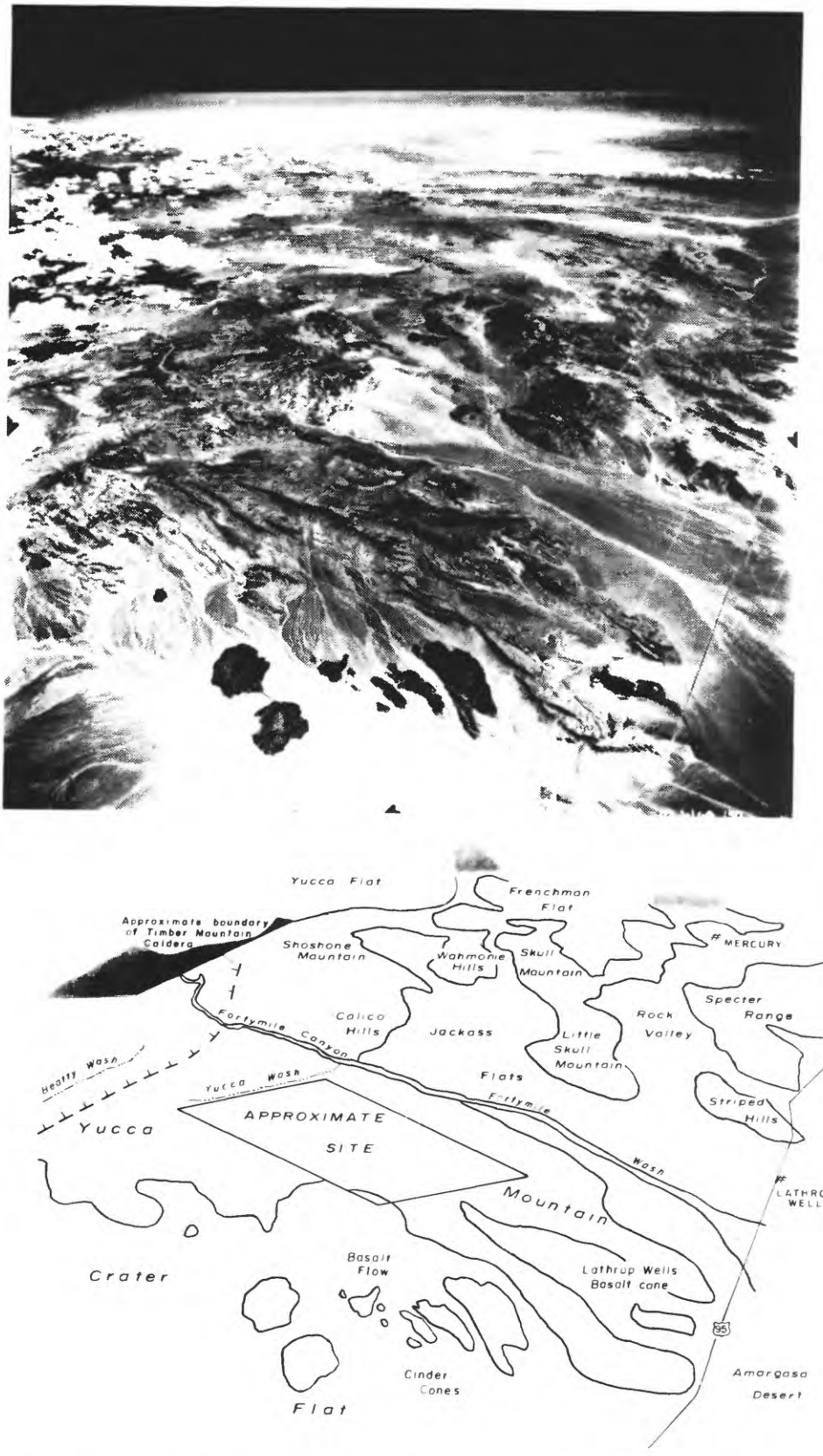

Figure 11.--High altitude oblique aerial photograph of the site and surrounding area. View is to east.

streams in Yucca Wash are incised into bedrock along some reaches and have cut a series of terraces in Pliocene(?) and Quaternary alluvial deposits along other reaches. North of Yucca Wash is a deeply dissected volcanic plateau called Pinnacles Ridge. The overall dendritic drainage pattern of the volcanic plateau is modified by structurally controlled reaches on some streams.

3) Flanking the southern end of Yucca Mountain on the south and east are complexes of alluvial fans and dissected alluvial fans forming a piedmont slope that is cut on the east by Fortymile Wash and extends into the Amargosa Desert on the south. This piedmont slope merges southward with the basin floor, which is covered with playa lake deposits 25 km south of Yucca Mountain. The playa intersects a piedmont slope that grades away from the Funeral Mountains on the west and controls the Amargosa River which follows the junction between opposing piedmont slopes in the northern Amargosa Desert. Piedmont landforms in the Site Vicinity are closely associated with Quaternary stratigraphy (Figure 12).

4) Drainage of the Site is mostly eastward to Fortymile Wash, and then southward to the Amargosa Valley. Fortymile Wash, which drains the Timber Mountain area north of the Site through Fortymile Canyon, is a narrow (150 to 600 m wide) erosional stream valley entrenched 13 to 26 m into Pliocene(?) and Quaternary alluvial deposits. This entrenchment of Fortymile Canyon decreases gradually downstream until the drainage joins with the piedmont slope 20 km south of Yucca Mountain near U.S. Highway 95.

5) Streams draining the Calico Hills, 15 km northeast of the Site, have deposited a complex system of alluvial fans that coalesce into a broad sandy piedmont slope to the south called Jackass Flats. Modifying the constructional landforms of the flats are the narrow erosional stream valleys of Fortymile Wash, along the western edge, and Topopah Wash and its tributaries in the eastern part.

6) Crater Flat is a broad constructional alluvial basin in which intermittent streams have been integrated into a subparallel drainage system that discharges to the south through a single outlet into the Amargosa Desert. Quaternary faulting along the west side of Crater Flat has uplifted Bare Mountain and resulted in the formation of steep alluvial fans below the mouths of deeply incised canyons. Pliocene and Quaternary basalt cones and small lava flows dot the surface of the southern half of Crater Flat.

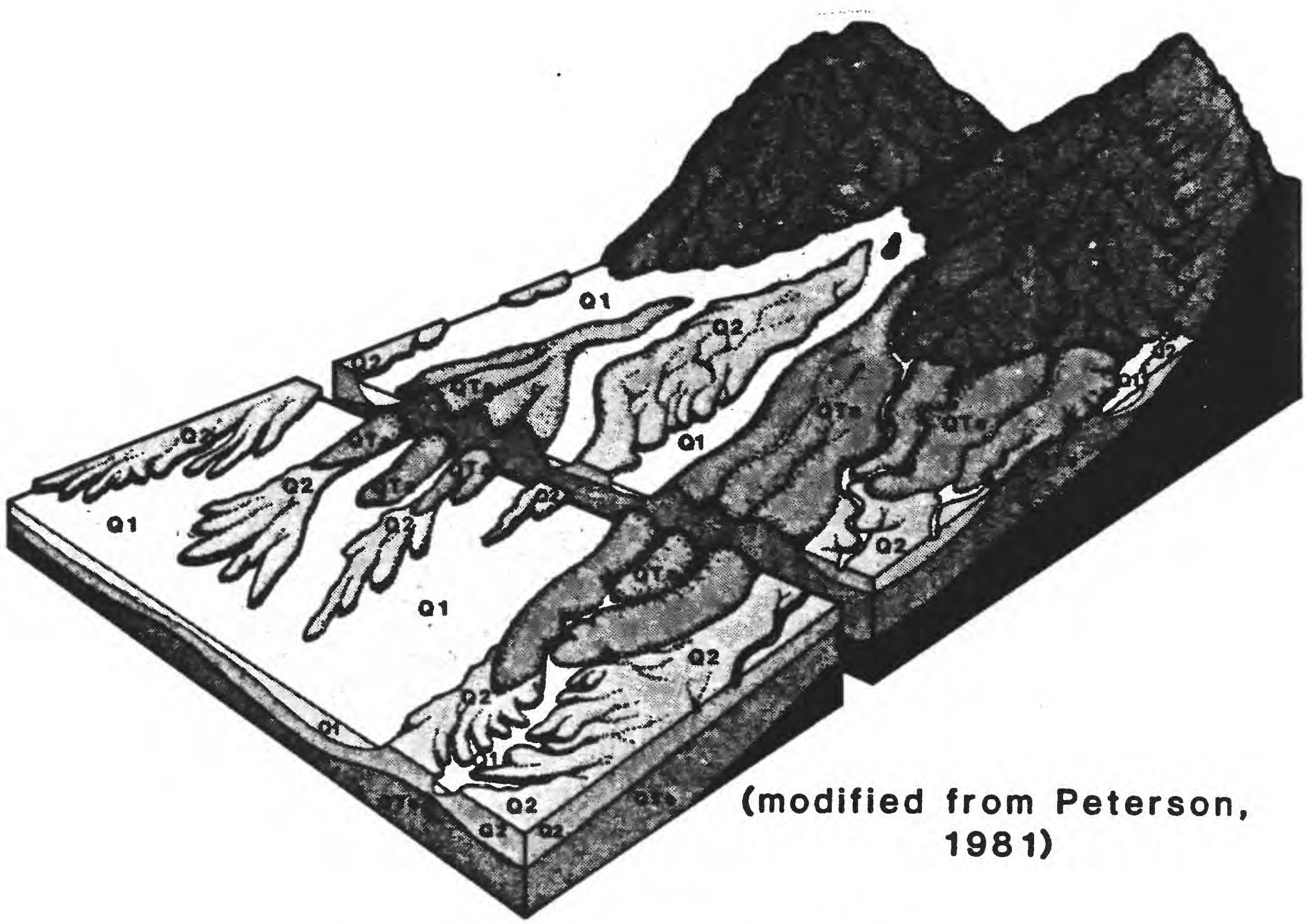

Q1 HOLOCENE ALLUVIAL AND EOLIAN DEPOSITS

Q2 UPPER AND MIDDLE PLEISTOCENE ALLUVIAL AND EOLIAN DEPOSITS

QTa LOWER PLEISTOCENE AND PLIOCENE DEBRIS FLOW DEPOSITS

Tv BEDROCK

FIG. 12

TYPICAL RELATION OF LANDFORMS AND QUATERNARY STRATIGRAPHY IN THE SITE VICINITY

Elevations in the Site Vicinity range from about 640 m in the Amargosa Desert south of the Site to 2,151 m at Shoshone Peak in the volcanic highlands northeast of the Site. The crest of Yucca Mountain reaches an elevation of approximately 1500 m, and the maximum local topographic relief within the Site is approximately 300 m.

Geomorphic Processes

Geomorphic processes in the Candidate Area are governed by the structural setting and climate. Active processes have been observed during geological mapping; however, detailed study and monitoring of these processes are incomplete. Understanding surficial processes under the present climatic conditions serves as a starting point for interpreting older surficial deposits, evaluating past changes of climate, and predicting the effects of future surficial processes within the bounds of predicted future tectonism and climate change.

The Candidate Area has an arid climate characterized by infrequent, but intense precipitation, strong insolation, large daily ranges of temperatures and relative humidity. These characteristics govern the alluvial slope processes and eolian processes at the Site, as well as the rates of physical and chemical rock weathering. In the present-day environment, rock weathering is dominated by physical weathering processes that cause repeated expansion and contraction of near-surface rocks: diurnal heating and cooling; freezing and thawing; and salt crystallization. Chemical weathering plays a minor role because of the lack of both the moisture and the decaying vegetable matter needed to form corrosive carbonic acids.

The annual precipitation ranges from 6 cm at the lowest elevations to 50 cm at the highest elevations and averages 10 to 25 cm in most parts of the area. Rain falls mostly during the winter; however, summer convective thunderstorms tend to produce the largest single storms and largest runoff events. Precipitation falls mostly in the mountains and the resulting hillslope runoff collects into channels that discharge into the closed intermontane basins. Several intermittent streams in the Site Vicinity are presently being monitored to determine the local characteristics of fluvial erosion and deposition, and the size and frequency of floods.

TABLE 1

MAXIMUM DEPTH AND RATES OF STREAM INCISION
IN TERTIARY AND QUATERNARY SURFACES IN THE YUCCA MOUNTAIN AREA

Surface[a] of Unit	Approx. Age (Years)	Maximum Depth (m)	Maximum Rate[b] (m/103 Years)	Location
Q2b	1.6 x 105 [c]	8.5	0.053	Fortymile Wash
Q2c	3 x 105 [d]	25.9	0.082	Fortymile Wash
Tpc	10 x 106 [e]	218.2	0.022	Western Yucca Mountain

Notes:

a) For meaning of unit designations, see Hoover and others, (1981).

b) Corrections for differences in slope, topographic relief, or drainage basin area have not been made in calculating the maximum rates of stream incision. All such corrections would tend to decrease the rates.

c) Q2b age is maximum determined by U-Th disequilibrium method.

d) Q2c age is average of two U-Th disequilibrium ages.

e) Tpc (Tiva Canyon Member of the Paintbrush Tuff) uplift age is determined from two minimum K-Ar ages for the Rainier Mesa Member, which overlies the traces of faults along which blocks of the Tiva Canyon Member were uplifted.

The runoff rarely reaches the basin floors; instead, it is absorbed into the alluvial piedmont slopes. Only very large floods discharge into the playas in the present climate, but the frequency of such large storms is not known. Large magnitude floods occur when long spring rains coincide with significant snowmelt in the mountains, or when an unusually severe storm that has not been depleted of moisture over the intervening mountains travels into the Candidate Area from the Pacific Ocean or Gulf of Mexico.

Mass movements are usually triggered by precipitation events. Landslides, rockfalls, debris flows, and mudflows all move under the influence of gravity, but seepage from runoff is usually necessary as a lubricant for bodies of loose rock and sediment to move. Large precipitation events tend to generate large mass movements.

Episodes of relatively increased mass-movement activity have occurred several times during the Quaternary. These episodes resulted from alternating intervals of relatively wet and dry climate. During more arid episodes little runoff was available to transport hillslope detritus, and rock debris tended to accumulate on hillsides. Runoff during wetter intervals transported the accumulated weathered detritus into the basin, where the sediment was deposited in large alluvial fans. This appears to have been the dominant fan-building process responsible for the older Quaternary deposits (Hoover and others, 1981).

Alluvial processes, as well as mass movement activity, do not appear to be as effective in moving detritus at the present time as they were during times of wetter climate during the Pleistocene. The large fans extending from range fronts to basin floors have been largely unaffected by these processes during the present episode of arid climate. Even large magnitude floods are confined to washes until the channel approaches more distal parts of the gravel fans. Many topographically high fan surfaces do not appear to have had any significant deposition or erosion by alluvial processes since middle Quaternary time. It appears that since middle Quaternary time, there have been no sustained periods of relatively wet climate during which coarse debris flows were deposited, similar to the remnant debris flows now exposed on the surfaces of most large fans.

Continued relative basin subsidence and range uplift during the Quaternary are another reason that fan surfaces are now incised and are not undergoing active deposition. Incision by Fortymile Wash into the main fan

deposits has not been deep, the surface of early to middle Quaternary fluvial deposits and debris flows (unit Q2c of Hoover and others, 1981) is less than 26 m above the present channel. Measurements of the depth of stream incision were made at several places in the Site Vicinity, and average rates of stream downcutting were calculated from dated stratigraphic horizons. The rate of stream incision at Yucca Mountain is less than 0.1 m per 1000 years during the last 300,000 years (Table 1). Part of this incision may be due to the increased discharge that resulted from the capture of Beatty Wash by Fortymile Wash sometime between 300,000 and 160,000 years ago rather than tectonic uplift.

Stream incision rates are only one measure of the total Quaternary erosion that has occurred in the Site Vicinity. No data are yet available for rates of hillslope erosion, deflation by wind, or sediment yield. These are the principal measurements necessary to characterize total Quaternary degradation at the Site.

The patterns of late Cenozoic tectonism and Quaternary climate changes serve as a basis for predicting the extremes of future geomorphic changes in the Site Vicinity. Fault movement at the Site could increase the topographic relief, which would serve to accelerate hillslope erosion and downcutting; however, small (<1m) individual fault movements would probably only have small local effects. Vertical offsets on alluvial fans could steepen surface gradients to the critical angle at which downcutting is initiated. Earthquakes could trigger mass movements such as landslides or debris flows. Predicted climate fluctuations in the Candidate Area over the next 10,000 years are based primarily on the projected CO_2 increase due to man's activities, and projected changes are an increase in the rate of warming and increased summer precipitation. If these changes occur, then a consequent increase in erosion should be expected. Increased runoff and sediment yield would probably denude hillslopes, and choke the washes with sediment. If sufficient runoff becomes available, sediment would be carried across the fans onto the basin floors. Increased temperatures would likely be reflected in decreased vegetation and an increase in wind activity. Both of these effects would enhance wind erosion and possibly dune formation in the basins. Further study of the present-day erosional processes and rates is necessary before the effect of possible future increased erosion on waste isolation can be evaluated.

FIGURE 13 GEOLOGIC TIME SCALE.REPRINTED WITH PERMISSION

from GEOLOGY Vol.11 no.9,Sept.1983

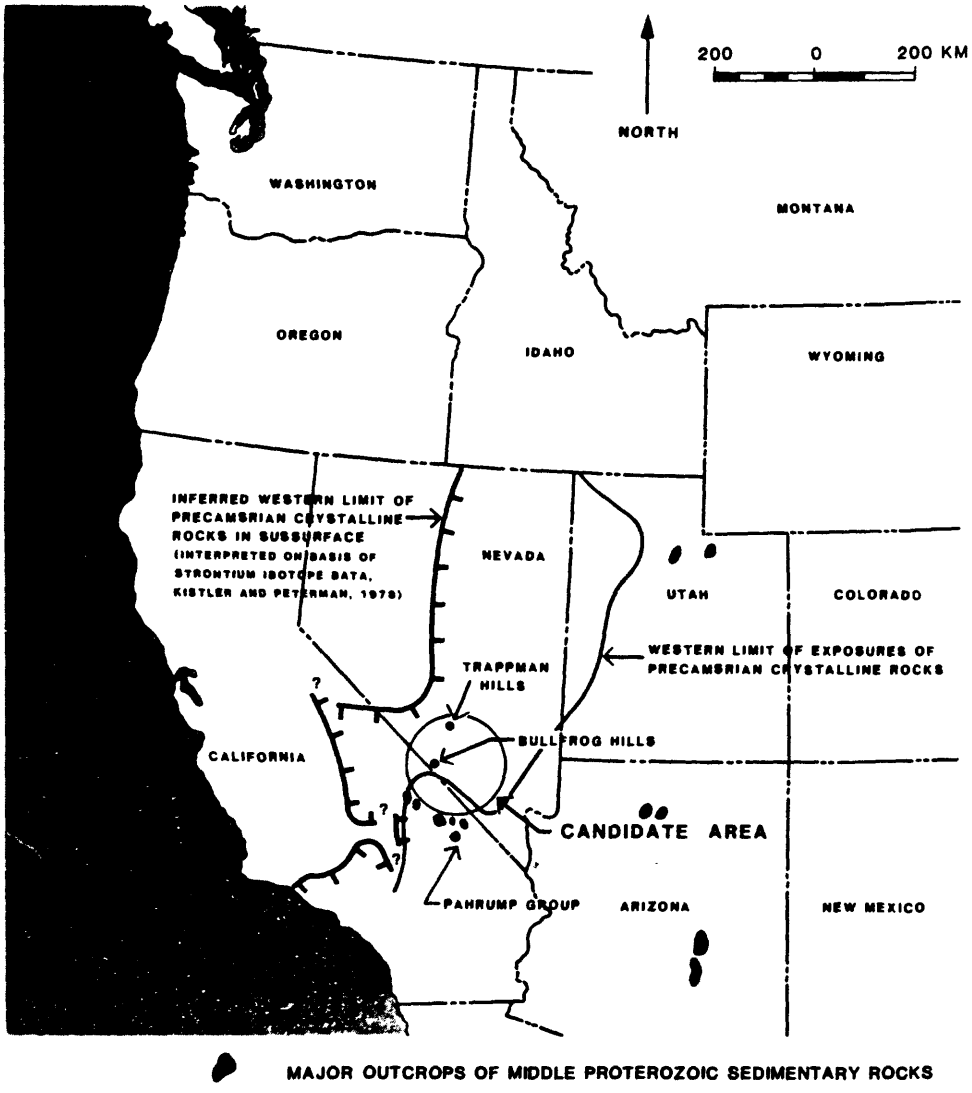

FIG. 14

DISTRIBUTION OF LOWER AND MIDDLE PROTEROZOIC CRYSTALLINE ROCKS AND MIDDLE AND UPPER PROTEROZOIC RESTRICTED BASIN DEPOSITS IN THE GREAT BASIN

STRATIGRAPHY

Rocks in the Candidate Area range in age from Early Proterozoic to Quaternary (Figure 13). The Upper Proterozoic and Paleozoic rocks, which occur throughout the area, are largely marine clastic and carbonate rocks deposited with gross concordance on the western continental shelf of ancient North America. Mesozoic marginal marine and nonmarine sedimentary rocks occur to the east and southeast of the Candidate Area. Mesozoic granitic plutons are common in the western part of the Candidate Area but sparse elsewhere. Many Upper Proterozoic and Paleozoic sedimentary rocks were metamorphosed during Mesozoic time. Most of the Cenozoic rocks are nonmarine volcanic and sedimentary units, predominantly tuff of Miocene age. Cenozoic granitic rocks occur in the southwest part of the Candidate Area and at one locality (Wahmonie, Figure 3) in the central part. Granitic rocks correlative with the Cenozoic volcanism presumably are also present at depth. Extensive Pliocene and Quaternary alluvial, eolian, and lacustrine deposits fill the intermontane basins. Pliocene and Quaternary basaltic rocks occur at scattered volcanic centers in the western and northern parts.

Stratigraphic Framework of the Candidate Area

Pre-Cenozoic

The documented geologic history of the Candidate Area extends back to the formation of Lower Proterozoic gneiss [1.8 b.y. old; (Wasserburg and others, 1959)] and schist. The gneiss and schist are intruded in the Death Valley area (Jennings, 1977) by porphyritic granite 1.4 to 1.3 b.y. old (Wasserburg and others, 1959). Similar gneiss and schist also crop out in the Bullfrog and Trappman Hills (Stewart and Carlson, 1978), closer to the proposed site, but their ages are undefined and they could be much younger (Figure 14; Stewart and Carlson, 1978).

During the Middle and Late Proterozoic, thick sequences of clastic and carbonate rocks were deposited unconformably on the older crystalline rocks in restricted basins that formed during the early stage of Precambrian rifting of the continental margin of western North America. These old sedimentary rocks, the Pahrump Group and Noonday Dolomite, occur only in the southwestern part of the Candidate Area (Jennings, 1977) (Figure 14).

The Cordilleran miogeocline, essentially the ancient continental shelf of western North America, was well defined by latest Proterozoic time (Stewart and Poole, 1974). A laterally extensive, westward-thickening wedge of carbonate and terrigenous detrital rocks was deposited on the continental shelf from the Late Proterozoic to Late Devonian (Figures 15 and 16). The Candidate Area lies largely within this continental-shelf terrane, where the stratigraphic sequence is about 7,200 m thick (Figure 17, in pocket). Upper Proterozoic and Lower Cambrian clastic rocks comprise the lower 2,700 m of the section and the lower of two major clastic aquitards in the region; Middle Cambrian through Upper Devonian stratified carbonate rocks comprise the upper 4,500 m of this section and are a regionally significant carbonate aquifer (Winograd and Thordarson, 1975). The entire sequence of Upper Proterozoic through Upper Devonian continental-shelf rocks thins southeastward to less than 1,000 m near the edge of the ancient stable craton (Figure 16).

An orogenic highland (Antler orogenic belt) that formed along the continental margin in Late Devonian and Early Mississippian time shed detritus eastward to a marine trough that occupied the former carbonate shelf (Figure 18) (Poole, 1974). The Upper Devonian and Mississippian Eleana Formation, a sequence of argillite, quartzite, conglomerate, and sparse limestone more than 2,300 m thick, was deposited in this trough, known as the Antler foreland flysch basin (Figures 16, 17, and 18). This and other associated clastic units comprise the upper of the two regionally important aquitards in the Paleozoic rock sequence (Figure 17). The foreland flysch basin deposits are thinner and finer grained toward the east where the basin shallowed. Toward the southern and eastern part of the Candidate Area, the clastic basin deposits grade into continental-shelf carbonate rocks of Mississippian age (Figures 16 and 18).

Carbonate platform facies rocks such as the Tippipah Limestone, itself more than 1,000 m thick, were deposited on top of the Mississippian basin deposits during the Pennsylvanian and Early Permian. These upper Paleozoic carbonate rocks comprise the upper carbonate aquifer (Figure 16) in the eastern part of the Candidate Area. According to Winograd and Thordarson (1975), the upper carbonate aquifer is probably not regionally significant in the western part of the Candidate area, including the Site.

The only Mesozoic sedimentary rocks exposed in the Candidate Area are shallow marine and nonmarine rocks that crop out in the Spring Mountains

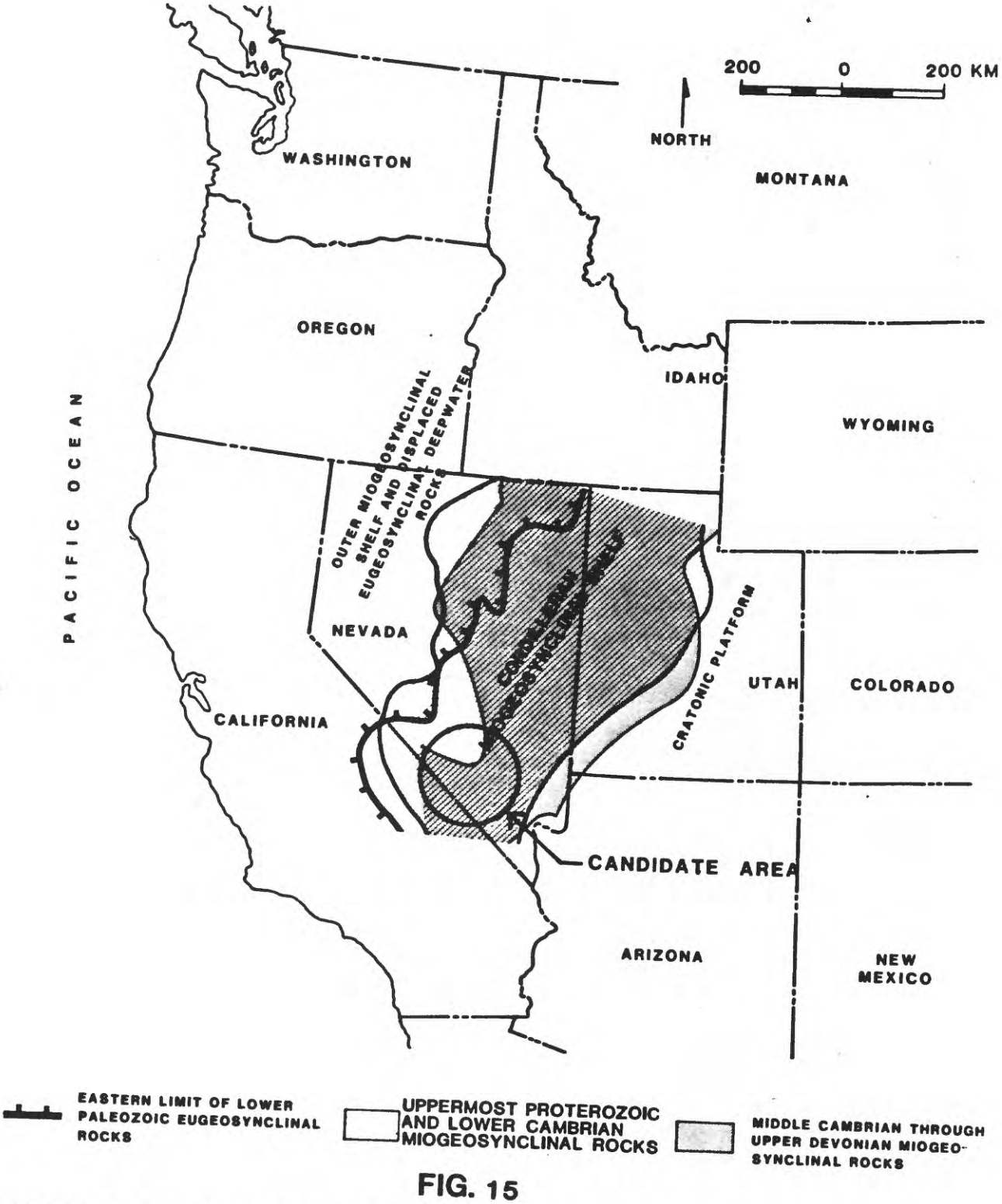

FIG. 15

LATEST PRECAMBRIAN THROUGH MID-PALEOZOIC PALEOGEOGRAPHY OF THE GREAT BASIN

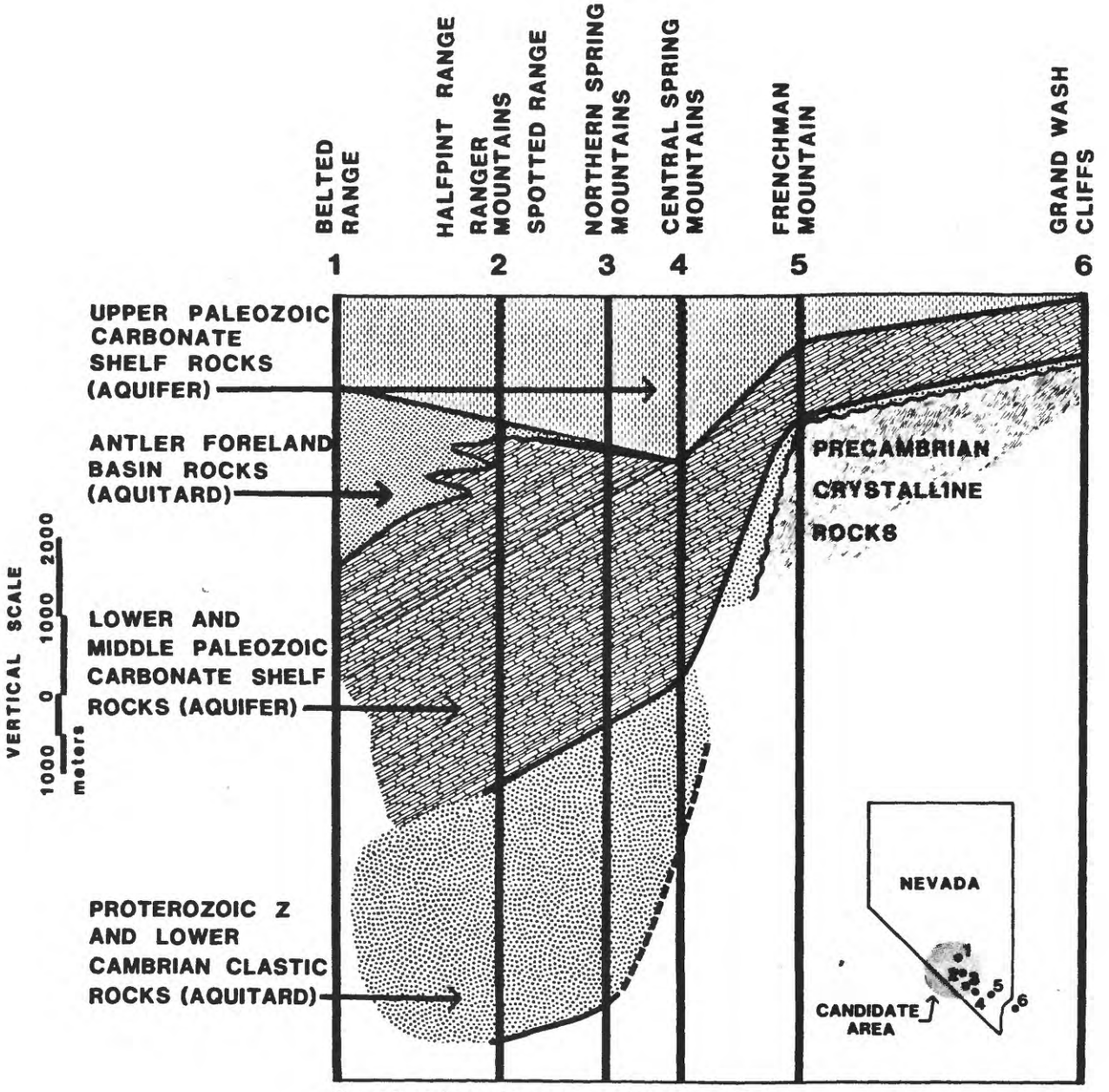

(modified from Stewart and Poole, 1974)

FIGURE 16

STRATIGRAPHIC COLUMNS ACROSS THE SOUTHERN GREAT BASIN

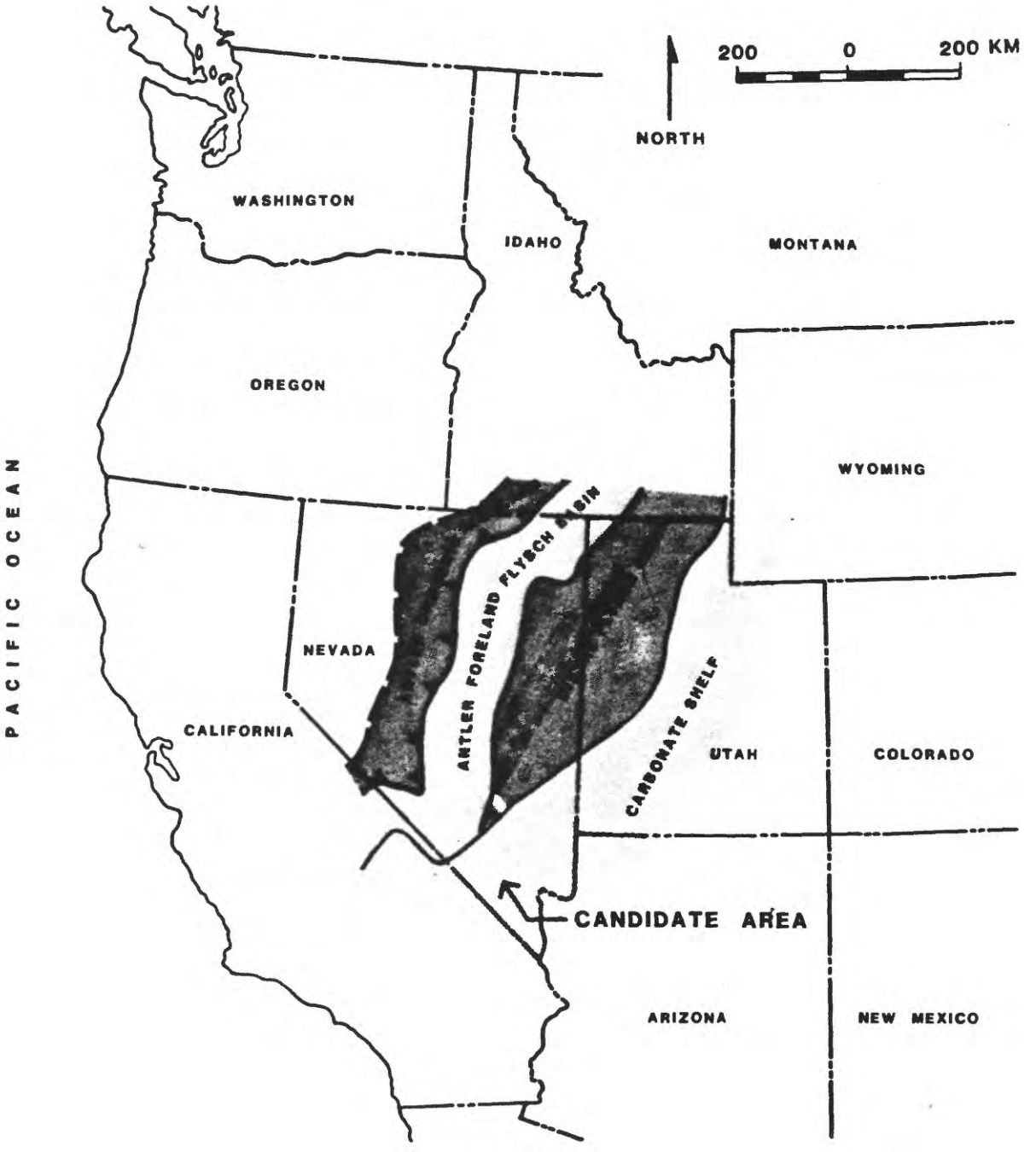

FIG. 18

LATE DEVONIAN AND MISSISSIPPIAN PALEOGEOGRAPHY OF THE GREAT BASIN

(Stewart and Carlson, 1978). Elsewhere, any such rocks were removed by erosion during Mesozoic orogenic events.

In late Mesozoic and earliest Cenozoic time, 180 to 60 m.y. ago (Armstrong and Suppe, 1973), plutons ranging in composition from diorite to granite were intruded in the west and southwest part of the Candidate Area (Jennings, 1977). Several granitic stocks of Cretaceous age intrude Paleozoic rocks in the northeast part of the Candidate Area.

Tertiary

No deposits of early Tertiary age are known in the Candidate Area. Volcanism began in northeastern Nevada approximately 40 m.y. ago and spread progressively south and southwestward (Armstrong and others, 1969; Scott and others, 1971; Stewart and others, 1977). Voluminous quartz-latite and rhyolite ash-flow sheets were erupted between 28 and 20 m.y. ago from large caldera complexes in central Nevada (Figure 19) (Ekren and others, 1971; Ekren and others, 1974a; Stewart and Carlson, 1976). The distal ash-flow deposits of some of these sheets reached the northern part of the Candidate Area. Great volumes of rhyolite ash flows and lavas were erupted intermittently between about 24 m.y. ago and 8 m.y. ago from numerous coalesced caldera centers in and near the northern part of the Candidate Area (Byers and others, 1976; Christiansen and others, 1977). The volcanic rocks that underlie Yucca Mountain were deposited about 14 to 11 m.y. ago during the later phases of this episode of caldera eruptions. During the past 10 to 8 m.y., volcanism was less widespread in the Candidate Area. Most of the activity during this period was confined to southern Death Valley (12 to 4 m.y.) and the region to the west (Owens Valley, Argus Range, Coso volcanic field). Volcanic rocks from 10 to 7 m.y. old show a bimodal distribution by volume between basalt and rhyolite; rocks younger than 7 m.y. are mostly basaltic. No rhyolitic deposits less than 6 m.y. old are known to have originated from volcanic centers within the Candidate Area.

Pliocene and Quaternary

Basaltic volcanism continued into the Pliocene and Quaternary along a north-northeast-trending belt of basaltic volcanic centers between Death

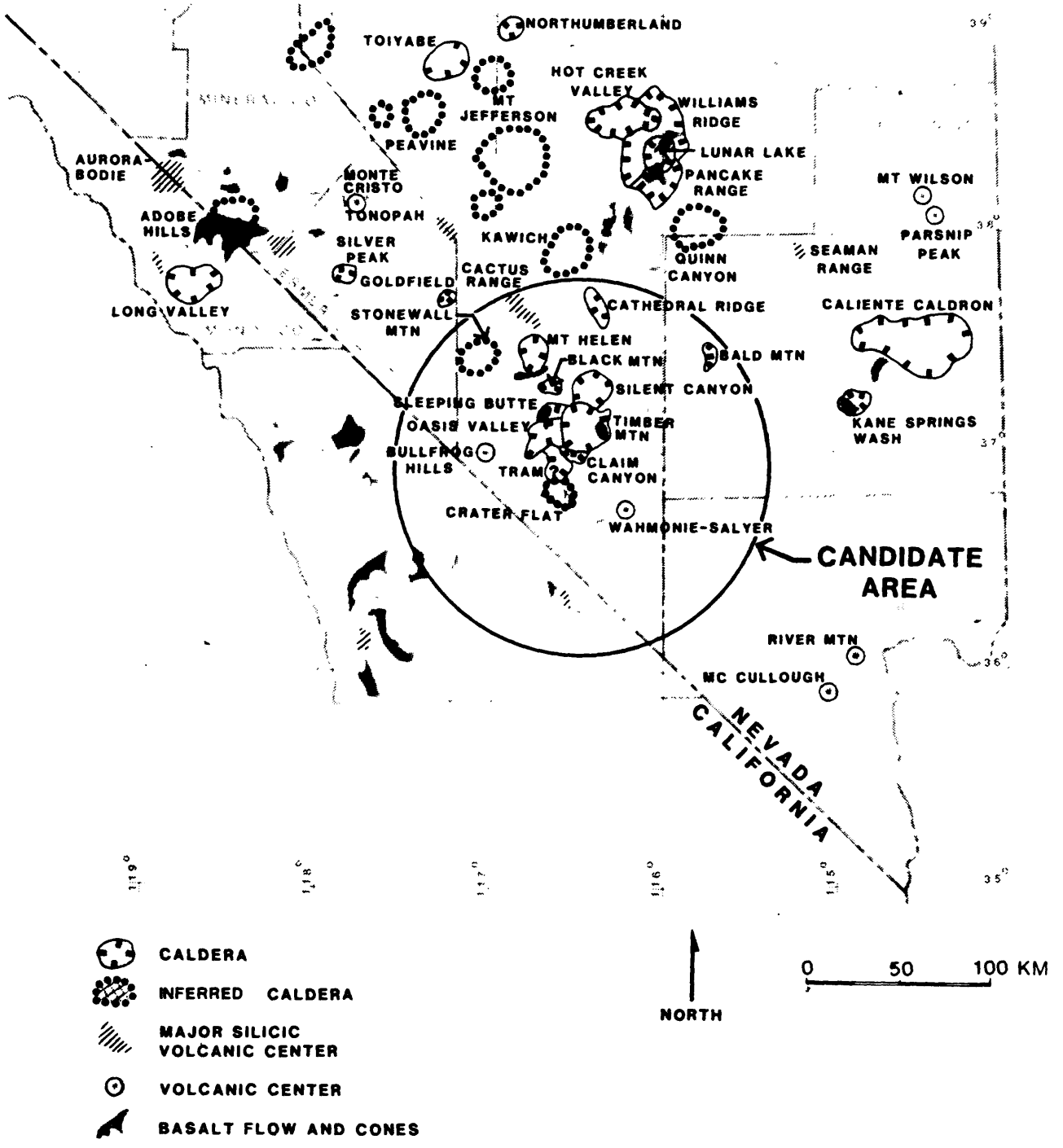

FIGURE 19
MAJOR CENOZOIC VOLCANIC CENTERS OF THE SOUTHERN GREAT BASIN

Valley and the Pancake Range. Scattered basaltic scoria cones and small lava flows of Quaternary age (0-2 m.y.) are present in northern and southern Death Valley, in the central part of the Candidate Area, and immediately west and southwest of the Site (Crowe and Carr, 1980) (Figure 20).

The Pliocene and Quaternary have been a time of erosion in tectonically developing highland areas and associated deposition in intermontane basins. Pliocene and Quaternary sedimentary deposits are mainly alluvial fan deposits that accumulated on piedmont slopes and merge with floodplain deposits and eolian sand sheets and dunes on the basin floors. Scattered spring, pond, and lacustrine deposits were formed in some basins.

A preliminary interpretation of the late Pliocene and Quaternary history of the central part of the Candidate area has been summarized by Hoover and others (1981), who concluded that a perennial lake occupied much of the Amargosa Desert from before 3 m.y. ago until less than 2.1 m.y. ago. A climate cooler and wetter than the present is interpreted for the Candidate Area at that time. The lake subsequently drained through a breached natural dam at the south end of the Amargosa Desert.

The climate is thought by Hoover and others to have become drier during the period between approximately 2 and 1 m.y. ago, causing vegetation to decrease and allowing increased erosion of slopes. Accumulation of widespread debris-flow deposits (unit QTa of Hoover and others, 1981) (Figure 21 and Table 2) is thought to have occurred during this time. Eventually, slopes were stripped of debris and (or) the climate became sufficiently arid that debris flows ceased. Pediments subsequently were cut across the debris-flow units.

A period of climatic fluctuations beginning after about 1 m.y. ago and continuing into the Holocene resulted in alternating periods of deposition and erosion. A study of vegetal remains in packrat middens led Spaulding (1983) to conclude that climate change sufficient to cause significant vegetation changes has not occurred in the area during the past 45,000 years. Even minor climatic fluctuations in the past 8,500 years, however, have been sufficient to trigger distinct erosional and depositional cycles according to Hoover and others (1981). The Holocene is characterized by relatively thin, discontinuous surficial fluvial and eolian deposits.

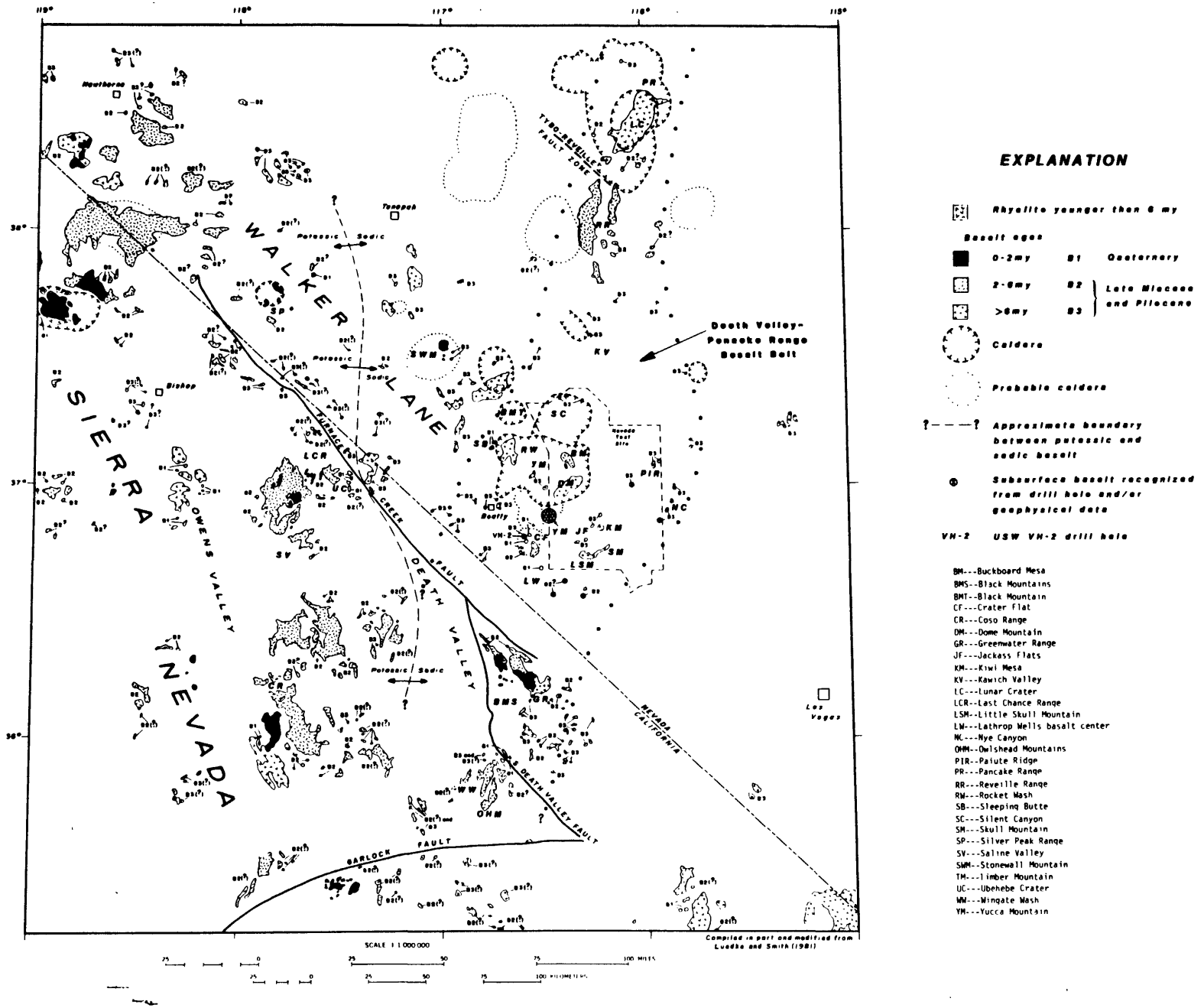

FIG. 20 VOLCANIC ROCKS YOUNGER THAN ABOUT 10 M.Y. AND CALDERAS OF THE SOUTHWESTERN GREAT BASIN, NEVADA AND CALIFORNIA

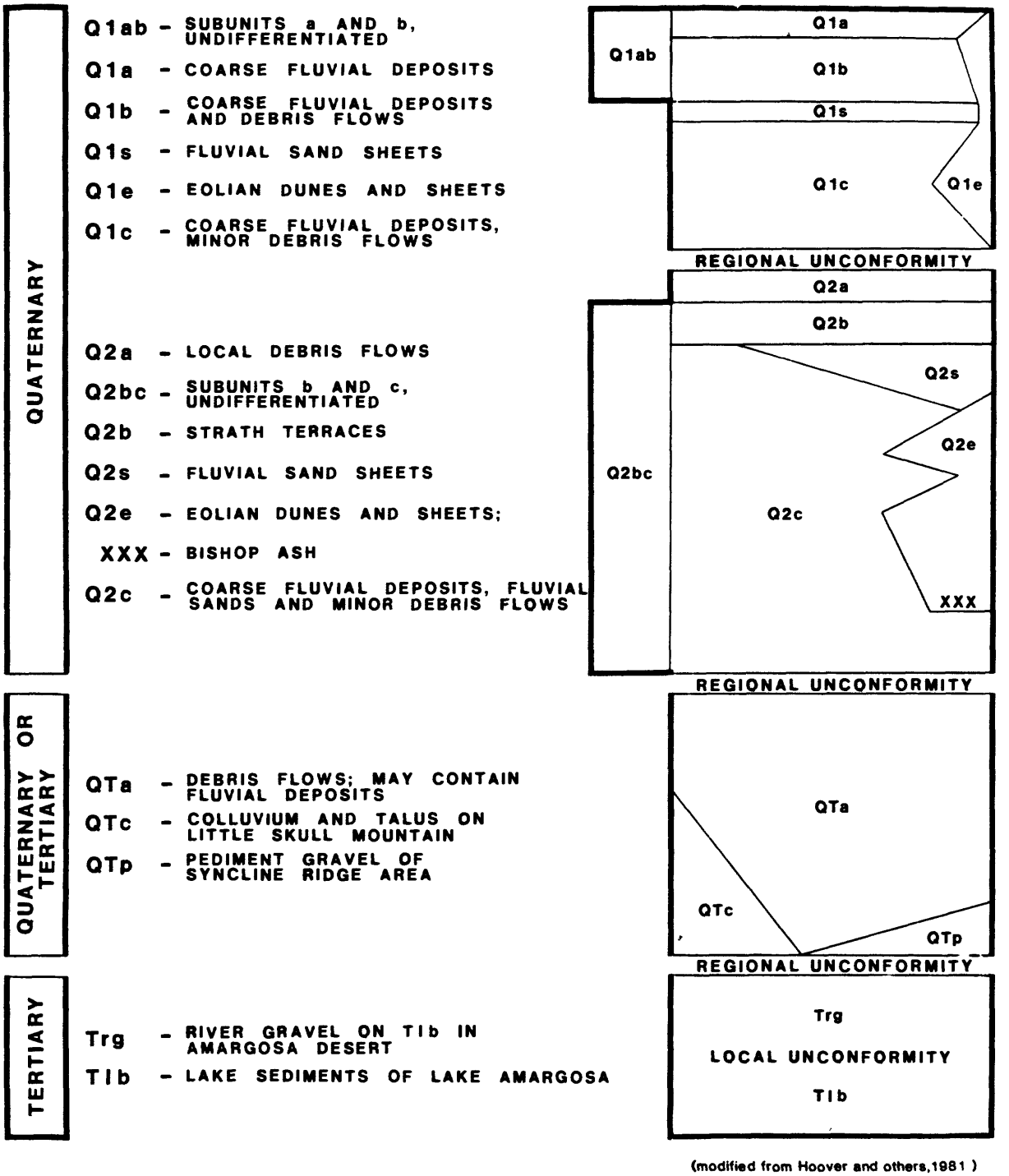

(modified from Hoover and others,1981)

Figure -21

STRATIGRAPHY OF SURFICIAL DEPOSITS IN THE CANDIDATE AREA

TABLE 2

AGES OF SURFICIAL DEPOSITS BY URANIUM-TREND AND OTHER METHODS

Surficial unit	Material	Age (k.y.)[1]	Method[2]	Location
Unit Qlc	Charcoal in fluvial gravel	8.3±0.075	C^{14}	Amargosa River bank 6 m below surface 2 km SE. of Beatty, Nev.
A horizon	Eolian silt	30±30	U-trend	SW Frenchman Flat Trench
A horizon?[3]	Loess	25±10	U-series	Basalt cinder cone 11 km NW of Lathrop Wells
Unit Q2a(?)[4]	Slope wash below fault scarp	40±10	U-trend	Crater Flat Trench 3
	Slope wash on steep slope	41±10	U-trend	Yucca Mountain Trench 13
	Fluvial gravel in wash	47±20	U-trend	Yucca Mountain Trench 2
Unit Q2b	Fluvial gravel in wash	145±25	U-trend	Yucca Mountain Trench 3
	Fluvial gravel on piedmont slope	160±18	U-trend	Gravel pit, Shoshone, CA
	Colluvium on steep slope	160±90	U-trend	Yucca Mountain Trench 13
Unit Q2s	Fluvial sand on piedmont slope	160±90	U-trend	ETS Trench, Jackass Flat
Unit Q2c-younger soil	Fluvial gravel in slope wash	270±30	U-trend	Crater Flat Trench 3
	Fluvial gravel on piedmont slope	270±35	U-trend	Jackass Divide Trench
	Fluvial gravel on pidmont slope	310±30	U-trend	Rock Valley Trench 1
Unit Q2c-older soil	Buried fluvial gravel on piedmont slope	430±40	U-trend	Jackass Divide Trench
	Fluvial gravel on piedmont slope	430±60	U-trend	S. Crater Flat Trench
Unit Q2e	Bishop ash in base	738±3[5]	Geochemical correlation[6]	Five locations in Jackass Flat and Amargosa Desert
Unit QTa				
-Younger than	Youngest ash in Lake Amargosa deposits	2.1±0.4 m.y.	Zircon fission track[7]	Carson Slough, Amargosa Desert

[1] ± one standard deviation

[2] Analyzed by:

C^{14}--S. W. Robinson, U.S. Geological Survey, Menlo Park, CA

U-trend--J. N. Rosholt, U.S. Geological Survey, Denver, CO

U-series--B. J. Szabo, U.S. Geological Survey, Denver, CO

[3] Correlated by appearance to A horizon

[4] Correlated to undated debris flows of unit Q2a by stratigraphic position and depositional environment

[5] Izett, G. A., (1982)

[6] Correlated by trace elements; analyzed by G. A. Izett, U.S. Geological Survey, Reston, VA

[7] Analyzed by C. W. Naeser, U.S. Geological Survey, Denver, CO

Stratigraphy of the Site

The rocks at and near the surface at the Site comprise a thick, gently-dipping sequence of Miocene ash-flow tuff, lava, and volcanic breccia, intercalated with relatively thin units of volcaniclastic rocks and flanked by younger unconsolidated alluvial deposits. The Miocene volcanic rocks range in composition from rhyolite to dacite. Surface mapping (Figure 3; Christiansen and Lipman, 1965; Lipman and McKay, 1965), supplemented by data from core and drill holes as deep as 1,800 m (Figure 22), provides excellent stratigraphic information. Some of the subsurface volcanic stratigraphy and the character of rocks underlying the volcanic sequence are inferred from geophysical data and by interpolation and extrapolation from surrounding areas.

Pre-Cenozoic Rocks

The depth to the pre-Cenozoic rocks underlying the volcanic sequence at the Site is poorly known. Gravity data suggests that pre-Cenozoic rocks are at least 3 km below the surface under much of the Site (Snyder and Carr, 1982). Geophysical models of the configuration of the upper surface of pre-Cenozoic rocks are discussed by Snyder and Carr (1982), who interpreted a depression in the gravity field over the northern part of the Site as the signature of an estimated 3000 m of tuff overlying pre-Cenozoic rocks there. They further interpreted the northern part of the Site as part of a tuff-filled caldera depression. It was not possible for Snyder and Carr, using only geophysical data, to determine whether the pre-Cenozoic rocks beneath the Site are Upper Proterozoic and Paleozoic strata or younger intrusive rocks.

An alternative interpretation, based on aeromagnetic data, has been offered by Bath and Jahren (1984). Relatively positive magnetic values over the north part of the Site are conspicuous in intermediate-altitude aeromagnetic data (Figure 23). Strongly magnetized metasedimentary rocks of the Eleana Formation crop out in the Calico Hills 15 km to the northeast of the Site (Baldwin and Jahren, 1982) and are associated with positive magnetic values similar to those over the northern part of the Site. Bath and Jahren (1984) therefore interpret the positive areomagnetic anomalies over the northern part of the Site and east of the Site over the Calico Hills (A2 through A7, Figure 23) as signatures of a magnetized tabular body of slightly metamor-

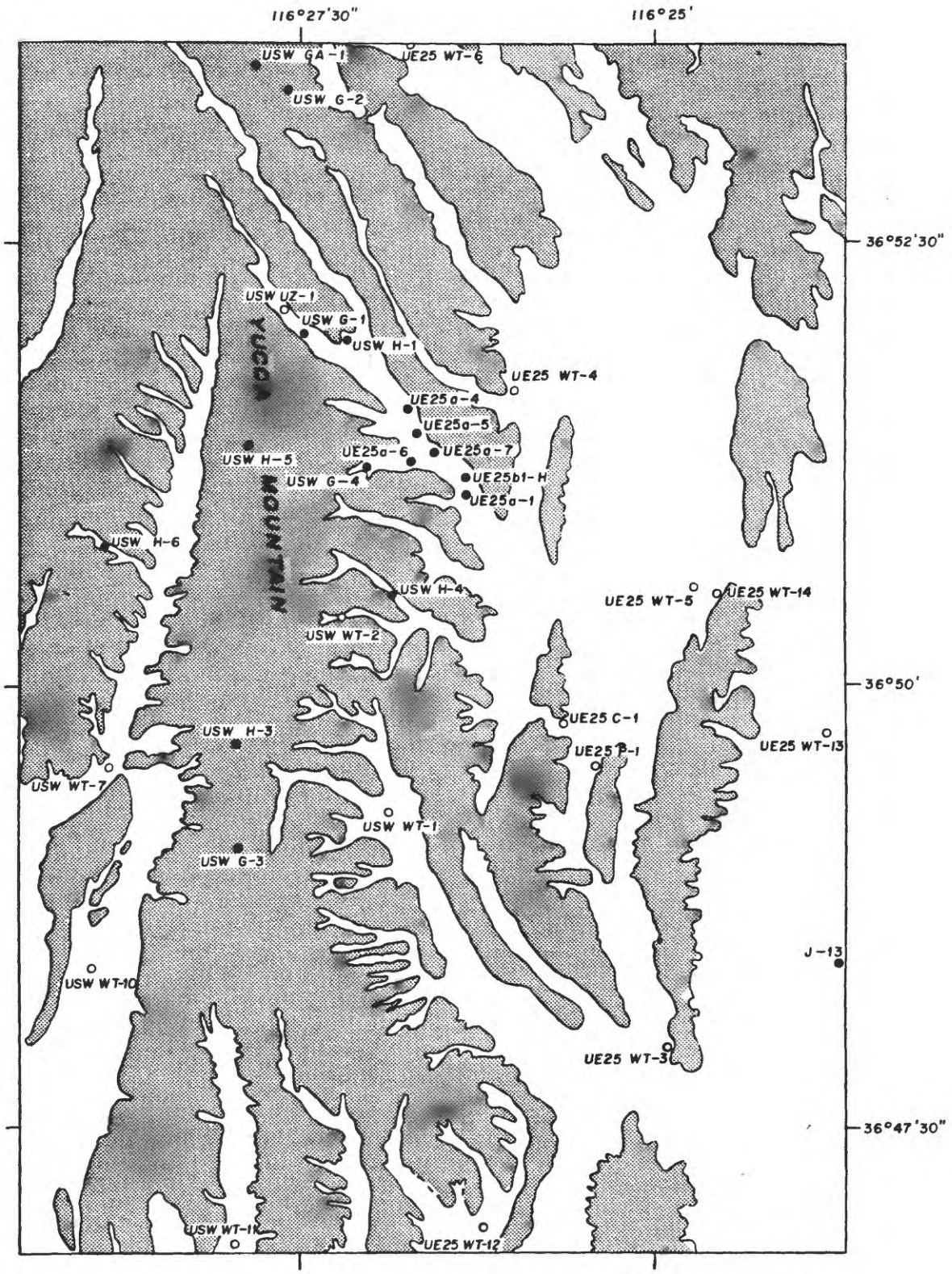

FIG. 22 LOCATION OF DRILL HOLES AT THE SITE.

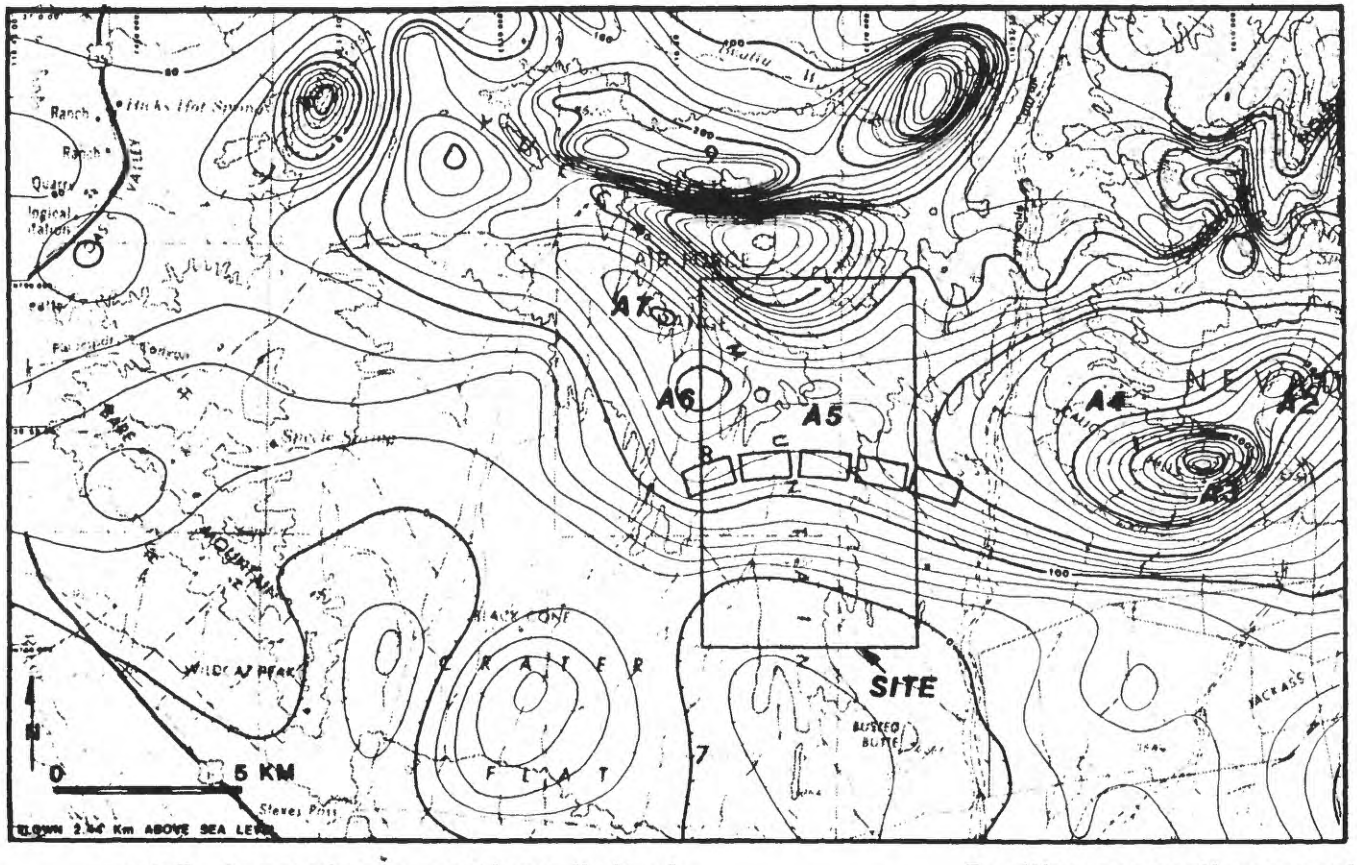

FIG. 23 INTERMEDIATE ALTITUDE AEROMAGNETIC MAP OF THE SITE AND SURROUNDING AREA. CONTOUR INTERVAL 20 GAMMAS

phosed Eleana Formation, extending westward from surface exposures in the Calico Hills to a subsurface level 900 m below sea level (2.2 to 2.4 km below the surface) under the northern part of the Site. They further suggest that the subvolcanic basement may contain deep-seated granitic rocks that provided a heat source for metamorphism, but there is no direct evidence of any such plutonic body.

A low-amplitude magnetic field occurs over the southern part of the Site (Figures 23; Bath and Jahren, 1984); relatively high gravity values over the southern part of the Site culminate in an elongate positive anomaly that trends southward from the southeast cover of the Site (Figure 24; Snyder and Carr, 1982). Snyder and Carr estimated a depth of between 1000 and 1200 m to pre-Cenozoic rocks at the culmination of this gravity high, which they interpreted as the signature of a relatively high-standing block of pre-Cenozoic rocks below the east edge of the Site. An exploratory drill hole (UE25p#1, Figures 22 and 24), completed in May 1983, was drilled to pre-Cenozoic rocks near the culmination of this positive gravity anomaly. This drill hole intersected dolomite at a depth between 1220 and 1250 m below the surface and continued in carbonate rocks to a total depth of 1806 m. Conodonts extracted from 6 core and cutting samples between the depths of 1319 and 1804 m are assigned Late Silurian ages (A.G. Harris, written commun., 1983). It is clear on the basis of this drill hole that at least part of the Site is underlain by Silurian carbonate rocks, which are part of the lower carbonate aquifer of Winograd and Thordarson (1975) (Figure 17). Relatively dense, nonmagnetic dolomite such as that encountered in drill hole UE25p#1 could produce the relatively high gravity and low magnetic values observed over much of the southern part of the Site, but a unique interpretation of the stratigraphy and structure of pre-Cenozoic rocks at the Site is not currently possible.

Volcanic Stratigraphy of the Site

Surface mapping and drill-hole data indicate that most volcanic units (Table 3) are continuous under the Site (Figure 25). However, lava and flow-breccia are fairly common in the subsurface in the north part of the Site but are rare to the south.

The rock being considered for a repository at Yucca Mountain is densely welded ash-flow tuff of the Topopah Spring Member of the Paintbrush Tuff. The

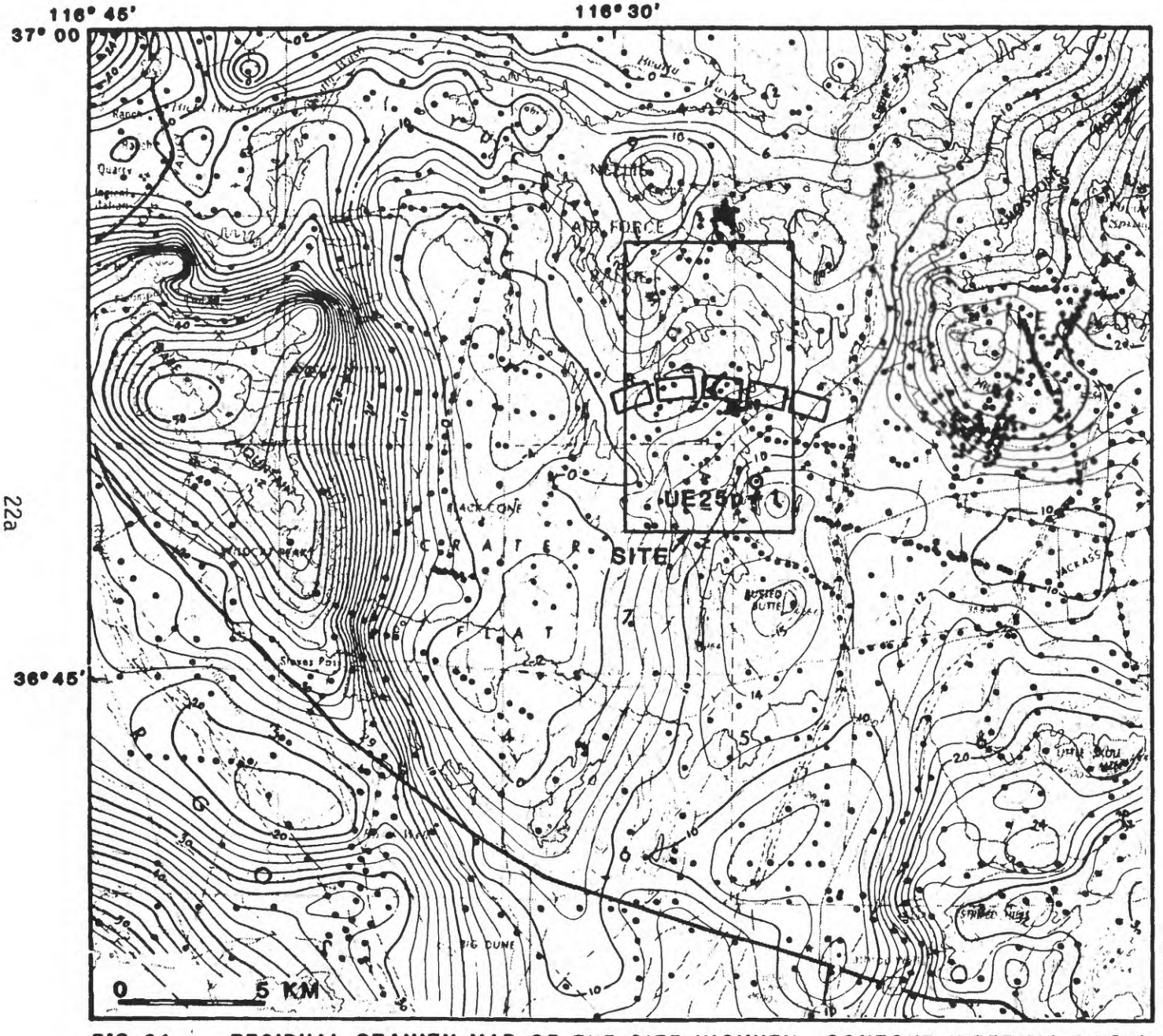

Approximate southern limit of magnetic anomaly from figure 3-25

⊙ UE25p#1

Drill hole to pre-Cenozoic rocks

Modified from Snyder and Carr (1982)

FIG. 24 RESIDUAL GRAVITY MAP OF THE SITE VICINITY. CONTOUR INTERVAL 2 mGal; REDUCTION AT 2.0g/cm

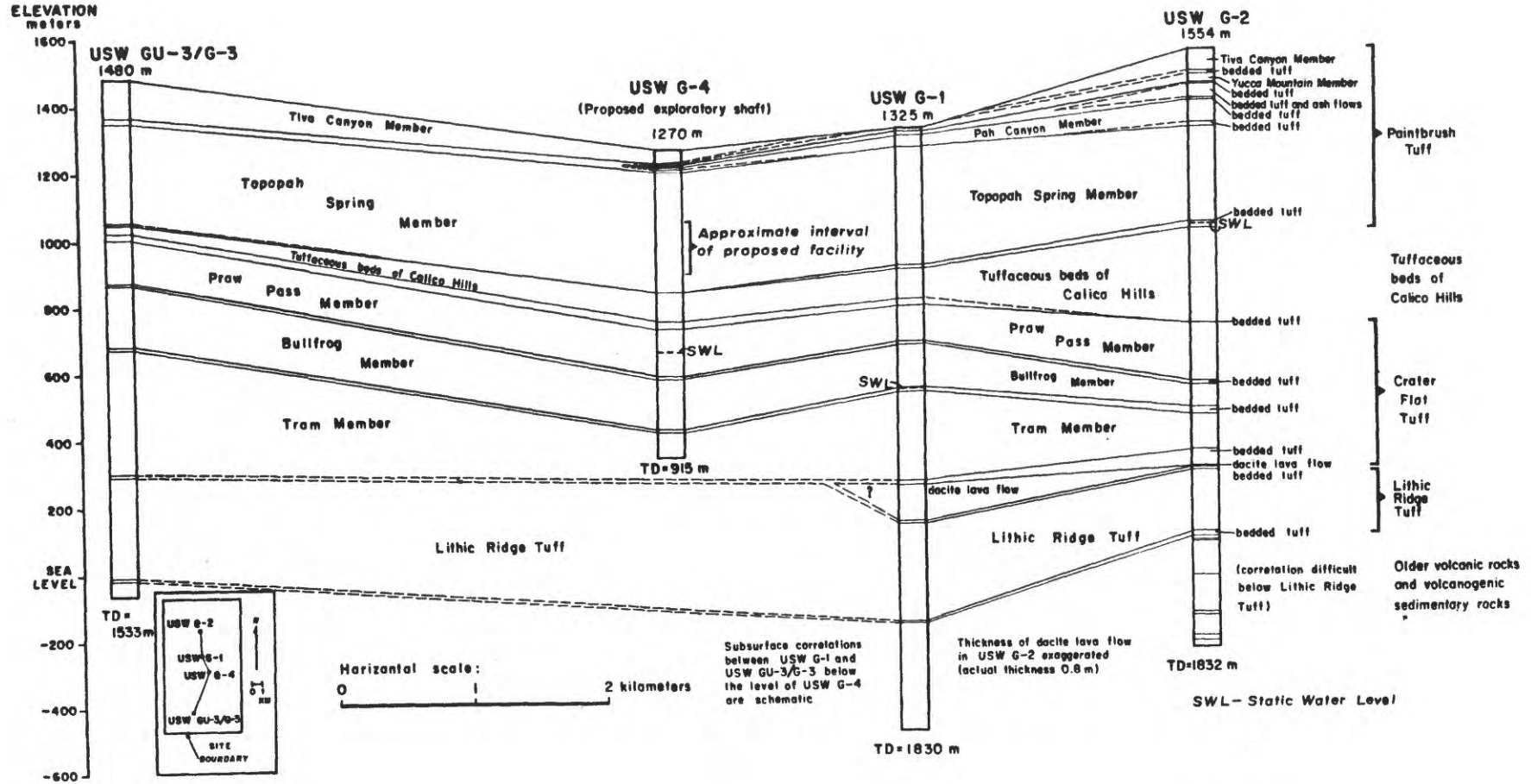

FIG. 25 STRATIGRAPHIC CORRELATION OF SELECTED DRILL HOLES AT THE SITE

genesis, emplacement, and crystallization history of an ash-flow cooling unit are briefly described here (see Smith, 1960, for detailed discussion). Ash flows are hot pyroclastic deposits, generally erupted from relatively shallow magma chambers. The eruptions are rapid and consist of a series of closely spaced pulses in which very hot, highly gas-charged, pumiceous ash clouds spread across the terrain, probably during collapse of the ascending eruptive column. If the glassy volcanic debris is sufficiently thick, sufficiently charged with volatiles, and hotter than approximately 500°C, it welds, by flattening of pumice and ash fragments, after coming to rest. The thicker or hotter ash flows may become densely welded, attaining densities of as much as 2.5 g/cm^3 with less than 10 percent porosity; colder or thinner flows may be unwelded or only partially welded with densities as low as 1.5 g/cm^3 and porosities as high as 40 percent. Nonwelded ash-fall tuff generally forms from the accumulation of cool, glassy ash settling out of ash clouds. A sequence of ash flows that cool together as a single unit has a secondary overprint of crystallization zones. Further alteration to secondary minerals such as clays and zeolites may result from interaction with groundwater, particularly in zones that are glassy or not densely welded.

The stratigraphy of the Site, determined on the basis of geologic mapping and drill core analysis, is summarized in table 3. An unconventional aspect of table 3 is its emphasis on bedded tuff. Intervals of this rock type, generally only a few meters thick but in places as much as 50 m thick, separate the welded tuff and other flow rock units. Poorly exposed and too thin to map at customary scales, the bedded tuff is nevertheless important to site characterization because its physical and chemical properties differ markedly from those of the flow rocks. Otherwise, stratigraphic nomenclature essentially conforms to that originally applied by Christiansen and Lipman (1965), Lipman and McKay (1965), Orkild (1965), and Byers and others (1976). Stratigraphic data obtained from the drill holes located on figure 22 are presented in detail by Spengler and others (1979b), Spengler and Rosenbaum (1980), and Spengler and others (1981), Maldonado and Koether (1983), Scott and Castellanos (1984), Spengler (written commun., 1983), and Rush and others (1983); the principal characteristics of the rocks are described below.

Older volcanic rocks and volcanogenic sedimentary rocks. The lowest rocks encountered in drilling, those beneath the Lithic Ridge Tuff, are difficult to correlate owing to their heterogeneity and varied degree of

TABLE 3

VOLCANIC STRATIGRAPHY AT THE SITE[a]

K-Ar Age (m.y.)	Magnetic Polarity[b]	Rock Unit	Range in Thickness (m)
10.2		Basalt dikes	
		* Timber Mountain Tuff	
11.3		* Rainier Mesa Member	0-46
		Bedded tuff	0-61
		* Paintbrush Tuff	
12.5	R	* Tiva Canyon Member	69-148
		Bedded tuff	1-15
	R	* Yucca Mountain Member	0-29
		Bedded tuff	0-47
	R	* Pah Canyon Member	0-71
		Bedded tuff	0-9
13.1	N	* Topopah Spring Member	287-359
		Bedded tuff	1-17
13.4[c]		Tuffaceous beds of Calico Hills	27-289
		Bedded tuff	0-21
		* Crater Flat Tuff	
	N	* Prow Pass Member	80-193
		Bedded tuff	2-10
13.5	N	* Bullfrog Member	68-187
		Bedded tuff	6-22
	R	* Tram Member	190-369
		Bedded tuff	3-50
	N	Dacite lava and flow breccia	0-249
		Bedded tuff	0-14
	I	* Lithic Ridge Tuff	
		Bedded tuff	3-7
13.9		Older volcanic rocks and volcanogenic sedimentary rocks	345+

[a] Names and rankings of some units do not conform to USGS usage. Formally recognized names are preceded by *.

[b] Magnetic polarity: N - normal, R - reversed, I - intermediate.

[c] Age determined on associated lava flow.

alteration; they are not known to crop out. Drill hole USW-G1 (Figures 22 and 25) penetrated 323 m of ash-flow tuff, interbedded with ash-fall tuff and reworked tuffaceous sediments. Most of the tuff is partially to moderately welded, and the tuffaceous sediments are moderately indurated. These rocks are altered and contain smectite (montmorillonite and related clays), analcime, and clinoptilolite, as well as traces of calcite and chlorite as alteration products (Spengler and others, 1981). Three subunits have been defined in drill hole USW-G1 on the basis of relative abundance of major minerals.

In drill hole USW-G2, 345 m of altered volcanic and volcanogenic rocks were penetrated below the bedded tuff beneath the Lithic Ridge Tuff. The sequence includes, in ascending order: (1) ash flow tuff--19 m; (2) bedded tuff, conglomerate and ash-flow tuff--17 m; (3) dacitic lava and flow breccia--66 m; (4) bedded and ash-flow tuff--10 m; (5) quartz latitic lava and flow breccia--132 m; and (6) rhyolitic lava and flow-breccia--101 m. These older rocks have not been correlated unequivicolly between USW-G1 and USW-G2; however, the lowest subunit in USW-G1 (subunit C of Spengler and others, 1981) may correlate with the uppermost ash-flow (4) in G2.

Lithic Ridge Tuff. A thick section of massive ash-flow tuff overlying the older ash-flow and bedded tuff has been named the Lithic Ridge Tuff (Carr and others, 1984). Its thickness ranges from 185 m (USW-G2) to 304 m (USW-GU3/G3). The unit is nonwelded to moderately welded and extensively altered to smectite clays and zeolites.

The Lithic Ridge Tuff is distinguished by a relatively low volume percentage of quartz phenocrysts (3-11 percent of total phenocrysts), notable amounts of sphene, and abundant lithic fragments including fragments of distinctive spherulitic rhyolite lava. Numerous slight variations in degree of welding, phenocryst ratios, and lithic fragment content suggest that the unit is the result of several eruptive surges.

Dacite lava and flow breccia. Dacitic lava and autoclastic flow breccia overlie the Lithic Ridge in deep holes in the northern and western parts of the Site but are absent elsewhere (Figure 25). Thickness of the unit is 22 m in drill hole USW-G2, 112 m in USW-H1, and 249 m in USW-H6. In drill hole USW-G1, most of the unit is flow breccia made up of angular to subangular fragments of dacite, commonly 2 to 10 cm long. The breccia is intercalated with a few lava flows 1 m to more than 17 m thick. In contrast, the unit in

USW-G2 consists largely of lava with flow breccia confined to the uppermost and lowermost parts.

The phenocryst content is variable, but mafic minerals, mostly hornblende and clinopyroxene, are prominent. Much of the unit is moderately to intensely altered to smectite clays and zeolites.

Crater Flat Tuff. Three rhyolitic ash-flow tuff sheets have been assigned to the Crater Flat Tuff on the basis of stratigraphic relations, petrography, and chemistry. They include, in ascending order, the Tram Member (Carr and others, 1984), the Bullfrog Member, and the Prow Pass Member (Byers and others, 1976).

The Crater Flat Tuff is distinguished from other units in the Site Vicinity by the relative abundance of quartz and biotite phenocrysts. In addition, the Prow Pass Member and, to a lesser degree, the Bullfrog Member contain distinctive reddish-brown mudstone lithic inclusions.

The ash-flow tuff part of the Tram Member ranges in thickness from 104 m (USW-G2) to 369 m (USW-GU3/G3), is moderately welded to nonwelded, and is underlain by 3 to 50 m of reworked and bedded tuff. The average phenocryst content is approximately 11 percent, of which approximately 30 percent is quartz. It is distinguished from many other tuffs by its reversed remnant magnetization (Table 3).

Two subunits are distinguished within the Tram on the basis of the relative abundance of lithic fragments; the lower subunit is lithic rich and the upper is lithic poor (Spengler and others, 1981). South and east of USW-G1, more than two-thirds of the basal part of the lower subunit characteristically contains zeolite minerals including clinoptilolite, mordenite, and analcime. Other alteration products include smectite, calcite, kaolinite and, in places, pyrite. The upper 20 m (UE25b-1H) to 65 m (USW-G1) of the lower subunit have less secondary alteration but approximately the same lithic content as the basal part. In drill hole USW-G1, the upper part of the lower subunit contains 10 to 15 percent smectite and 10 to 15 percent zeolites, including clinoptilolite, mordenite, and analcime. Inclusions of lava fragments constitute as much as 33 percent of the rock volume.

The upper subunit of the Tram, 126 to 171 m thick, is partly welded and has a microcrystalline groundmass. Zeolite and clay minerals are scarce or absent, and lithic fragments commonly constitute less than 5 percent of the rock.

Conspicuous differences in parts of the Tram are recognized in drill hole USW-G2 (Maldonado and Koether, 1983). The upper subunit described above is absent in USW-G2. The uppermost interval in USW-G2, 46 m thick, contains 50 to 95 percent lithic fragments of tuff and lava of both rhyolitic and intermediate composition. The abundance of lithic fragments nearly masks the pyroclastic texture. The lithic-rich interval rests gradationally above ash-flow tuff with 10 to 30 percent lithic fragments. The lateral stratigraphic relations between the Tram in drill hole USW-G2 and the lower two subunits of the Tram in USW-G1 are not known. Detailed study of the Tram in USW-GU3/G3 suggests that it comprises 28 separate magmatic pulses (Scott and Castellanos, 1984).

The Tram is separated from the overlying Bullfrog Member by 6 to 22 m of bedded and reworked tuff.

The ash-flow tuff comprising most of the Bullfrog is 68 m (USW-G2) to 187 m (USW-GU3/G3) thick. In northern drill holes it seems to be a simple cooling unit in which nonwelded to partially welded zones enclose a moderately welded core, but in the south (USW-GU3/G3) it is compound, split by a 1 m-thick bed of sedimentary tuff. Most of the upper part of the member is devitrified or shows evidence of vapor phase crystallization. In drill holes USW-G1 and USW-G2, the upper part of the unit is partially altered to zeolites and (or) clay; in UE25b1-H, only the lower 21 m have been slightly altered to clay.

As much as 10 m of ash-fall tuff and tuffaceous sediments, which are commonly zeolitized, separate the Bullfrog from the overlying Prow Pass Member.

The ash-flow tuff of the Prow Pass Member, 80 m (USW-H6) to 193 m (USW-G2) thick, is similar in appearance and petrography to the Bullfrog, but the two members are distinguished because (1) mudstone fragments in the Bullfrog are fewer and smaller than in the Prow Pass and occur in equal amounts with rhyolitic lava fragments; and (2) the Bullfrog contains more biotite and hornblende. The Prow Pass is also distinguished from other units of the Crater Flat Tuff by its orthopyroxene and by extreme resorption of quartz phenocrysts. Phenocryst content is approximately 10 percent, mostly potassium feldspar and plagioclase. Generally, the Prow Pass is devitrified and only slightly welded, and locally it is zeolitized. The top and bottom parts are commonly altered to clay and zeolites. A zone of slight to intense zeoliti-

zation and silicification, 25 to 55 m thick, occurs in the lower part, except in drill holes USW-G1 and USW-GU3/G3. The upper part of the Prow Pass is vitric to partly vitric in several holes.

A sequence of ash-fall tuff, reworked tuff, and tuffaceous sandstone as much as 20 m thick separates the Crater Flat Tuff from the overlying tuffaceous beds of the Calico Hills.

Tuffaceous Beds of Calico Hills. In outcrop, the tuffaceous beds of the Calico Hills comprise a sequence of ash-flow and ash-fall tuff, volcaniclastic sediment, and rhyolitic lava (McKay and Williams, 1964). At the Site, the Calico Hills unit consists of massive, homogeneous, nonwelded ash-flow tuffs totaling 27 m (USW-H3) to 289 m (USW-G2) thick, which are separated in places by ash-fall and reworked tuff beds as much as 4 m thick. The nonwelded tuff is mostly crystal poor (less than 5 percent), but locally it is rich in lithic fragments, some as much as 6 cm long. In the northern part of the Site, the entire unit is zeolitized but it remains vitric in the south (USW-GU3/G3). Zeolites (predominantly clinoptilolite and mordenite) constitute 60 to 80 percent of the rock volume (Spengler and others, 1979b; Spengler and others, 1981).

Ash-fall and reworked tuff beds 1 to 17 m thick separate the tuffaceous beds of the Calico Hills from the overlying Paintbrush Tuff.

Paintbrush Tuff. The Paintbrush Tuff, more than 460 m thick, makes up nearly all of the exposed rocks at Yucca Mountain (Lipman and Christiansen, 1964; Orkild, 1965; Lipman and others, 1966; Byers and others, 1976).

The four members in ascending order are: (1) Topopah Spring, (2) Pah Canyon, (3) Yucca Mountain, and (4) Tiva Canyon. The Topopah Spring and Tiva Canyon Members consist predominantly of densely welded, devitrified ash-flow tuffs that enclose between them a sequence of nonwelded to partially welded ash-flow tuff and tuffaceous sediments that includes the Pah Canyon and Yucca Mountain Members. The Pah Canyon and Yucca Mountain Members are thickest in the northwest part of the Site, thinning southeastward.

The ash-flow tuff of the Topopah Spring Member, 287 m (drill hole USW-G2) to 369 m (drill hole USW-H1) thick, is the thickest and most extensive member of the Paintbrush Tuff. As this unit is the potential medium for a repository it is discussed in some detail.

The Topopah Spring is a compound cooling unit with a nonwelded, glassy base and top that grade abruptly inward through zones of partial welding into

a thick, densely welded, devitrified center. The nonwelded to partially welded glassy base grades upward into a black, densely welded vitrophyre commonly about 14 m thick. Phenocryst content generally is less than 5 percent, although it attains 17 percent near the top. It is the only member of the Paintbrush Tuff lacking accessory sphene and having normal thermal remnant magnetization (Byers and others, 1976, p. 25).

A thick interval of densely welded, rhyolitic, phenocryst-poor tuff gradationally overlies the vitrophyre in the central part of the Topopah Spring. This densely welded tuff contains 2 or 3 distinctive subunits that have abundant lithophysal (gas) cavities. Such cavities comprise as much as 30 percent of the total volume in northern drill cores but decrease in abundance southward. The cavities are spherical to lenticular and in core specimens are as large as 7.5 cm near the middle of each subunit, gradationally decreasing in size and abundance toward subunit boundaries. (Cavities as large as 20 cm have been found in outcrops.)

Near its top, the Topopah Spring contains a quartz-latitic, phenocryst-rich (about 17 percent) zone, approximately 6 m thick, known as the caprock. The caprock is overlain by vitrophyre as much as 1 m thick, which is in turn overlain by 1 to 12 m of glassy, nonwelded to partially welded tuff. Superimposed across zones of similar welding characteristics are zones of devitrification and vapor-phase crystallization (Lipman and others, 1966).

The Pah Canyon and Yucca Mountain Members are relatively thin, nonwelded ash-flow tuffs which are the distal edges of flow sheets that thicken to the northwest (Lipman and Christiansen, 1964; Orkild, 1965). The Pah Canyon attains a maximum thickness of 71 m, the Yucca Mountain 29 m. The Pah Canyon contains 5 to 15 percent phenocrysts, mainly alkali feldspar, plagioclase, and biotite. In contrast, the overlying Yucca Mountain Member is a distinctively uniform, shard-rich tuff containing small amounts of pumice, phenocrysts, and lithic fragments.

The uppermost unit of the Paintbrush Tuff in the Site, the Tiva Canyon Member, is 90 to 140 m thick in outcrop. It is a multiple-flow, compound cooling unit made up of ash flows that erupted approximately 12.5 m.y. ago from the Claim Canyon caldera segment north of Yucca Mountain (Lipman and others, 1966; Byers and others, 1976). The Tiva Canyon is almost entirely densely welded and forms most of the surface of Yucca Mountain. The phenocryst mineralogy of the Tiva Canyon is similar to that of the Topopah Spring,

with the notable exception that sphene is present as a phenocryst mineral in the Tiva Canyon. The Tiva Canyon is compositionally zoned in a manner similar to the Topopah Spring. Ten mappable units are distinguished in the Tiva Canyon. These units are informally designated in ascending order: (1) columnar, (2) hackly, (3) lower lithophysal, (4) red clinkstone, (5) gray clinkstone, (6) rounded step, (7) lower cliff, (8) upper lithophysal, (9) upper cliff, and (10) caprock (Scott and others, 1983). The rounded step subunit is laterally equivalent to the combined red and gray clinkstone subunit.

The Tiva Canyon thickens southward from approximately 90 m to nearly 140 m, then thins again to 125 m in the southernmost part of the area. Within the Tiva Canyon, the relative proportion of the total unit represented by the thicknesses of the two lithophysal subunits decreases southward from approximately 30 percent to 10 percent. As the lithophysal zones thin, the nonlithophysal zones thicken.

Timber Mountain Tuff. The Rainier Mesa Member (11.3 m.y. old) of the Timber Mountain Tuff is locally present in valleys on the flanks of Yucca Mountain (Figures 3 and 5). It unconformably overlies downfaulted blocks of the Paintbrush Tuff but was either not deposited on or was removed by erosion from the top of the higher-standing fault blocks that form most of Yucca Mountain.

At the Site, the Rainier Mesa Member has a maximum thickness of approximately 46 m. It is nonwelded and glassy at the base, grading upward into partly welded devitrified tuff near the interior. Phenocrysts (10 to 25 percent) are mainly quartz and alkali feldspar, with some plagioclase and biotite (Lipman and McKay, 1965).

Basalt. The youngest volcanic rocks at Yucca Mountain (10 m.y. old) are basalt dikes less than 1 m thick that intrude a fault and nearby fractures at the head of Solitario Canyon in the northwest part of the Site (Figure 3). The basalt is very fine grained and locally vesicular, with sparse microphenocrysts of olivine, plagioclase, and rare clinopyroxene grading into a microlitic groundmass. The basalt was brecciated near it margins by later movement along the fault.

Surficial Deposits

Surficial deposits have been divided into four general units by Hoover and others, (1981) on the basis of physical properties and geomorphic characteristics. These characteristics include: (1) topographic position, (2) drainage development, (3) soil profile development, (4) variations in desert pavement, (5) lithology, and (6) interpreted depositional environment. The stratigraphy of these units was previously summarized in figure 21. This stratigraphy implies four general episodes of basin aggradation separated by episodes of protracted erosion. The general ages of the units have been interpreted from uranium-trend dates, an experimental isotopic dating technique (Rosholt, 1980) and correlation of intercalated volcanic ash deposits with ash deposits that have yielded conventional isotopic dates (Table 2). The rates of deposition and lengths of time represented by unconformities are not known.

TECTONIC AND VOLCANIC FRAMEWORK OF THE CANDIDATE AREA

Pre-Cenozoic Tectonism

The major elements of the pre-Cenozoic tectonic framework of western North America have been concisely summarized by Burchfiel and Davis (1975), among others. Only those events affecting the tectonic history of the Candidate Area are summarized here.

The earliest recognized phase of tectonism in the Candidate Area is recorded in Lower and Middle Proterozoic rocks in the Death Valley area. This tectonism, metamorphism, and igneous activity occurred over a long period of geologic time, generating the Precambrian crystalline rocks that form the stratigraphic basement for stratified rocks throughout the region.

Complex rifting began in the Middle Proterozoic ultimately resulting in the establishment of a passive continental margin along the western edge of North America in latest Proterozoic time. The rifted margin controlled patterns of latest Proterozoic and early Paleozoic sedimentation.

The passive margin persisted until Late Devonian time when compressive tectonism, the Antler orogeny, affected much of the western margin of North America. During the Antler orogeny, lower and middle Paleozoic rocks from the outer continental-shelf to the deep-ocean floor were thrust eastward on a complex system of low-angle faults over the western part of the continental shelf. The resulting thrust complex formed a highland along the continental margin that, during Mississippian time, shed clastic material eastward into a marine foreland basin occupying the area of the former inner continental shelf. The axis of the Mississippian sedimentary basin passes through the Candidate Area (Figure 18). Renewed stability in the area of the continental shelf during the Pennsylvanian and Early Permian resulted in the deposition of a thick sequence of carbonate rocks in the Candidate Area.

Beginning in the Late Permian (approximately 250 m.y. ago) and continuing through the Mesozoic (65 m.y. ago), the western edge of North America evolved into an active continental margin, characterized by the convergence of lithospheric plates and accretion of new magmatic and tectonic terranes by processes related to plate subduction (Davis and others, 1978; Hamilton, 1978). The style of tectonic activity varied along the continental margin through late Paleozoic and earliest Mesozoic time, but by the Late Triassic, the

margin was undergoing "similar magmatic, sedimentary, and metamorphic phenomena along its entire length--a consequence of oblique(?) convergence and subduction of Pacific Ocean lithosphere" (Davis and others, 1978, p. 9).

The details of the tectonic processes and events occurring along the continental margin during the Mesozoic are not important here, because the Candidate Area lay farther inland. Tectonism along the margin, however produced a broad belt of deformation, igneous activity, and metamorphism within the adjacent continent (Figure 26). Pre-Cenozoic rocks in the southwest part of the Candidate Area are part of a mobile belt of deformation, metamorphism, and igneous activity that evolved through Mesozoic time. Rocks deformed and metamorphosed at mid-crustal levels during the Mesozoic are now exposed in the Death Valley area. Rocks deformed within the upper few kilometers of the crust contain brittle structures such as folds and thrust faults, and rocks deformed at deeper crustal levels contain ductile folds and strong penetrative metamorphic fabrics.

A broad belt of granitic plutons passes through the southwest part of the Candidate Area. The ages of these plutons span most of Mesozoic time. Mid-Cretaceous granitic rocks (Naeser and Maldonado, 1981) are exposed in three of the ranges around Yucca Flat, 50 km northeast of the Site. These granitic rocks lie along an east-trending aeromagnetic anomaly and were interpreted by Hinrichs (1968) and Bath and others (1983) as upward protrusions from a large east-trending pluton. A similar east-southeast trending positive aeromagnetic anomaly (Figure 23) was interpreted by Bath and others, (1983) as evidence that another granitic complex underlies part of Yucca Mountain, Calico Hills, and Wahmonie (Figure 3). The only exposures of granitic rocks associated with this magnetic anomaly are at Wahmonie, where the intrusives are of Tertiary age (Ekren and Sargent, 1965). As discussed previously, the anomaly shown on figure 23 also was interpreted as evidence that metamorphosed Eleana Formation underlies the northern part of the Site (Bath and Jahren, 1984).

East of the belt of Mesozoic metamorphism and plutonism, Paleozoic continental-shelf rocks were deformed in a broad foreland fold and thrust belt that formed in the late Mesozoic. The locus of thrust faulting in the foreland thrust belt generally progressed eastward with time through the late Mesozoic, and the youngest, easternmost thrusts form a continuous zone along the western margin of the Paleozoic cratonic platform east of the Candidate Area (Figure 26). This folding and thrust faulting redistributed some of the Proterozoic and Paleozoic clastic and carbonate rocks in the Candidate Area.

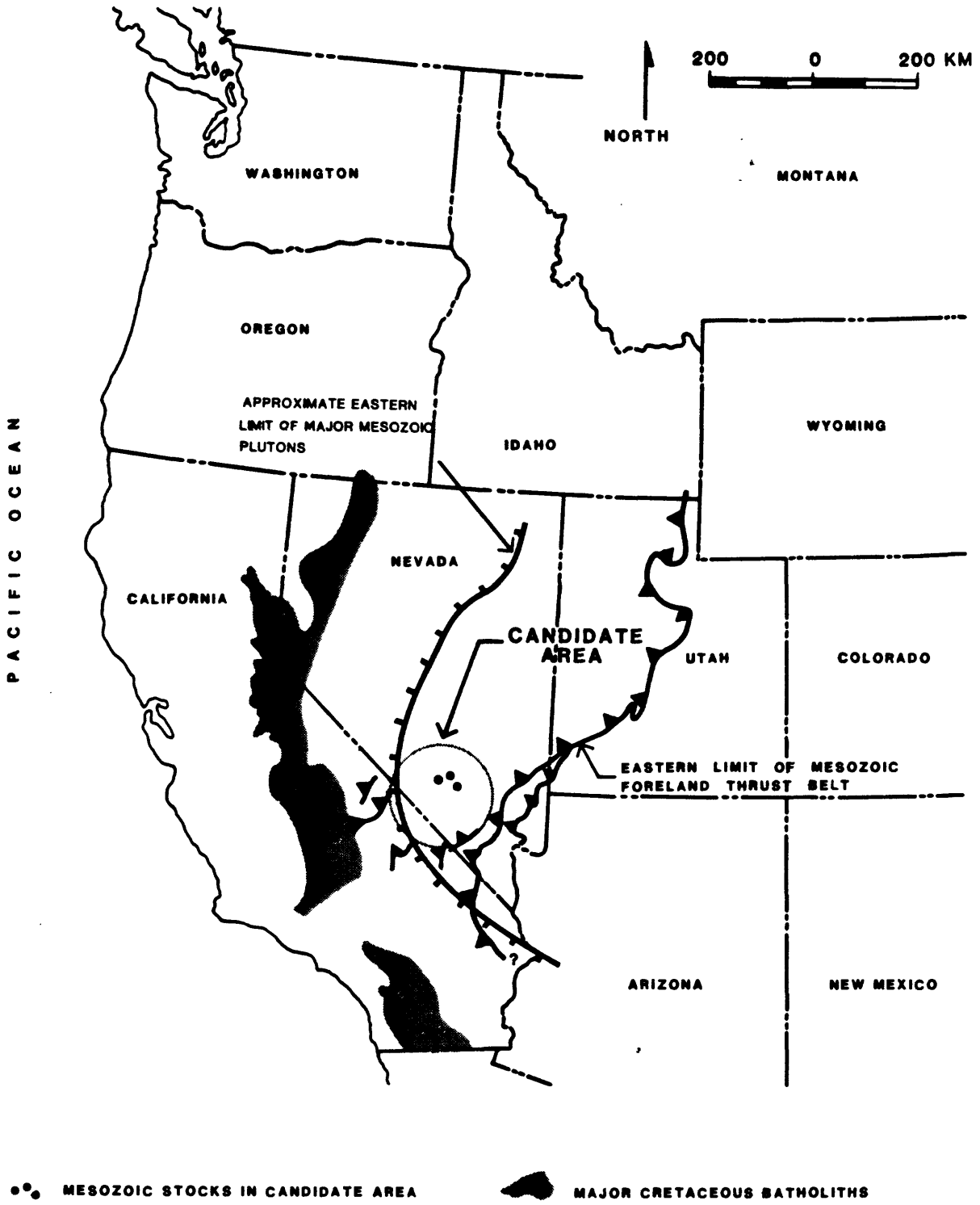

FIGURE 26
MESOZOIC TECTONIC ELEMENTS EAST OF SIERRA NEVADA BATHOLITH

The geometry and distribution of the thrust faults passing through the Candidate Area are poorly known because of discontinuous exposure. Numerous short segments of gently dipping faults are exposed in the eastern and central parts of the Candidate Area and in northern Death Valley, but some of these faults are now recognized as Tertiary low-angle normal faults formed during extensional tectonism. Others are of uncertain origin. Several systems of known and presumed Mesozoic thrust faults, placing Upper Proterozoic and lower and middle Paleozoic rocks over rocks as young as Permian, pass through the Candidate Area. Segments of thrust faults are exposed along the west side of Yucca Flat, in the Spotted Range, Specter Range, Calico Hills, at Bare Mountain, and in the northern Death Valley area (Figure 3; Jennings, 1977; Stewart and Carlson 1978). Laterally continuous thrust faults are exposed in the northern Spring Mountains and in the Nopah and Resting Spring Ranges (Burchfiel and others, 1974, 1982).

Folds are also important in influencing the distribution of pre-Cenozoic rocks. Folds vary widely in form, size, and distribution. In the ranges surrounding Yucca Flat, large overturned folds are associated with thrust faults. At Bare Mountain, 20 km west of the Site, much of the upper Precambrian and Paleozoic section is steeply dipping to overturned below a major thrust fault, which itself appears to be broadly folded. The timing of these folds relative to the thrust faulting is not known. Outcrop-scale, ductile folds are common in metamorphosed rocks in the northwest part of Bare Mountain; these small folds have no effect on the distribution of major stratigraphic sequences, but they may be related to larger scale folding that does affect map patterns in the area. Work in progress is attempting to delineate folds in the pre-Cenozoic rocks beneath the Site Vicinity. However, only broad patterns are likely to be established within the limits of practical subsurface exploration.

Cenozoic Tectonism

The most conspicuous structural features of the Candidate Area are the block-faulted basins and ranges and associated strike-slip faults produced by crustal extension (Figure 27). Most of this faulting occurred during the late Cenozoic and some is historic.

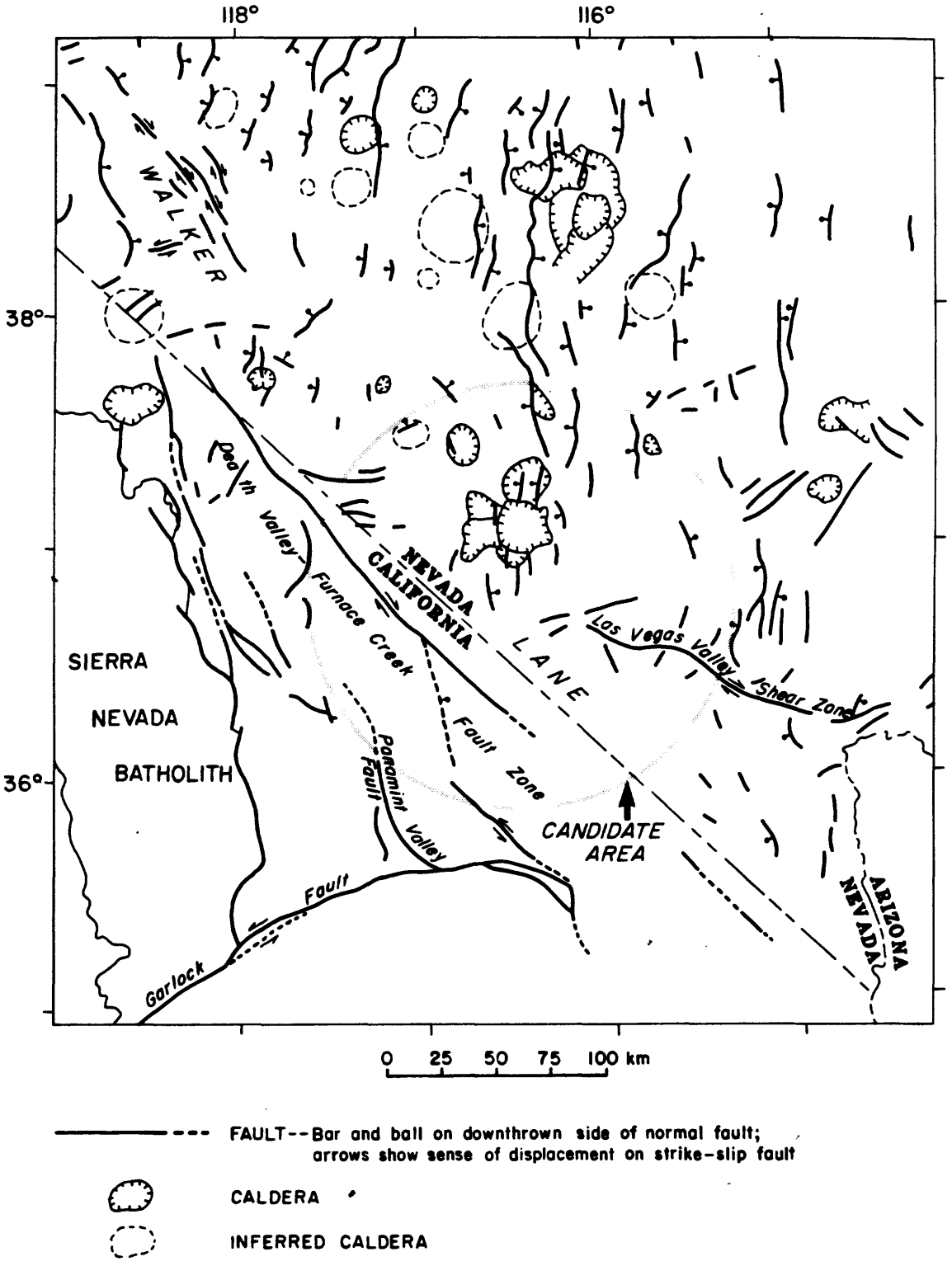

FIG. 27 --SIMPLIFIED MAP OF MAJOR CENOZOIC TECTONIC FEATURES IN THE SOUTHWESTERN GREAT BASIN.

No record of Paleocene or Eocene tectonism in the Candidate Area has been identified because no rocks of that age are exposed. This was the time of the well-known Laramide deformation in the Rocky Mountain region, several hundred kilometers to the northeast, and a pronounced hiatus in magmatism in the Great Basin (Burchfiel and Davis, 1975; Cross and Pilger, 1978; Dickinson, 1981). Sparse direct evidence for early Tertiary faulting and folding in east-central and northeastern Nevada demonstrates at least local tectonic activity in the Great Basin during that time, but the setting and regional extent of that deformation are unknown. The absence of early Tertiary deposits suggests that much of the area was then elevated and undergoing erosion (Stewart, 1980).

During late Eocene to early Miocene time a northwest-trending belt of volcanism, approximately 200-km wide, was gradually established across the Great Basin, including the northeastern part of the Candidate Area. Little or no contemporary tectonic deformation seems to have occurred however, as the ash-flow sheets erupted during this time display little or no angular discordance and have lateral continuity (Stewart, 1980). Much of the local deformation of middle Tertiary ash-flow units is attributed by Stewart to caldera structure. The earliest indication of Cenozoic tectonism in the Candidate Area is also based on indirect evidence. Tectonically generated coarse conglomerate and monolithologic breccia in the early Oligocene Titus Canyon Formation, occurring along the northeast flank of the Grapevine Mountains 30 to 40 km southwest of the Site, were recognized by Cornwall and Kleinhampl (1964) and Reynolds (1969). These deposits were interpreted as evidence of early Oligocene normal faulting by Reynolds (1969). The areal extent and significance of such faulting is unknown, but Reynolds suggested that despite local faulting between Cretaceous and early Miocene time, erosion and sedimentation resulted in a progressive reduction of topographic relief that was not renewed by major faulting during that period.

Extensional tectonism may have occurred continuously in the Basin and Range since late Eocene or early Oligocene time, but a distinction between extensional tectonism and Basin-and-Range faulting has been emphasized by Zoback and others (1981). Two important extensional phases that overlap in time have been identified in the history of the Basin-and-Range: (1) older extensional faulting, associated with voluminous silicic volcanism, from latest Eocene to middle Miocene time (Crowe, 1978; Dickinson and Snyder, 1979) and (2) Basin-and-Range faulting, middle Miocene and younger, which controls

the present-day topography of the Basin-and-Range Province (Stewart, 1978). The time of the onset of Basin-and-Range faulting is uncertain and may vary from place to place.

A change in the plate tectonic configuration of the western continental margin of the United States that began in the late Oligocene or early Miocene had a profound effect on both tectonism and volcanism in the Great Basin (Atwater, 1970; Christiansen and McKee, 1978). The late Mesozoic and early Tertiary pattern of oblique plate convergence and subduction of oceanic crust relatively eastward beneath the continental margin gradually evolved into a transform configuration characterized by right-lateral, strike-slip movement on northwest-trending faults, such as the San Andreas fault system. The complex extension and widespread right-lateral shear that characterized the Great Basin during the late Tertiary began at the same time as the reordering of the continental margin and continues at the present.

Structures characteristic of Basin-and-Range extension in the Candidate Area include 1) block-faulted basins and ranges, 2) major zones of strike-slip faulting, 3) low-angle normal faults, and 4) major detachment faults, which are gently dipping surfaces along which rocks deformed at strikingly different crustal levels in the geologic past are now juxtaposed through processes of crustal extension (See Crittenden and others, 1980; Wernicke, 1981; and Hamilton, 1982 for discussions of detachment faulting and crustal extension). All of these structures appear to be complexly interrelated both in time and areal distribution. Structures related to caldera collapse developed locally through most of the Miocene. The similar timing and areal distribution of extensional tectonism and Cenozoic volcanism in the Great Basin suggest a common tectonic control, but spatial and temporal relationships between faulting and volcanism are difficult to demonstrate.

Basin-and-Range block faulting has occurred in the southern, eastern, and northernmost parts of the Candidate Area (for example the Nopah, Resting Spring, Desert, Pintwater, Pahranagat, and Belted Ranges and adjacent basins) and at Yucca Mountain. Basin and Range structures also occur in the Death Valley area, but their tectonic setting may differ from that of the other areas, as discussed below.

Three models proposed to explain the structure of Basin-and-Range block faults were summarized by Stewart (1978). The block faults have been interpreted as: (1) horst-and-graben structures, (2) tilted blocks bounded by

planar faults, and (3) rotated blocks bounded by downward flattening (listric) fault planes. Zoback and others, (1981) reviewed the evidence for each model. As Stewart (1978) pointed out, Basin-and-Range blocks are not rigid coherent masses formed by vertical movement along profound rangefront faults, but are broken to varied degrees by faults distributed throughout the blocks. Yucca Mountain is a typical example of such a structural style.

Rangefront faults may form on one or both sides of a mountain block. Mountain blocks generally rotate between 0° and 30° from horizontal but locally beds dip steeply or even are overturned. Structural relief between adjacent Basin-and-Range blocks is commonly between 2 and 5 km. Frontal faults predominate but blocks can be internally faulted as well.

Strike-slip faults are also important in the tectonic framework of the Great Basin. A major northwest-trending belt of right-lateral strike-slip faults, called the Walker Lane, disrupts the regional structural grain in the southwestern part of the Great Basin along the California-Nevada border (Figure 27) (Locke and others, 1940; Longwell, 1960; Stewart, 1967, 1978). The marked curvature near this belt of many of the otherwise northerly trending structures and ranges in the southern Great Basin has been attributed to bending along the belt (Albers, 1967). Total displacement along the Walker Lane, which occurs in part as fault slip and in part as bending, may be 130 to 190 km (Stewart and others, 1968). Timing of the bending and shearing is uncertain. They may have begun as early as the Jurassic (Albers, 1967) or after deposition of the 29 m.y. old Horse Spring Formation (Ekren and others, 1968), but movement related to extensional tectonism was restricted to Cenozoic time. Some shear zones considered to be part of the Walker Lane are covered by undeformed upper Miocene or Pliocene volcanic rocks. Elsewhere within the belt, Pliocene and Quaternary deposits are displaced by strike-slip faults (Albers, 1967). Much of the uncertainty surrounding the age of displacement along the Walker Lane arises from the complex history of the belt and uncertainty as to which structural features in the southern Great Basin should be considered part of the Walker Lane.

A concealed zone of right-lateral strike-slip faulting, called the Las Vegas Valley shear zone, was postulated by Longwell (1960) to explain bending and offset of pre-Cenozoic rocks and structural features across the Las Vegas Valley in the southeast part of the Candidate Area. The total displacement along the Las Vegas Valley shear zone has been estimated to be between 44 and

69 km; 21 km or more of the displacement can be attributed to bending observed in the mountain ranges north and south of Las Vegas Valley (Wernicke and others, 1982). Displacement across the shear zone probably occurred between 15 and 11 m.y. ago according to Fleck (1970) and Anderson and others (1972).

The Death Valley and Furnace Creek faults are major en echelon strike-slip faults that form a northwest-trending zone of right-lateral shearing, 300 km long, in the southwest part of the Candidate Area (Stewart, 1967). Right-lateral displacement along the Death Valley-Furnace Creek fault system has been estimated to be between 10 and 80 km (Stewart and others, 1968). Movement along the Death Valley-Furnace Creek fault zone may have begun as early as middle Miocene time (Reynolds, 1974a). The present topographic relief of Death Valley is largely the result of fault movement from Pliocene time to the present (Reynolds, 1969, 1974a; Brogan, 1979).

Two sets of strike-slip faults occur in the central part of the Candidate Area: (1) northeast-striking faults with small left-lateral offsets, and (2) northwest-striking faults or flexure zones of right-lateral offsets or bending (Poole and others, 1965; Ekren and others, 1968, 1971; Carr, 1974). The northwest-striking, right lateral faults, which are parallel to the trend of the Walker Lane, are apparently complementary to the northeast-striking, left-lateral faults, such as the Cane Spring and Mine Mountain fault systems (Figure 3). Movement along the two sets of faults, active about 17 to 11 m.y. ago, appears to have been contemporaneous. Near Frenchman Flat, 50 km east of the Site, a prominent system of north- to north-northwest-striking Basin-and-Range faults (Stewart and Carlson, 1978), which probably formed more than 14 m.y. ago (Barnes and others, 1965; Byers and Barnes, 1967), curves to the southwest in harmony with the curvature typical of the Walker Lane. Paleozoic rocks and the Mesozoic thrust belt are also rotated in a manner consistent with right-lateral shearing.

Gently dipping faults separating younger rocks above from older rocks beneath and involving both Paleozoic and Cenozoic rocks occur in many parts of the Candidate Area. Such structures are well developed at Bare Mountain, 20 km west of the Site (Figure 3; Cornwall and Kleinhampl, 1961), in the eastern part of the Candidate Area (Guth, 1981), and in the Death Valley area (Hunt and Mabey, 1966; Jennings, 1977). Most of these structures are Cenozoic in age and are related to Cenozoic extension.

The relation between normal and strike-slip faulting in the Candidate Area is controversial. The late Cenozoic deformation of the entire Basin and Range has been attributed to a diffuse zone of transform displacement between the Pacific plate and stable North America (Atwater, 1970; Christiansen and McKee, 1978). An intracontinental transform origin for the Las Vegas Valley shear zone has been postulated by Fleck (1970), Davis and Burchfiel (1973), and Guth (1981). Movement along the Las Vegas Valley shear zone was interpreted by Guth (1981) as accommodating the different amounts of extension that have occurred during the Miocene in the block-faulted terrane to the north and the relatively unextended Spring Mountains to the south. Zones of right-lateral shear in the Great Basin have also been interpreted as wrench faults, which are regarded as the cause rather than the consequence of block faulting (see Stewart, 1978 for a review). The block faulting that formed the deep central part of Death Valley was attributed by Burchfiel and Stewart (1966) to local oblique extension necessary to accommodate the en echelon arrangement of the Death Valley and Furnace Creek faults in a right lateral shear system.

The amount of late Cenozoic extension in the Basin and Range has been estimated by Hamilton and Myers (1966), to be between 50 and 100 km or an 8% to 18% increase over the original width. These authors suggested that if inferred early and middle Cenozoic extension is considered and if faults flatten with depth, a more realistic estimate of the total Cenozoic extension may be 300% or more. Between 10 and 20% late Cenozoic extension was proposed by Stewart (1971), whereas total extension in the southern Great Basin of at least 65% and possibly as much as 80 to 100% was suggested by Wernicke and others, (1982).

The extension was not evenly distributed in the Candidate Area. Extension of 30 to 50% in parts of Death Valley was estimated by Wright and Troxel (1973). Extension between the Sheep Range at the eastern edge of the Candidate Area and the Pintwater Range is estimated to be about 80%, and local extension of as much as 150% may have occurred in the Desert Range (Guth, 1981). No significant Cenozoic extensional features have been mapped within the northern Spring Mountains (Burchfiel and others, 1974; Guth, 1981). Considerable block and strike-slip faulting has occurred west of the Spring Mountains in the southern part of the Candidate Area (Burchfiel and others, 1983), although no estimate of extension has been made for that area. Neither have any estimates been made for extension in the central part of the Candidate Area.

Extensional tectonism in the Great Basin may have begun in early or middle Cenozoic time, but details of early extension are lacking. The beginning of Basin-and-Range block faulting is commonly considered to coincide with the transition from calc-alkalic to bimodal volcanism, which occurred approximately 17 m.y. ago (Stewart, 1978). The first appearance of fault-controlled sedimentary basins resembling those seen today was between 13 and 11 m.y. ago (Stewart, 1980).

The spatial and temporal patterns of Basin-and-Range block and strike-slip faulting throughout the Candidate Area are not well documented. The time of faulting has been determined in a few areas within narrow limits. Cenozoic faulting around the northeastern part of Death Valley was episodic (Reynolds, 1974a,b), even though extension in the region was probably continuous. North- and northeast-trending faults formed between 20 and 16 m.y. ago and between about 14 and 13 m.y. ago. Doming, folding, and faulting along north-trending faults occurred between 11 and 7 m.y. ago (Reynolds, 1974a). Faulting has been nearly continuous since about 7 m.y. ago, forming the present-day topographic relief in Death Valley. Late Pleistocene and Holocene fault scarps are common along the length of the Death Valley-Furnace Creek fault zone (Reynolds, 1969; Brogan, 1979).

There is sparse evidence for early and middle Cenozoic faulting in the eastern part of the Candidate Area (Ekren and others, 1968). Strike-slip faulting along the Las Vegas Valley shear zone and between Yucca and Frenchman Flats was interpreted as middle to late Miocene (15 to 11 m.y. ago; Poole and others, 1965; Fleck, 1970; Anderson and others, 1972). Deep sedimentary basins such as Yucca and Frenchman Flats in the east-central part of the Candidate Area were interpreted by Carr (1974) as post-Miocene structures; Carr observed that faulting continued in those areas during the Holocene.

Some normal faulting occurred in the central part of the Candidate Area contemporaneously with early volcanic activity (about 16 to 14 m.y. ago; Christiansen and others, 1977), but this faulting must have produced little topographic relief, because it had little effect on the distribution of younger ash-flow sheets (Byers and others, 1976). Ash-flow sheets of the Paintbrush Tuff (12.5 to 13 m.y. old) are uniformly distributed suggesting that they were erupted over an area of low relief. The Timber Mountain Tuff at Yucca Mountain (11.1 to 11.4 m.y. old) is restricted to topographic basins and rests on the Paintbrush Tuff with buttress unconformity; much of the

faulting that outlines the structural blocks therefore developed between 12.5 and 11.4 m.y. ago. Faulting also occurred after deposition of the Timber Mountain Tuff, because ash-flow sheets of the Thirsty Canyon Tuff (7 to 8 m.y. old) thin against relatively high-standing blocks of Timber Mountain Tuff on Pahute Mesa, and the Timber Mountain Tuff is cut by faults in the Yucca Mountain area. The Timber Mountain Tuff at Yucca Mountain is commonly cut by the same faults that cut the Paintbrush Tuff, but displacements of the Timber Mountain Tuff are generally smaller than those of the Paintbrush Tuff, and displacements of Quaternary deposits are smaller than those of the Timber Mountain Tuff. Observations such as these have led some workers to suggest that the rate of faulting has diminished at the Site over the past few million years (Carr, 1982b).

Additional work is needed before the temporal and spatial relations of Cenozoic faulting in the Candidate Area are well enough known for quantitative evaluation of future tectonism. However, some general patterns have emerged. Early and middle Cenozoic faulting may have occurred in the Candidate Area, but probably created no great topographic relief. Major extensional faulting occurred in much of the area during the middle and late Miocene. This faulting varied considerably in style, timing, and areal extent. Many of the deep structural basins and areas of high present-day topographic relief within the Candidate Area formed during Pliocene and Quaternary time; faulting continues in many areas.

Pleistocene Tectonism

Numerous faults with Quaternary surface displacements are recognized in the Candidate Area, but rates of movement and ages of most recent movements are commonly difficult to determine because materials necessary to date them are scarce. Fault scarps having evidence of Quaternary movement are of two general types in the Candidate Area (Figure 28, in pocket): (1) steep linear or curvilinear mountain fronts and lineaments in old surficial deposits, and (2) distinct fault scarps. Figure 28 is a preliminary map showing most of the prominent mountain fronts and surface lineaments in the area; some segments less than about 10 km long are not shown. Many mountain fronts display little or no direct evidence of displacement, yet the steepness of the fronts and the linear shape of flanking alluvial fans suggest relative uplift of the mountain

block during the Quaternary. A striking example of a curvilinear mountain front is the east side of Bare Mountain, 15 km west of the Site (Figure 3). Only a few small scarps in alluvium are preserved along the mountain front, but the entire front is morphologically youthful with smooth, undissected slopes and little desert pavement developed on the fan surfaces. Topographic lineaments of a few meters width are not included on the preliminary map of Quaternary fault scarps and lineaments because most wide lineaments are interpreted as marking old buried and/or eroded fault zones. Most faults with no topographic relief are interpreted to be Pleistocene. All Pleistocene faults shown on Figure 28 are considered to be active faults which could move again.

A zone of faults having demonstrable Pleistocene displacement extends southward from Sand Spring Valley, 120 km northeast of the Site, through Yucca Flat and curves southwestward into the Amargosa Desert (Figure 28). A set of surface faults in the Pahrump Valley is inferred to be a continuation of this zone, which was called the NTS Paleoseismic Zone by Carr (1974). It generally corresponds with a zone of relatively high current seismicity (Rogers and others, 1981) and has an S shape similar to that of the Nevada Seismic Zone where it crosses the Walker Lane.

Twenty-three trenches were excavated across known or suspected surface breaking faults at Yucca Mountain in order to evaluate the history of Quaternary faulting. Four trenches encountered bedrock at shallow levels and exposed only thin Quaternary deposits that were not useful in limiting the age of fault movement. A reconnaissance study of the remaining trenches was done to determine the stratigraphy of exposed Quaternary units and the extent of fault displacements. The locations of the trenches are shown on Figure 3, and the results of the trench studies are summarized in Table 4. No demonstrable offsets of Holocene deposits were recognized in any of the trenches, however Holocene materials were thin or absent in most trenches. Deposits interpreted as late Pleistocene were faulted in one trench in Crater Flat (CF-3 on Figure 3; Swadley and Hoover, 1983). Deposits interpreted as early Pleistocene were offset in two trenches in Crater Flat (CF-1 and CF-2 on Figure 3; Swadley and Hoover, 1983) and in a trench on the west side of Yucca Mountain (No. 8, Figure 3). Fractures interpreted as fault related cut Quaternary deposits in several trenches on Yucca Mountain.

TABLE 4

SUMMARY OF STRATIGRAPHIC AND STRUCTURAL DATA FROM TRENCHES ACROSS FAULTS IN THE SITE VICINITY

Trench No.	Stratigraphic Unit Exposed*	Structural Features
2	Q1c, Q2c	None
4B	Q1c	None
6	Q1c	None
8	QTa, Q2c	Fault cuts QTa
9	Q1c, Q2c	None
10A	Q2c	None
10B	QTa	None
11	Q2b, Q2c, QTa	None
12	Q2	None
13	Q2b, Q2c	None
14	Q2e	Fractures
16A	Q2e	None
16B	Q2e	Fractures
17	Q2e	Fractures
CF1	QTa, Q2	Fault cuts QTa, not Q2
CF2	QTa, Q2	Fault cuts QTa, not Q2
CF3	Q2c, Q2b	Fault cuts Q2c, not Q2b
A1	Q2e	Fractures
A2	Q2c	None

All trenches located by number on Figure 3.

*See Hoover and others (1981) for a discussion of stratigraphic units.

Holocene Faulting

Two areas of unequivocal Holocene surface rupture due to faulting are present within the Candidate Area: (1) Yucca Flat, 50 km northeast of the Site, and (2) the Death Valley-Panamint Valley area, which comprises the southwestern third of the Candidate area. The possibility of Holocene surface movement on the eastern rangefront fault at Bare Mountain, 20 km west of the Site, and on the Rock Valley fault zone, 30 km southeast of the Site, cannot be ruled out, nor can the possibility of small Holocene movements on other Quaternary faults. Active seismicity occurs along some fault zones in the Candidate Area that have had Pleistocene movement but that show no evidence of Holocene surface rupture, indicating that absence of surface displacements does not necessarily mean absence of Holocene faulting.

The latest natural movement along the Yucca fault system in Yucca Flat was estimated by Carr (1974) to have occurred between 10,000 and 1,000 years ago. Other fault scarps in Yucca Flat are older than Holocene. Large cracks have formed in the playa at the south end of Yucca Flat and at several other playas in the area several times during approximately the last 50 years. Subsidence because of differential compaction may be the cause of some contemporary cracking in these playas, but most linear cracks were considered to be tectonic by Carr (1974). Local surface rupture related to underground weapon testing is also common at the Nevada Test Site.

Numerous Holocene fault scarps occur in Death Valley and Panamint Valley, areas of obvious youthful tectonism. At least one scarp in Death Valley was interpreted as approximately 2,000 years old (Hunt and Mabey, 1966). At present very little seismicity is occurring along the Death Valley-Furnace Creek fault zone, which is 50 km from the Site at its closest approach. A study by Smith (1979) of numerous youthful scarps in Panamint Valley, approximately 90 km west of Yucca Mountain, demonstrated that many of the faults had right-lateral strike-slip displacements of as much as 20 m. Recurrence intervals of 700 to 2,500 years were calculated for major earthquakes in that area.

Youthful fault scarps are present on both the east and west sides of Bare Mountain. Only short fault scarps are present on the east side, but the southern part of the eastern rangefront is morphologically youthful. Upper Pleistocene deposits have been offset by rangefront faulting, but no Holocene offsets have been demonstrated. The Beatty fault forms a nearly continuous,

that the onset of basaltic and bimodal volcanism coincided with the termination of crustal convergence and associated subduction, and the development of a transform plate boundary along the western continental margin (Atwater, 1970), but the timing of plate tectonic and volcanic events is not well enough known to determine specific relationships.

Five middle Miocene caldera complexes have been recognized in the central part of the Candidate Area. Structural controls on their distribution are uncertain. Volcanic centers in southern Nevada seem to be concentrated where large right-lateral faults die out or split into branches or en echelon arrangement; according to Carr (1974), especially favorable loci are places where northwest-striking right-lateral faults step right several kilometers, and where their ends are connected by northeast-striking complementary faults. Studies of volcanic centers have been too few to document specific structural control of volcanism.

Late Cenozoic Volcanism

The distribution of volcanic rocks younger than approximately 10 m.y. within the southern Great Basin is shown on Figure 20. Two belts of volcanism, which merge in the Death Valley area, are recognized:

(1) Quaternary basalt and local major silicic volcanic centers that are concentrated along the southwestern border of the Great Basin (Western Great Basin volcanic belt); and
(2) volcanic centers younger than 8 m.y. old that extend from southern Death Valley north-northeastward through the Candidate Area to central Nevada (Death Valley-Pancake Range basalt belt).

Silicic volcanism in the southern Great Basin diminished in the late Miocene, and basaltic volcanism surpassed it in volume. Sites of active basaltic and subordinate silicic volcanism progressively shifted toward the margins of the southwestern Great Basin beginning about 10 m.y. ago (Crowe, and others, 1983a). The Death Valley-Pancake Range belt emerged as a distinct volcanic feature at about 7 or 8 m.y. ago. Volcanic activity continued within the Death Valley-Pancake Range belt and along the southwestern margin of the Great Basin during the Quaternary, whereas volcanic activity in adjacent areas diminished.

Separate belts of basalt younger than 10 m.y. old cannot be distinguished petrologically in the southwest part of the Candidate Area. Through the central part of the Candidate Area to the Kawich Valley, the Death Valley-Pancake Range volcanic belt is defined by the distribution of scattered basalt centers ranging in age from 0.3 to 8 m.y. (Figure 20). The northern part of the belt includes the voluminous basalt fields in the Reveille Range (4 to 5 m.y. old) and the Lunar Crater volcanic field in the Pancake Range (<1 to 4 m.y. old). The northern end of the Death Valley-Pancake Range volcanic belt approximately coincides with the northwest-trending Nevada rift as described by Zoback and Thompson (1978).

Two distinct types of basalt fields younger than 10 m.y. old have been recognized within the Candidate Area based on reconnaissance geologic mapping of all volcanic fields:

Type I: Large volume (>3 km^3), relatively long-lived (active for several million years) fields containing various types of basalt. Extremely silicic volcanic rocks are associated locally with these fields.

Type II: Small volume (typically $\leq$0.1 km^3) scoria cones or clusters of cones and associated basaltic lavas. These centers generally formed during brief eruptive events (<1 m.y. in duration) separated by longer periods of inactivity (generally >2 m.y.).

Characteristics of these basaltic fields are summarized in Table 5.

The regional tectonic setting of the Death Valley-Pancake Range belt and the detailed setting of individual fields have been examined to determine the structural controls of volcanism, but with little success. Structural associations can be made on a regional basis, but their exact relation to the origin of specific volcanic centers is not known. The north-northeast trend of the Death Valley-Pancake Range belt is perpendicular to the extension direction for the south-central Great Basin suggested by Zoback and others, (1981) and hence is parallel to the most likely direction of dike injection.

Three distinct structural settings have been recognized for basalt centers in the Death Valley-Pancake Range belt (Crowe and Carr, 1980). These include:

TABLE 5

CHARACTERISTICS OF BASALTIC VOLCANISM FIELDS IN THE CANDIDATE AREA

Field	Field Type	Description	Tectonic Setting	Age (m.y.)
Death Valley	II	A. Southern Death Valley -- single scoria cone, no lavas B. Older lavas of Shoreline Butte	Close to Furnace Creek Fault, near its intersection with north-northeast-trending faults	2-0.5
Greenwater-Black Mountain	I	Three cycles of bimodal activity from south to north and older to younger: 1. Quartz bearing basalts, olivine basalts, and mafic andesite	General "pull-apart" or spreading area between Furnace Creek and Death Valley Fault Zones. Vents along north to north-northeast-trending fault zones	8-4
NTS Region-- silicic cycle basalts (examples: basalts of Basalt Ridge, Dome Mountain, Kiwi Mesa, and Skull Mountain)	I	Large volume lava sheets and shields	Ring fracture zones or Basin and Range faults within or near rhyolite caldera complexes.	11-8
NTS Region-- "rift" cycle basalts (Examples: basalts of Silent Canyon, Rye Canyon, Paiute Ridge, Buckboard Mesa, Sleeping Butte, and Crater Flat)	II	Small volume scoria cones with minor lava erupted during distinct pulses of activity throughout the NTS region	Basin and Range faults in general but including (1) their intersection with caldera ring fracture zones, and (2) north-northeast-trending "rifts" possibly related to right-stepping offsets in strike-slip shear zones of Walker Lane Belt	8-0.3
Kawich Valley	II	Isolated scoria cones, lavas and small plugs	Basin and Range faults	10-8
Reveille Range	I	Sheets and local shields of scoria cones and large volume lavas including local trachyandesite and trachyte plugs or domes	North-northeast-trending "rifts" between northwest-trending strike-slip faults and north-south trending Basin and Range faults	8-4(?)
Lunar Crater (Pancake Range)	I	Numerous single or coalesced Strombolian and Surtseyan centers with small to large volume lavas	Localized along major north-northeast-trending "rift" zone that crosses a much older (20-30 m.y.) caldera complex (Ekren and others, 1974). Older basalts are mostly related to caldera ring fracture, younger to north-northeast-trending "rifts"	4-0.1(?)

(1) North-northeast-trending zones of extension between active or formerly active northwest-trending strike-slip faults;
(2) Ring-fracture zones of inactive cauldrons; and
(3) Basin-and-Range faults.

Not all areas containing these tectonic features are sites of volcanic activity; therefore, sites of future volcanic activity cannot be predicted directly on the basis of these structural features. The above tectonic settings represent areas of relatively higher risk of volcanism than areas lacking these features. It is not known whether faults and fractures provide passive structural pathways for the ascent of magma or whether faulting has a more active relationship to volcanism.

Volcanism during the last 10 m.y. associated with the Death Valley-Pancake Range belt in the central part of the Candidate Area can be divided into two categories:

(1) Older basalt spatially related to silicic volcanic centers and erupted during the waning stages of large-volume silicic volcanism (Basalt of the silicic episode);
(2) Basalt that is generally younger than and spatially unrelated to the silicic volcanic centers (Rift basalt).

The basalt of the silicic episode was generally extruded in large-volume eruptions (>3 km^3), exhibiting a relatively wide range in composition (basalt to basaltic andesite or latite), and from 12 to about 8.5 m.y. old, with a notable peak in volume, 10 m.y. ago. Rift basalt may locally overlap the age of basalt of the silicic episode, but can be distinguished because rift basalt is either spatially unrelated to silicic centers, or, where spatially related, the rift basalt is demonstrably younger than the silicic rocks.

Rift basalt is alkaline olivine basalt and hawaiite (Vaniman and others, 1982). Two episodes of rift basalt are distinguished by age and trace element composition (Crowe and others, 1983b). These are: (1) older rift basalt (8.8 to 6.5 m.y. old), which has trace element abundances typical of alkali basalt throughout the Great Basin (Crowe and others, 1983b); and (2) younger rift basalt, which is strongly enriched in trace elements other than rubidium. The basalt of the younger episode (<4 m.y. old) occurs in the central part of the Candidate Area and in southern Death Valley.

The eruptions of the rift basalt were generally of small volume (<0.1 km^3) and formed isolated scoria cones and lavas at scattered localities. Scoria fall sheets originally surrounded and extended downwind from the cones, but have been largely removed by erosion. The style of eruption of this basalt, by analogy to historic eruptions, was Strombolian. This style of isolated, small volume, short duration eruption has been the only type of volcanic activity recognized within the central part of the Candidate Area during the last 8 m.y. Rates of volcanic activity for rift basalt as measured by number of cones for a specified area and time period have been consistently low. The basalt centers of Quaternary age in the Candidate Area are located in southern and northern Death Valley, Crater Flat immediately west of the Site, and north of Beatty, Nevada. There has been no volcanic activity in the Candidate Area for the last 200,000 to 300,000 years (Crowe and Carr, 1980).

STRUCTURAL GEOLOGY OF THE SITE AND THE SITE VICINITY

Yucca Mountain is made up of a series of north-trending structural blocks, consisting of gently eastward dipping Miocene volcanic rocks, rotated along west-dipping Basin-and-Range normal faults (Figures 5 and 6). The potential waste repository would be located within the largest of these blocks. The pattern of north-trending Basin-and-Range blocks appears to extend westward from Yucca Mountain beneath the alluvial fill of Crater Flat to Bare Mountain (Figure 3), where bounding faults dip eastward. North of Yucca Mountain is the Timber Mountain caldera complex. Southeast of Yucca Mountain, the ranges around Jackass Flats are characterized by faults that strike northeast.

The Calico Hills to the northeast are domed and complexly faulted. A central area of slightly metamorphosed Paleozoic sedimentary rocks is surrounded and overlain by hydrothermally altered Tertiary volcanic rocks (Figure 3). Doming may have resulted from Tertiary magmatic activity (Maldonado and others, 1979).

Structure of Pre-Cenozoic Rocks

Gravity data have been used to estimate that the depth to pre-Cenozoic rocks ranges from as little as 1 km near the southeast corner of the Site to more than 3.5 km at the northwest part, and about 4 km under Crater Flat (Snyder and Carr, 1982). Uncertainty in the density contrasts used for the gravity model makes depth predictions accurate only to within ± 30 percent, or approximately 1000 m for the deeper estimates. The magnitudes of these predicted depths are supported by a seismic refraction model (Figure 29) by Hoffman and Mooney (1983) Additional seismic refraction surveys in progress will aid in resolution of depths to pre-Cenozoic rocks and subsurface structure.

A distinct northeast-trending gravity high between Busted Butte and the Calico Hills, was interpreted by Snyder and Carr (1982) as a structural high in the pre-Cenozoic rocks or, alternatively, as an eroded northwest-facing escarpment on pre-Cenozoic rocks. A saddle in this regional gravity high between Yucca Mountain and the Calico Hills may represent a significant structural and (or) stratigraphic discontinuity coincident with Yucca Wash. The

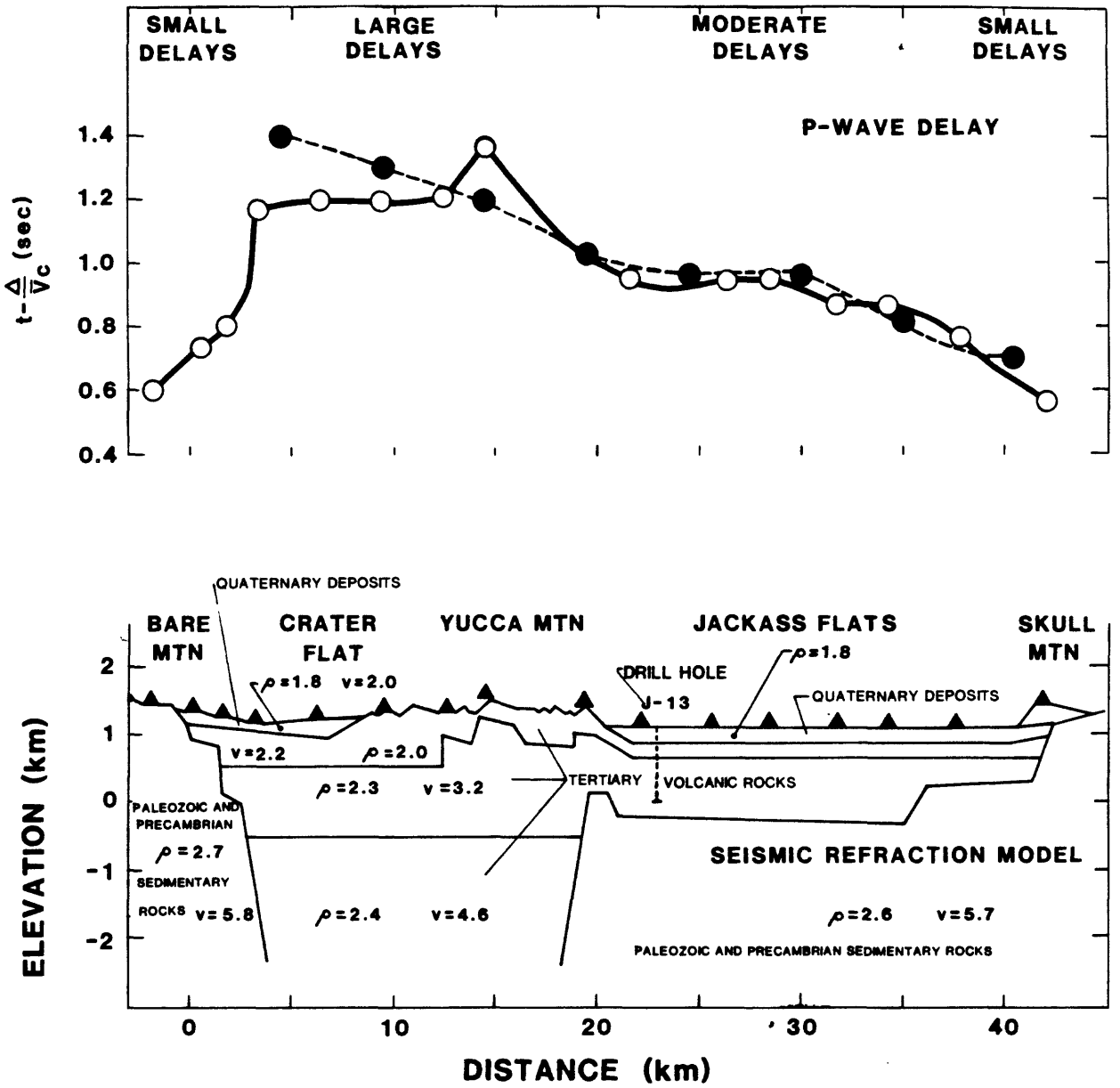

LEGEND

- OBSERVED
- CALCULATED
- ▲ CALCULATION POINT
- ρ ASSUMED DENSITY (g/cm³)
- v ASSUMED VELOCITY (km/sec)

t = TIME

Δ = DISTANCE

$\bar{V}c$ = 6km/sec = AVERAGE CRUSTAL VELOCITY

FIGURE 29

SEISMIC REFRACTION AND P-WAVE DELAY PROFILES FROM BARE MOUNTAIN TO SKULL MOUNTAIN

gravity models preferred by Snyder and Carr suggest at least 2000 m of structural relief in the sub-Tertiary rocks between Yucca Mountain (Busted Butte) and Crater Flat. They interpret the Crater Flat structural depression to be a combination of graben structures and old calderas; these calderas may have been the source for the Crater Flat Tuff that occurs in the subsurface at the Site (Carr, 1982a,b). As noted previously, the possible presence of a large east-trending intrusive body beneath the northern end of the Site has been suggested (Snyder and Carr, 1982).

Surface Structural Geology

Three sets of steeply dipping faults occur within the Site (Figure 30). Recognition of these faults, based primarily on geologic mapping, has been aided by interpretation of low-level aeromagnetic (Figure 31) and electrical resistivity (Figure 32) data. Many faults that involve alluvium have been trenched (Figures 3 and 30) to confirm their presence and to aid in dating them.

One set of faults at the Site consists of widely spaced, typical Basin-and-Range normal faults, which generally strike north to northeast and have relatively large displacements. These faults control the basic geomorphic features of Yucca Mountain (Figures 5). A second set of faults, largely occurring between Drill Hole Wash and Yucca Wash, strikes northwest (Christiansen and Lipman, 1965; Lipman and McKay, 1965; Scott and others, 1982). These faults have little vertical displacement. They display near-horizontal slickensides, and at least one has several tens of meters of right-lateral strike-slip displacement. Near the north end of Yucca Mountain, a series of linear northwest-trending washes were created by erosion along these strike-slip faults. A third set of faults, largely restricted to the southern part of the Site, strikes north-northwest. These faults tend to be more closely spaced than the other fault sets and have small vertical displacement. They apparently rotate strata to dip as much as 50° eastward.

Both the north-northeast-striking and north-northwest-striking faults dip steeply westward. The north-northeast-striking faults decrease in both displacement and abundance northward over a distance of about 5 km.

The Site can be divided into seven blocks (Figure 33) on the basis of structural patterns. These are called the (1) Solitario Canyon, (2) central,

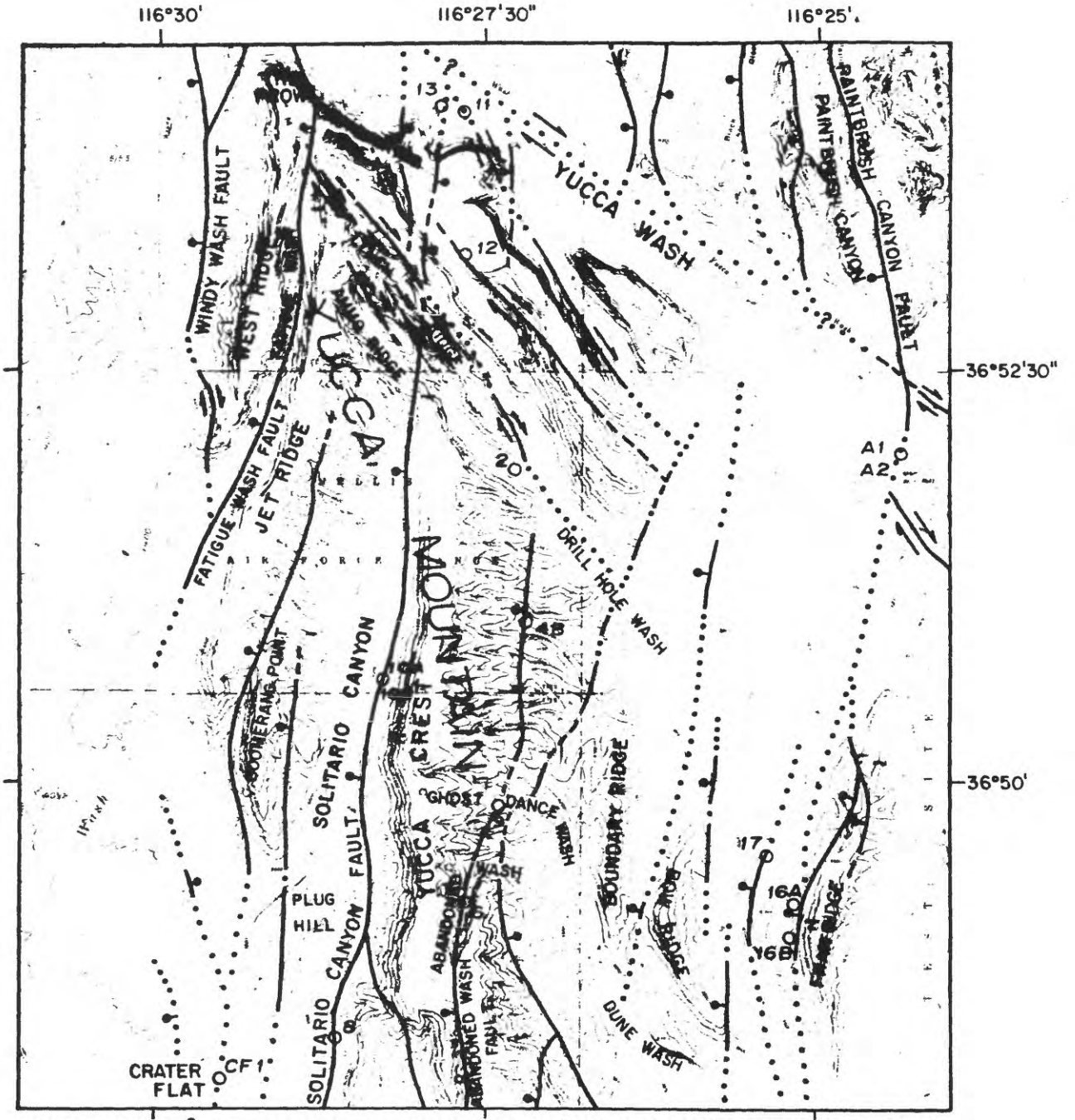

FIG. 30
FAULTS AT YUCCA MOUNTAIN INTERPRETED FROM GEOLOGIC MAPPING

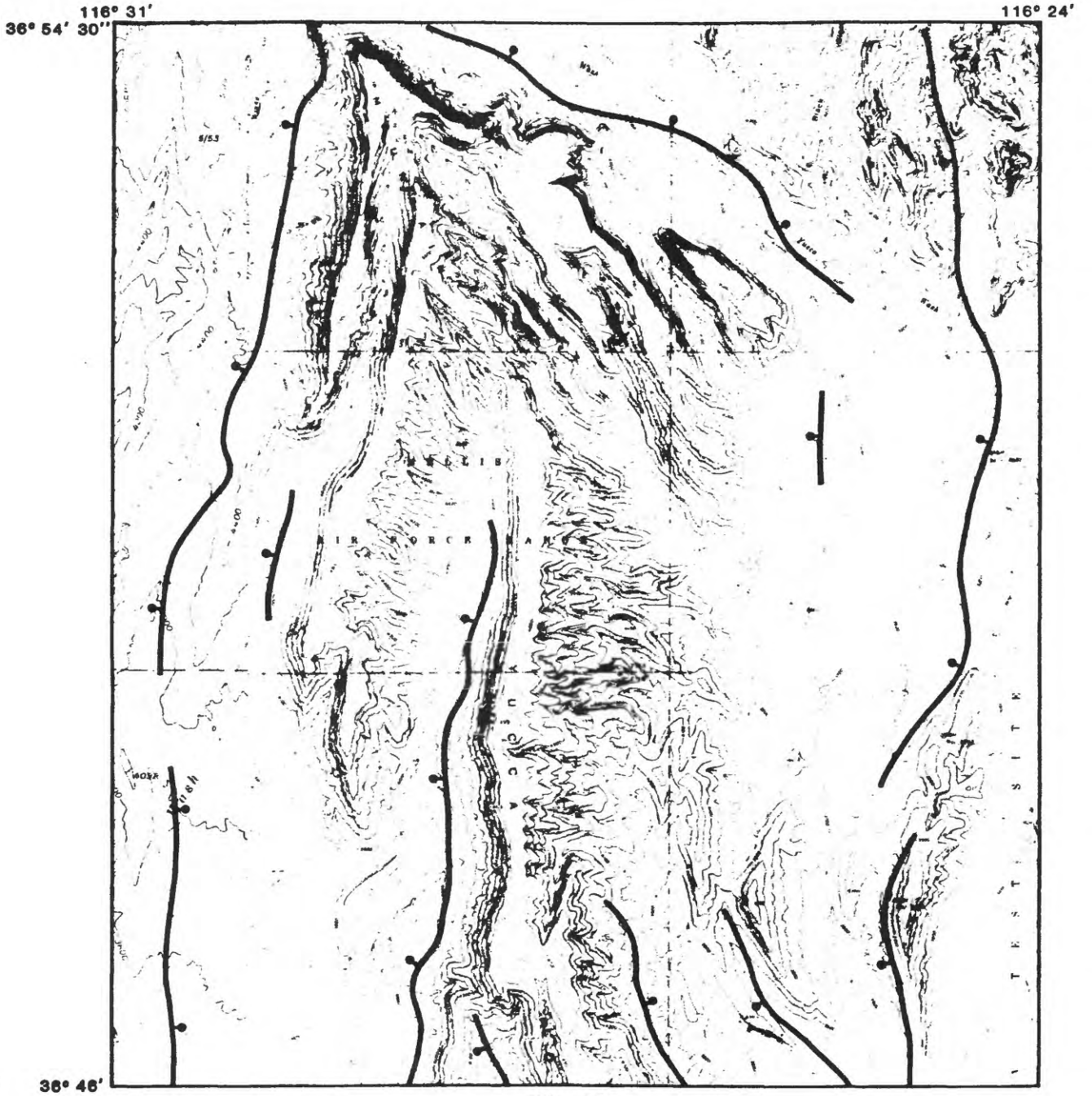

FIG. 31
FAULTS AT YUCCA MOUNTAIN INTERPRETED FROM LOW-LEVEL AEROMAGNETIC DATA

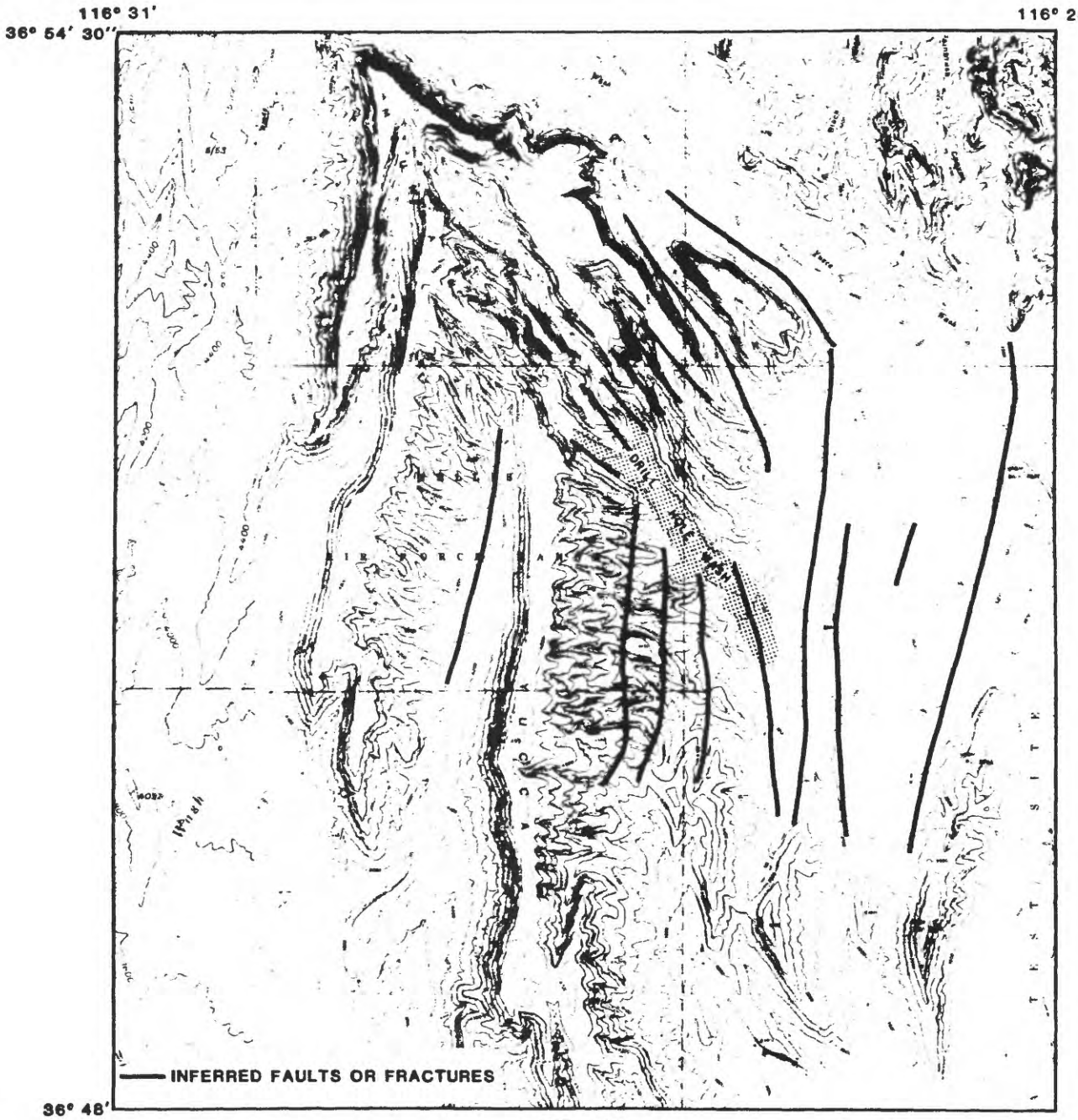

FIG. 32
FAULTS AND (OR) FRACTURES AT YUCCA MOUNTAIN INTERPRETED FROM ELECTRICAL RESISTIVITY DATA

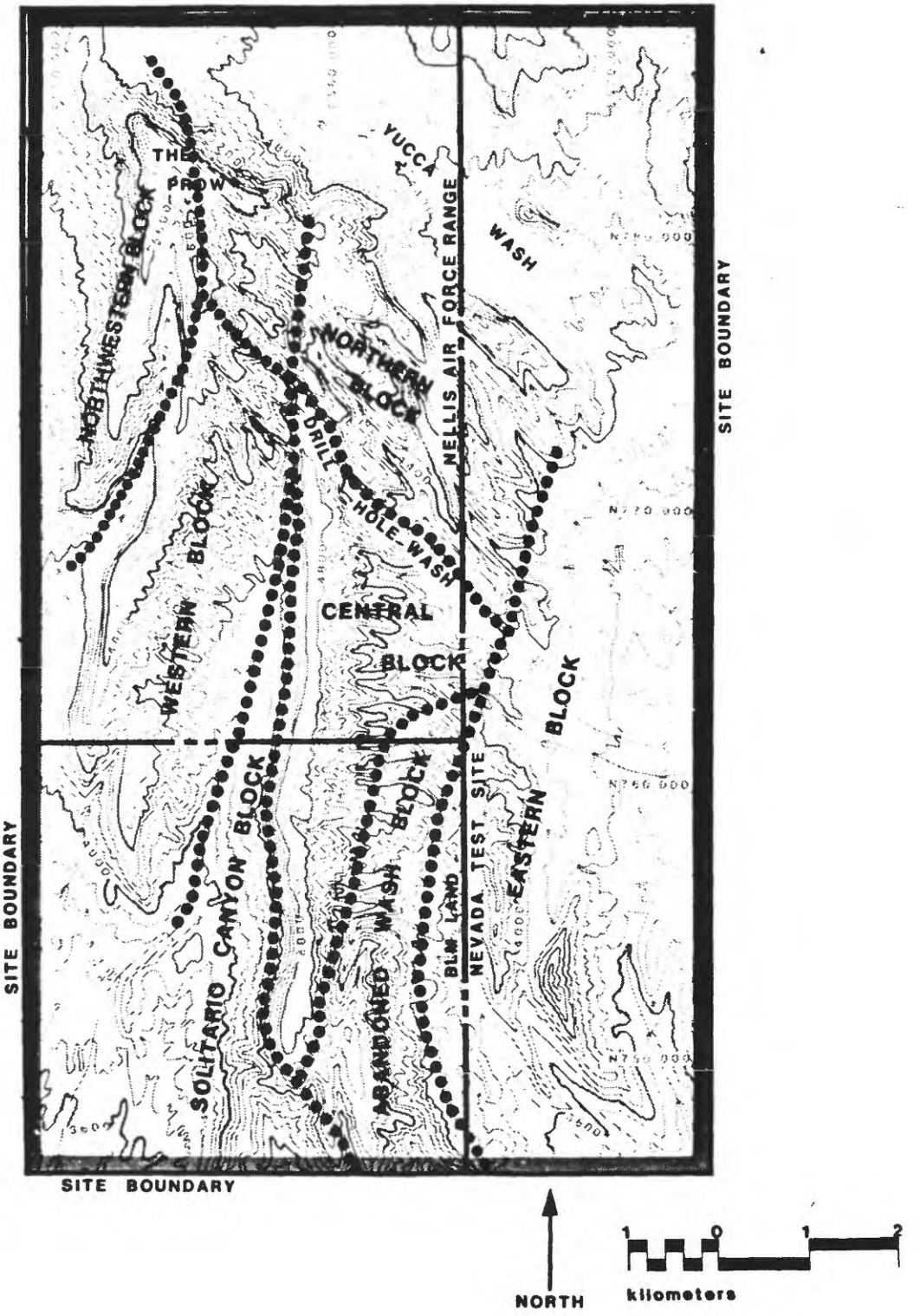

FIGURE 33
STRUCTURAL BLOCKS AT THE SITE

(3) northern, (4) Abandoned Wash, (5) eastern, and (6) western and (7) northwestern blocks.

1. Solitario Canyon Block. This block is characterized by north-northeast-trending tectonic breccia zones as much as 30 m wide. These alternate with zones of closely spaced normal faults, 1 to 50 m apart, which have displacements from a few centimeters to as much as 250 m. Only representative faults can be shown on the geologic maps (Figure 5) and on Figure 30. The dip of the faults generally is 60° to 70° W. (range: 35° to 80° W.), but several faults dip steeply eastward. The frequency and displacement of fault and breccia zones decrease northward toward the head of Solitario Canyon, where individual faults coalesce into a single 20-m-wide fault zone with less than 30 m of vertical displacement. The easternmost of these faults, called the Solitario Canyon fault, forms the western boundary of the potential repository. Attitudes of bedding and foliation planes defined by welded pumice fragments range from horizontal to steeply overturned. Nearly all of the faults developed before deposition of the Rainier Mesa Member of the Timber Mountain Tuff (11.3 m.y. ago), but at least one fault along the southwest edge of the Site cuts Quaternary alluvial deposits.

2. Central Block. A scarcity of large-displacement faults and a uniform 5° to 10° eastward dip of beds characterize this block (Figure 5). Two north-northeast-striking normal faults of small displacement cut the block near Drill Hole Wash. The easternmost of these can be traced approximately 2.5 km southward from the wash, where it splays into a series of north-northeast-striking faults. This fault has as much as 14 m displacement. The westernmost fault, which extends into the northern block, can be traced for approximately 1.5 km and has as much as 5 m of displacement. Fractures striking about N10°W to N20°W and dipping 80°SW are widespread. Other fractures striking north to north 20° east and dipping steeply northwest and southeast are present but less common. In the southern half of the block, normal faults, spaced 30 to 100 m apart and with apparent displacements of less than 3 m, occur parallel to the northwest-striking fractures. Near the

southern and eastern boundaries of the block, beds locally dip more than 10° east, particularly where fractures and faults are more abundant. Geometric constraints on structure sections (Scott and Bonk, 1984) suggest the presence of numerous closely spaced small-displacement faults in the southern half of the central block. Such faults have not been detected in the field, possibly because of their small displacement. It is possible that small faults, which can be important to the hydrologic character or mineralization of the block, are more numerous than surface maps indicate (Figures 5 and 30).

3. Northern Block. Layering in this block dips uniformly about 7° southeastward, which could be the original depositional attitude. Two main sets of faults cut the northern block (Figures 5 and 30). One set consists of north-northeast-striking, west-dipping normal faults, spaced about 600 m apart and with 3 to 10 m of offset. The other set consists of northwest-striking, strike-slip faults. Most of these faults occur between Drill Hole and Yucca Washes. That the most recent movements on these faults have been strike slip is shown by the presence of near horizontal slickensides. The sense of net offset is unknown except for two localities, one about 600 m west of drill hole USW-G2 and the other about 800 m east of drill-hole USW-G2, where the outcrop pattern is consistent with right-lateral displacement. Poor exposure of these faults could be related to their presence within and parallel to washes and (or) to the lack of significant vertical offset.

A series of horsts and grabens bounded by northward trending normal faults occur along the cliff overlooking Yucca Wash. Roughly one fault occurs each 300 m. The vertical offset on each of these faults is as great as 100 m adjacent to Yucca Wash but displacement decreases southward to no measurable offset within 1 km.

Mass movement of a slide block, 300 m by 450 m in area, has occurred along the ridge south of Yucca Wash (Scott and Bonk, 1984). The toe of this feature is beneath alluvium in the wash. The block is broken into at least 12 segments that strike parallel to the wash and dip

between 70° and 20° into the wash. Breccia is common as are small faults about 1 m apart. Hanging wall scarps several meters high attest to the youth of this feature.

4. Abandoned Wash Block. This area is cut by many north-northwest-striking, steeply west-dipping fractures and faults. Dips of beds steepen progressively from the southern part of the central block eastward into the Abandoned Wash block, where dips of 20°E to 40°E are common and dips as steep as 70°E occur locally. Beds steepen abruptly near north-northwest-striking faults. These faults commonly have displacements of 3 m or less (Figures 34 and 35). Although slickensides on most of these faults plunge down dip, slickensides on one fault plunge 10° northward, indicating that, at least locally, the latest displacement had a strike-slip component.

   The abrupt changes in bedding attitude and fault density in the Abandoned Wash block appear to be related to one of the principal faults cutting the Site. The north-trending part of Abandoned Wash contains a steeply west dipping fault with about 25 m of dip-slip displacement (Ghost Dance fault in Figure 5), which extends northward from Abandoned Wash almost to Ghost Dance Wash where it is covered by talus in an area cut by several north-northeast-striking faults. The eastern boundary of the Abandoned Wash block is marked by faults that dip steeply eastward.

5. Eastern Block. This area contains many north-northeast striking normal faults, most having displacements of 1 to 5 m. A few faults having much greater displacements repeat the east-dipping Topopah Spring-Tiva Canyon sequence in the eastern part of the block. In the western part of the block, the density of faults is as great as one every 100 m and faults strike north-northwest. Bedding dips between 15° and 50°, considerably steeper than in the central block. Most faults in the eastern block dip steeply westward but a few dip east, producing narrow grabens.

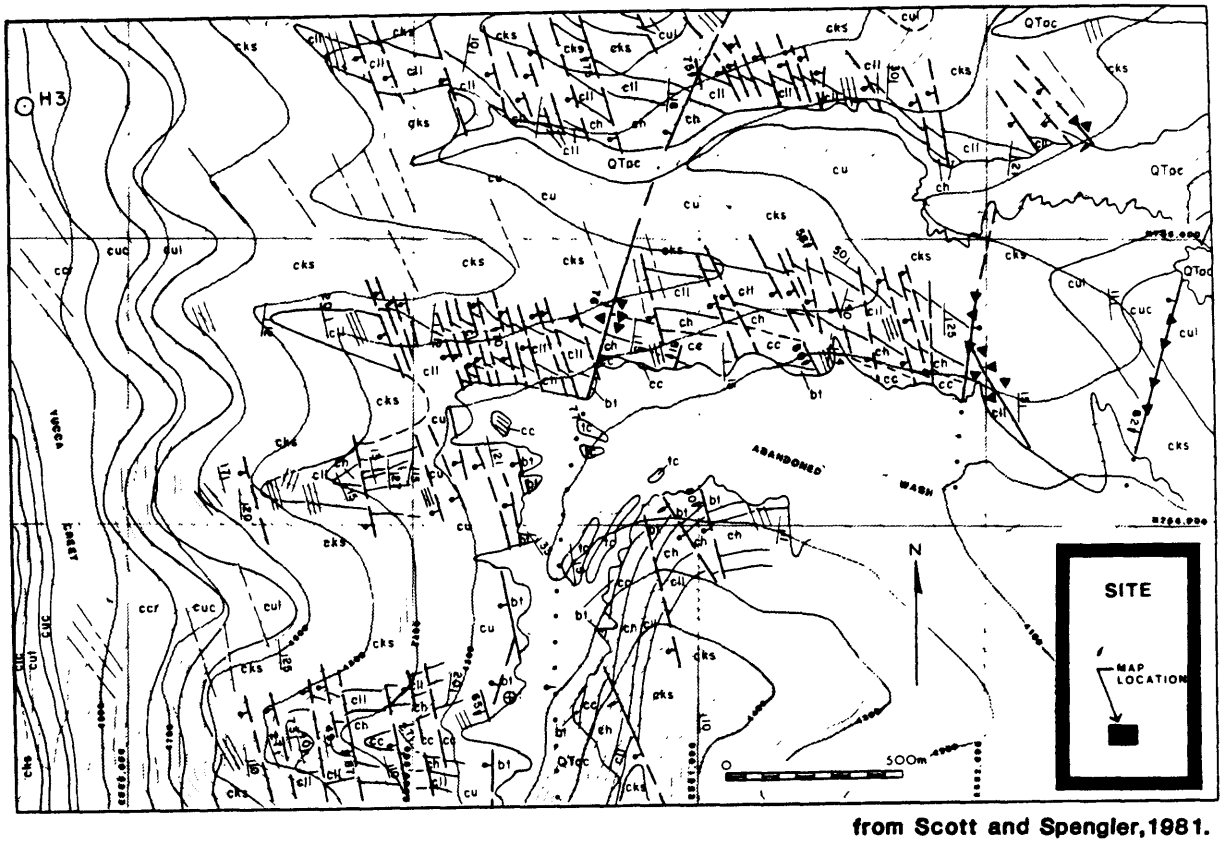

from Scott and Spengler, 1981.

EXPLANATION

cc–columnar zone

bt–bedded tuffs

tc caprock zone

QTac–alluvium and colluvium

cu–Tiva Canyon Member of Paintbrush Tuff

Ccr–caprock zone

Cuc–upper cliff zone

Cul–upper lithophysal zone

cks–clinkstone zone

cll–lower lithophysal

ch–hackly zone

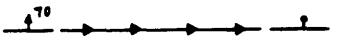

faults showing dip, bar and ball on downthrown side, triangle shaped arrow shows trend and plunge of slickensides.

FIGURE 34 GEOLOGIC MAP OF THE ABANDONED WASH BLOCK AT YUCCA MOUNTAIN.

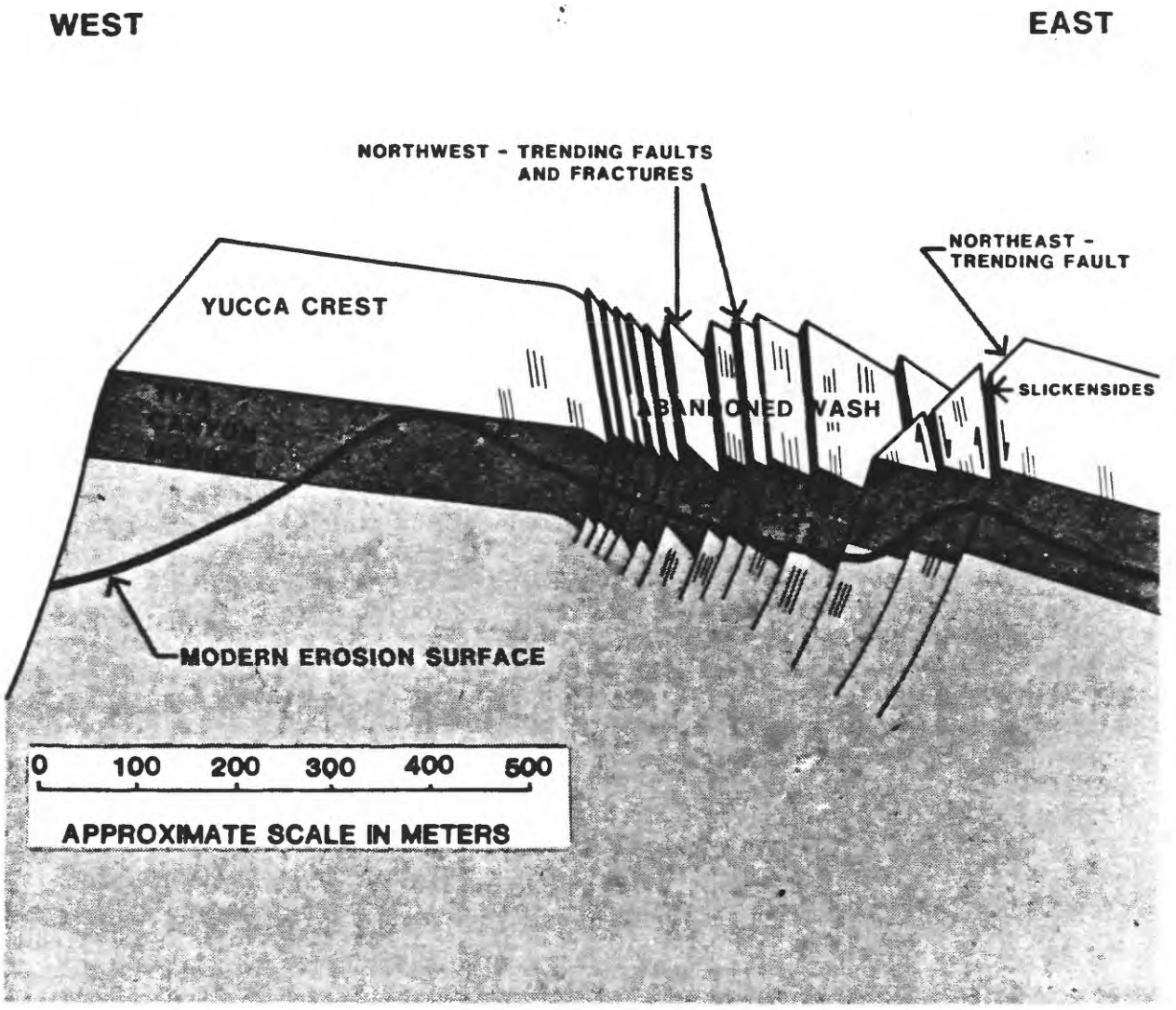

FIGURE 35

SCHEMATIC BLOCK DIAGRAM OF CLOSELY SPACED FAULTS IN THE ABANDONED WASH BLOCK, YUCCA MOUNTAIN

6. Western Block. In the western block, westward-dipping normal faults are spaced approximately 100 m apart. Vertical displacement on these faults decreases northward from a maximum of 3 to 20 m. Foliation in the ash-flow tuffs dips from 6°E to 7°E at the northern end of the block and increases to nearly 15°E at the southern end. Relative to the central block, strata in the western block are more steeply tilted and faults are more common. A few northwest-striking faults occur in the northernmost part of the western block but are characteristically absent elsewhere in the block.

A basalt dike, dated at 10 m.y. old (W. J. Carr written commun., 1984) intrudes the Solitario Canyon fault at the saddle between the western block and the central block. The dike has been disrupted by subsequent fault movement. Similar dikes trend north to northwest in the northernmost part of the western block.

7. Northwestern block. The northwestern block is separated from the western block by a large west-dipping normal fault in Fatigue Wash (Figure 5). This fault has at least 100 m of displacement at its southern end, decreasing northward to about 10 m where the fault crosses The Prow into Yucca Wash.

Similar to the western block, strata in the northwestern block dip about 6°E near The Prow but dip nearly 15°E farther south. There, a complex of anastomosing north-west-striking normal faults slices through the ridge (Figure 5). All exposed fault surfaces dip southwestward. Most slickensides indicate oblique-slip with a right-lateral component.

The western side of the block is bounded by the Windy Wash fault (Figure 5), a west-dipping normal fault with more than 225 m of vertical displacement. Several smaller normal faults of the same general attitude cut the western slope of West Ridge, but none cut the caprock of the Tiva Canyon Member.

Slickensides on fault planes indicate the direction of most recent fault movement. There are three main groups of consistently oriented slickensides on faults at Yucca Mountain (Figure 36). Groups 1 and 2 (on Figure 36) occur on the steeply westward-dipping faults that are interpreted as having perdominantly normal displacement on the basis of their large stratigraphic throw. Group 1 slickensides indicate dip-slip displacement; Group 2 slickensides plunge less than 20°SW and indicate a dominant component of strike slip, which is left lateral on the basis of stratigraphic separation. Although predominately normal faults, some of these faults last moved in a strike-slip fashion.

Group 3 slickensides occur on nearly vertical, northwest-striking faults and plunge less than 25°; offset beds indicate right-lateral strike slip. A few faults dipping steeply to the southwest at the southern end of West Ridge (Figure 5) have slickensides (Group 4, Figure 36) that indicate nearly pure dip slip with a small component of right-lateral strike slip.

Most of the displacement on the north to north-northeast striking normal faults occurred between 12.5 and 11.3 m.y. ago. Offset of the 12.5 m.y. old Tiva Canyon Member is greater than that of the 11.3 m.y. old Rainier Mesa Member. Pliocene and Quaternary surficial deposits locally are faulted against the Tiva Canyon Member in Solitario Canyon. Quaternary alluvium is offset near the east side of Crater Flat. Small displacements of probable Quaternary alluvium also are evident along the Windy Wash and Paintbrush Canyon faults (Figure 5).

Cross-cutting relationships suggest that most of the displacement along the northwest-striking, right-lateral faults also occurred between 12.5 and 11.3 m.y. ago. Faults cut the 12.5 m.y. old Tiva Canyon Member of the Paintbrush Tuff with as much as 10 to 30 m of displacement, but only slightly disturb the 11.3 m.y. old Rainier Mesa Member of the Timber Mountain Tuff.

A few east-striking faults near The Prow displace the tuffaceous beds of Calico Hills about 3 m but do not cut the overlying Topopah Spring Member (Figure 5). These faults may be volcanogenic, related to the east-trending boundary of the nearby Claim Canyon Cauldron to the north.

Fractures are common in exposures of the densely welded Tiva Canyon and Topopah Spring Members at Yucca Mountain. Because it is impractical or impossible to determine whether each crack in the rock is a joint, without displacement, or a fault, having displacement, all cracks are called fractures

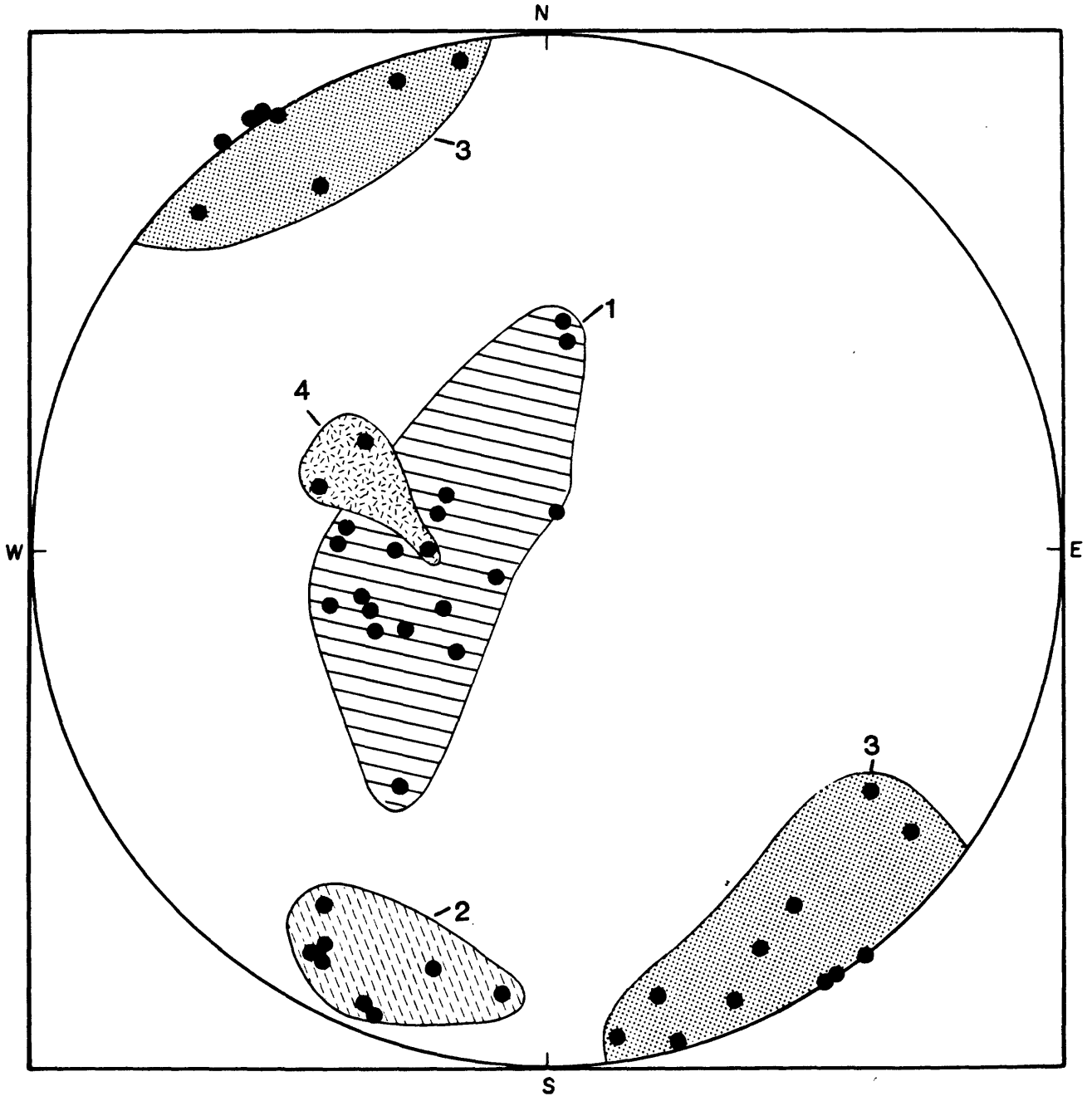

FIG. 36 STEREOGRAPHIC PROJECTION OF SLICKENSIDES ON FAULTS ON YUCCA MOUNTAIN.

LOWER HEMISPHERE EQUAL-AREA PROJECTION

unless slickensides, offset, or breccia indicate movement. Fractures in rocks may affect (1) water or vapor transport of radionuclides from a repository to the accessible environment, (2) groundwater recharge and movement, and (or) (3) mining conditions at a repository. For example, hydraulic conductivities of fractured densely welded ash-flow tuff in the saturated zone are 3 to 8 orders of magnitude greater than matrix hydraulic conductivities of the same rock (Winograd and Thordarson, 1975; Scott and others, 1983).

Fractures are of particular importance as barriers or conduits for flow of ground water. In this regard, both surface and subsurface fractures at the Site can be characterized in two classes: open or closed. Open fractures can be simple apertures or permeable breccia zones, some of which contain open cavities. Closed fractures can consist of simple fractures with hairline apertures or wider apertures sealed by secondary mineralization. They also can have more complex surfaces of dense fault gouge, or breccia healed with secondary minerals.

Fracture frequencies at the Site have been determined on the basis of fracture counts along linear surface traverses and in drill-core. Fractures that cut the traverse or core axis at small angles are probably more abundant in the surrounding rock than indicated by the number of such fractures intersecting a traverse or core. Consequently a numerical way to express fracture frequency in terms of fractures per unit volume derived by Scott and others (1983) was used in developing the following discussion. The method provides a basis for comparison rather than an absolute count of fractures.

Fracture frequencies were determined for five surface traverses in the Tiva Canyon Member and one, near the Prow, in the tuffaceous beds of Calico Hills (Figure 37). Fracture frequencies determined for short traverses in continuously exposed Tiva Canyon Member are about 6 to 8 per m^3. In contrast, fracture frequencies of 2 to 4 per m^3 were determine for long traverses in the Tiva Canyon. Two factors contribute to the lower fracture frequencies for long traverses. First, the long traverses were made across the moderately welded caprock as well as the more densely welded middle part of the Tiva Canyon, but short traverses were confined to the densely welded part. Fractures are generally more abundant in densely welded tuff than in moderately welded tuff. Second, the long traverses were over areas covered by talus which commonly covers gullies beneath which high fracture densities might be expected. South-facing slopes, which generally have better bedrock exposure

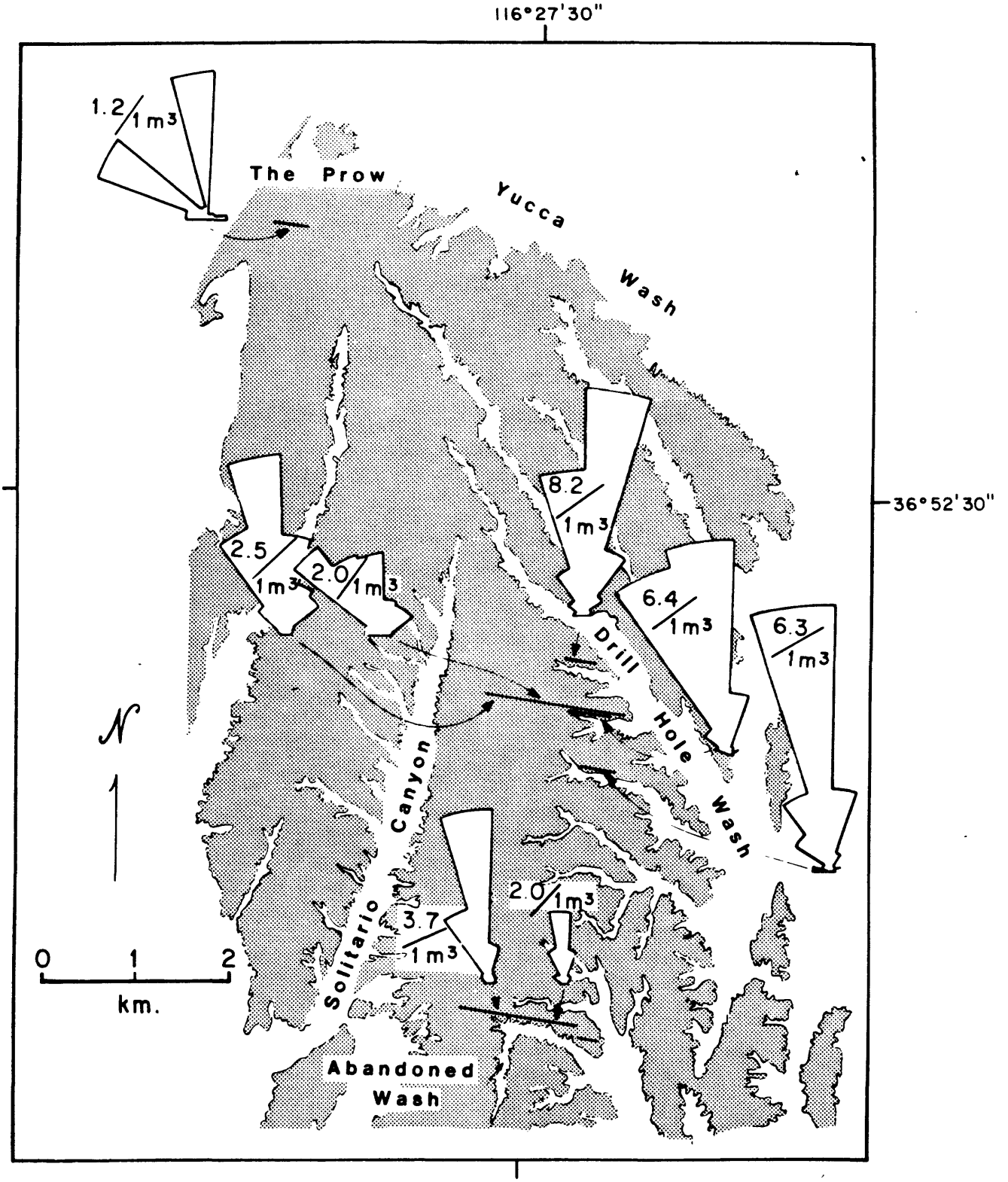

FIG. 37 ROSE DIAGRAMS OF THE STRIKES OF FRACTURES ENCOUNTERED ALONG TRAVERSES PERPENDICULAR TO THE AVERAGE FRACTURE ATTITUDE. FIVE TRAVERSES WERE MADE IN TIVA CANYON MEMBER. A SIXTH TRAVERSE WAS MADE AT THE PROW IN THE TUFFACEOUS BEDS OF CALICO HILLS. THE OUTLINE OF YUCCA MOUNTAIN IS THE CONTACT OF TERTIARY VOLCANIC ROCKS WITH QUATERNARY DEPOSITS. SOME TRAVERSES HAVE MORE THAN ONE DIAGRAM.

than north-facing slopes, have about twice the fracture frequencies of north-facing slopes. These observations suggest that the most reliable fracture densities are those measured along short traverses that afford maximum exposure and uniform lithology.

Fractures in volcanic rocks are produced by cooling, tectonism, and unloading or dilatation owing to removal of overburden. Fractures produced by dilatational stress at the Site have not been distinguished from those produced by tectonic stress; the attitudes of dilatational fractures are likely to be heavily influenced by the active tectonic stress field. Cooling fractures are not considered to be as important as tectonic fractures at Yucca Mountain, because fractures have a strong preferred orientation consistent in both welded and nonwelded tuff throughout the mountain (Figure 37). Nevertheless, fractures are more abundant in welded tuff than in nonwelded tuff. Apparently, nonwelded tuff responds to a given stress by developing fewer fractures, perhaps by taking up stress intergranularly. Further work is in progress to test the validity of these preliminary conclusions.

The fractures in the northern, western, and northwestern blocks, where no traverses were made, also have a dominant north-northwestern strike. Most of the eastern block has the same dominant fracture set. However, some areas, particularly those associated with north-northeast striking faults, have dominantly north-northeast striking fractures. The longest and smoothest fractures appear to define two sets: a dominant north-northwest striking set and a strong but secondary north-northeast striking set.

Subsurface Structural Geology

Drill-hole data have been helpful in assessing the subsurface structure. Primary layering in the northern drill holes dips 3°E to 8°E. In drill hole USW-GU3/G3 farther south, the dip changes from 7°E near the surface to about 10°S at 1500 m depth. No sharp discordance in attitudes of foliation or bedding has been recognized at depth.

The distribution of fractures relative to rock type in core is similar to that at the surface; more fractures occur in brittle densely welded tuff than nonwelded or bedded tuff. The fracture data from drill hole USW-GU3/G3 are used here as an example (Scott and Castellanos, 1984). Data from drill holes in the northern part of the Site were presented by Spengler and others (1979b).

Fracture frequency in USW-GU3/G3 core is expressed in two ways. The first reports the number of fractures encountered in each 3.05-m (10-ft) interval without correction for attitude or deviation of the hole from vertical; these data are shown on Plate 1 of Scott and Castellanos (1984) alongside selected lithologic features. The second compares frequency per unit volume (m^3) with physical-property stratigraphy (Figure 25 of Scott and Castellanos, 1984). Scott and Castellanos reached several conclusions from this comparison. There is a correlation between large fracture frequency and degree of welding and related physical properties. Fracture frequency in densely welded tuff, which ranges from about 15 to 40 fractures/m^3, varies little over tens of meters of core. Lithophysal zones tend to have slightly fewer fractures than intervals without lithophyse, 14 compared to 20 fractures/m^3. Unwelded tuff has as few as 1 fracture/m^3. There is an abrupt decrease in the frequency of fractures that is independent of welding below a depth of about 940 m in drill hole USW-GU3/G3. Moderately welded tuff above 940 m has 8 to 23 fractures/m^3, but below that depth there are only 2 or 3 fractures/m^3 in a similar rock type. This difference may be influenced by (1) variations independent of depth such as an increase in the amount of clay and zeolite alteration, (2) increased confining pressure, and (or) (3) some other unrecognized factor.

Attitudes of subsurface fractures have been determined from oriented cores (strike and dip), from downhole television camera surveys above the water table (strike only), and from conventional cores (inclination only without correction for drill hole deviation). Fracture attitudes in oriented core from drill hole USW-GU3/G3, for example, are similar to attitudes measured at the surface (Scott and Castellanos, 1984). Preliminary analysis of fault and fracture orientations also suggests general parallelism between dominant fault and fracture attitudes in USW-GU3/G3, steeply west-southwest dipping.

Subsurface information from the Paintbrush Tuff provides indirect evidence for a strike-slip fault zone parallel to Drill Hole Wash (Spengler and others, 1979b; Spengler and Rosenbaum, 1980). Several strike-slip faults have been mapped in upper Drill Hole Wash (Figure 5), and similar faults may exist under alluvium in lower Drill Hole Wash. In oriented core from drill hole UE25a-4, numerous northwest-striking, steeply dipping fractures parallel the trend of the wash. In UE25a-1, where no oriented cores were recovered,

numerous steeply dipping fractures were recorded. Fractures in drill holes UE25a-4, -5, -6, and -7 define prominent sets striking N12°W and N37°E, both dipping between 70° and 90° (Spengler and Rosenbaum, 1980). Surface mapping along with drill hole information limit maximum vertical displacements on faults in the wash to less than 3 m.

Drill-hole deviation at Yucca Mountain is generally southwestward (Figure 38). The uniform direction of drill hole deviation is likely a function of physical anisotropy in the rock. Drill holes are not deflected parallel to the direction of dip of primary layering, as commonly occurs in holes drilled in stratified rock. Instead, the deviation appears to generally parallel the dominant dip direction of fractures.

Three attempts with seismic reflection were made to map subsurface structure within the Site (McGovern and Turner 1983). Despite the high resolution methods and powerful source and receiver arrays, no mappable reflection events were recorded at Yucca Mountain. Apparently, state-of-the art reflection seismology profiling was ineffective in evaluating the structure of the Site because of local field conditions within the Site, such as rock type and complex structure.

Active Stress Field

Extension in the area of the southern Great Basin including the Site is in a N50°W direction according to a stress model proposed by Carr (1974). This model was based on a synthesis of tectonic and seismic data available in 1973 and a few stress and strain measurements. The time that the current stress configuration began is not known precisely, but the extensional episode responsible for the present topography in the Great Basin is thought to have begun between 10 and 4 m.y. ago (Zoback and Thompson, 1978; Zoback and Zoback, 1980; Zoback and others, 1981).

Study of drilling induced fractures in drill holes at Yucca Mountain provides additional information about the active stress field. Televiewer logs in drill holes USW-G1 and USW-G2 show extensive drilling-induced hydraulic fractures in the shallow parts of the holes. These fractures have not been recognized in corresponding intervals of core. The fractures dip steeply (>85°) and have a uniform strike of N20°E to N25°E. Their orientation indicates that the least horizontal principal stress direction of the in-situ

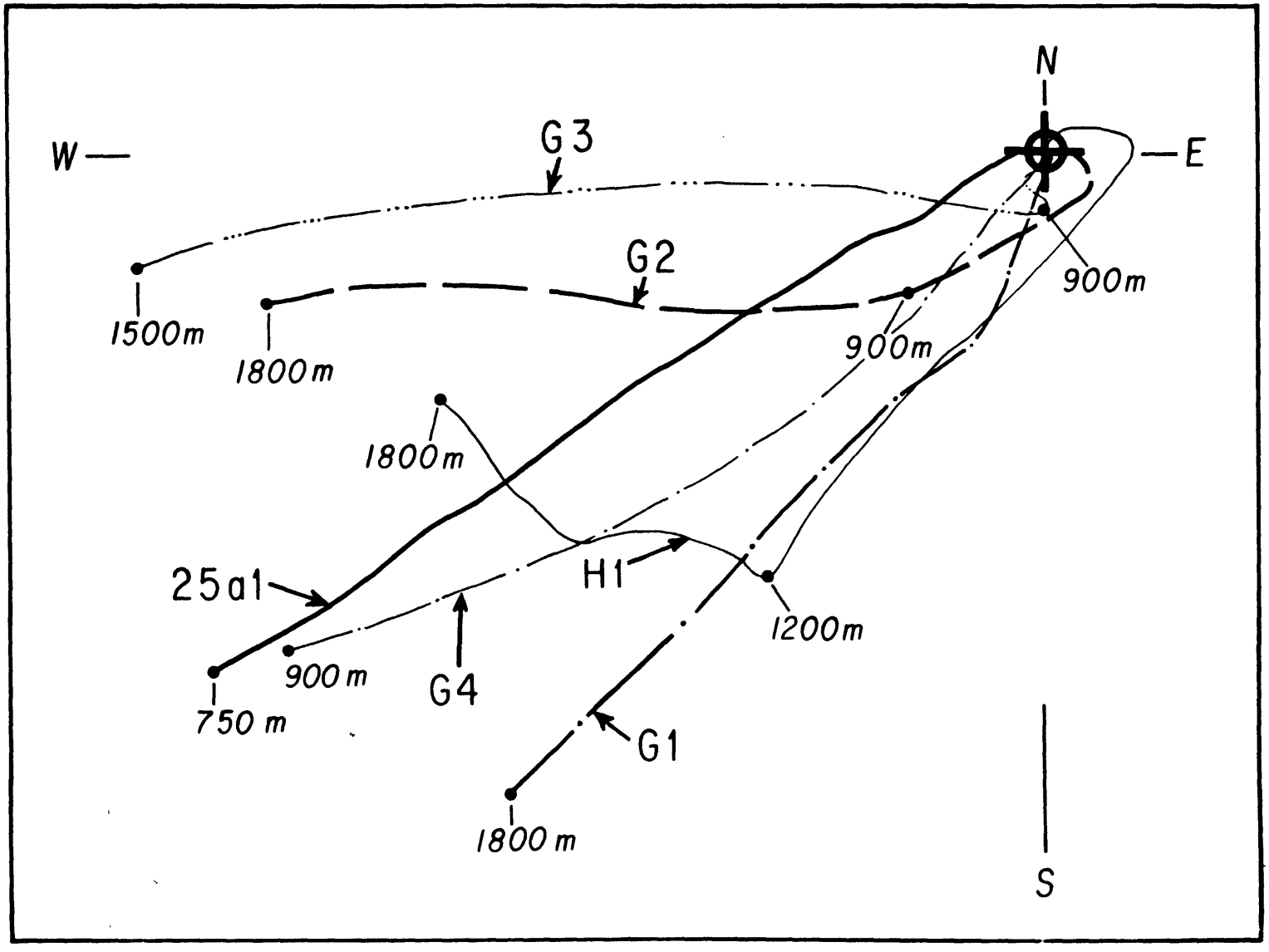

FIG.38 DRILL-HOLE DEVIATIONS ON YUCCA MOUNTAIN.NOTE THAT NO HORIZONTAL SCALE IS GIVEN BECAUSE THE AMOUNT OF LATERAL DEVIATION VARIES. LINE LENGTHS ARE NORMALIZED TO REPRESENT PERCENT OF HORIZONTAL DEVIATION.

stress field is about N65°W to N70°W, which is generally consistent with the interpretation of Carr (1974). The mean strike of 11 suspected drilling induced fractures between depths of 830 and 1330 m in drill hole USW-GU3/G3 is N16°E, generally consistant with data from other drill holes.

Stress measurements from experimental hydraulic fracturing of these drill holes show low magnitudes for the least horizontal principal stress, S_h, relative to the vertical principal stress (Figure 39). These low stresses provide an explanation for the presence of drilling-induced hydrofractures. Drilling-induced fractures are expected to extend and propagate when the fluid pressure in them exceeds S_h. As seen in Figure 40, if the pore pressure curve were shifted to the right by filling the drill hole with fluid above the ambient water table and applying downhole pumping pressure during drilling, the fluid pressure in fractures would exceed S_h and the fractures would extend. The fact that during drilling the fluid level in these wells rarely reached the surface probably means that the fluid escaped into the hydraulic fractures.

The large difference in magnitude between the least stress (S_h) and the greatest stress (the vertical stress, S_v) will affect the design and construction of a repository facility, and has important implications for the possibility of incipient normal faulting. Frictional sliding on preexisting faults optimally oriented to the stress field is controlled by the coefficient of friction, u, and the pore pressure, P_p. In a normal faulting regime, frictional sliding can be expected on optimally oriented faults whenever the ratio of $(S_v - P_p)/(S_h - P_p)$ exceeds the value $((u^2 + 1)^{1/2} + u)^2$ (Zoback and others, 1978). For reasonable values of u (between 0.6 and 1.0; Byerlee, 1978) the values of S_h determined in USW-G1 and USW-G2 are close to those at which frictional sliding might be expected to occur on the faults which strike N25°E to N30°E.

Work is in progress on interpretation of hydraulic fracturing test results from hole UE25p#1 and on some unusual pressure-time curves recorded in hole USW-G2.

Vertical and Lateral Crustal Movement

The period of regional lateral crustal shortening that characterized the Mesozoic was followed during the Cenozoic by lateral crustal extension throughout the Basin and Range. The local patterns of uplift, tilting, and

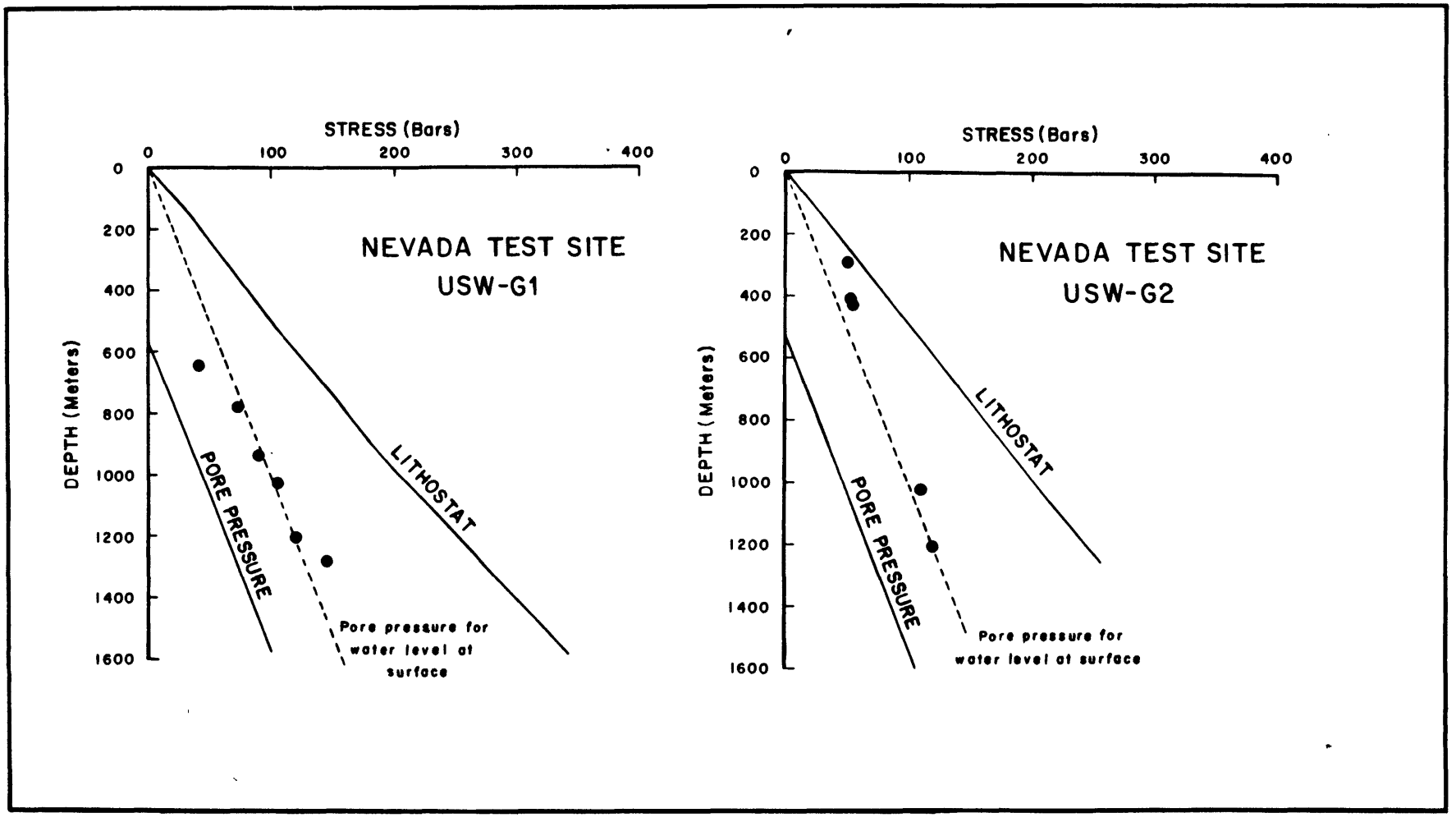

FIG. 39 LEAST PRINCPAL STRESS ,Sh, AS A FUNCTION OF DEPTH IN TWO YUCCA MOUNTAIN DRILL HOLES.THE VERTICAL STRESS (lithostat) AND PORE PRESSURES AT DEPTH ARE SHOWN FOR REFERENCE.DASHED LINE INDICATES FLUID PRESSURE WHICH RESULT FROM FILLING THE HOLE TO THE SURFACE WITH WATER.

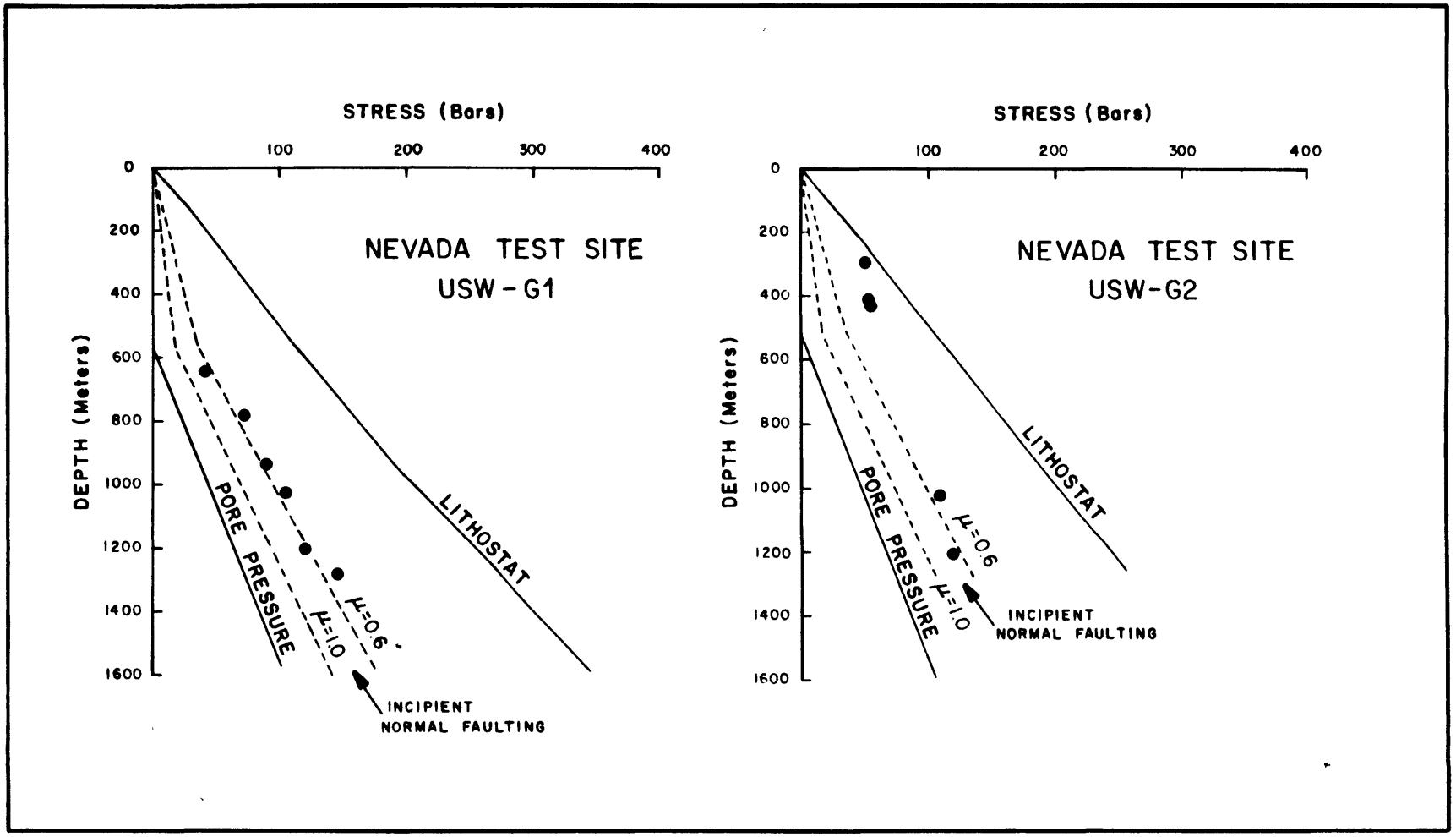

FIG.40 RELATION OF LEAST PRINCIPAL COMPRESSIVE STRESS ,Sh, TO FAULTING.THE VERTICAL STRESS (lithostat) AND PORE PRESSURE AT DEPTH ARE SHOWN FOR REFERENCE. DASHED LINES INDICATE BOUNDARY BETWEEN STABLE VALUES OF Sh (to the right of the dashed line) AND VALUES OF Sh CORRESPONDING TO FRICTIONAL SLIDING ON OPTIMALLY ORIENTED PREEXISTING FAULTS (to the left of dashed line) FOR COEFFICIENTS OF FRICTION ,u, OF 0.6 AND 1.0

subsidence in the Site Vicinity are typical of shallow crustal response to regional extension and attendant volcanic activity in the Great Basin. The region currently is undergoing active lateral crustal extension. Geodetic data sufficient to resolve historical crustal movements are not available, but a geodetic network has been installed.

SEISMICITY OF CANDIDATE AREA AND SITE

One of the principal difficulties associated with the assessment of seismic hazard in the Candidate Area is that the historic record of earthquake activity in this sparsely populated region is poorly known. The lack of detailed seismic information within the Candidate Area for most of historical time limits the accuracy and completeness of the earthquake record and our ability to evaluate future seismic activity.

Seismicity of the Candidate Area

National and university catalogs of historical earthquakes (such as NOAA, California Institute of Technology, University of Nevada at Reno, University of California at Berkeley, and University of Utah) are the only sources of seismic data for earthquakes that occurred in the Candidate Area before about 1960, and few seismographs were deployed within the area during that time. Some more detailed seismic data was obtained between 1960 and 1970 from several studies of limited scope and duration, generally related to nuclear testing at the Nevada Test Site. Few of these data were incorporated into the national and university catalogs.

King and others (1971) compiled a list of earthquakes for southern Nevada from the national and university catalogs and data collected from a sparse network operated from 1960 to 1973. The data collected from this network during 1971, 1972, and the first half of 1973 were reported by Bayer and others (1972), Bayer (1973a), Bayer (1973b), and Bayer (1974). Rogers and others (1976) assembled a list of historic earthquakes occurring before 1975 for a 500,000 km^2 region centered on the Nevada Test Site, using data from these catalogs and other limited studies. This list has since been expanded and revised and is now updated through 1983 (A. M. Rogers, USGS, personal commun., 1983).

The completeness of the earthquake record for the region including the Candidate Area has been evaluated in several studies. Greensfelder and others (1980) and Willis and others (1974) concluded that the catalog of earthquakes occurring in the region since 1932 is complete for all earthquakes greater than or equal to magnitude (M) 4 to 5. Rogers and others (1977a), using a catalog compiled for their study, inferred that the detection of earthquakes

in the M 4 to 5, 5 to 6, 6 to 7, and 7 to 8 ranges is complete for the most recent 40, 50, 60, and 130 years, respectively. This catalog includes earthquakes from west-central Nevada and southern California, areas that have more earthquakes and have been observed for longer periods than the southern Great Basin. The conclusions of Rogers and others (1977a) on completeness for M 4 to 5 is in accord with that of Greensfelder and others (1980) and Willis and others (1974). In the analysis of the natural seismic hazard, the rates for each magnitude range were determined using only data from the 40-, 50-, 60-, and 130-year intervals of completeness.

The seismic record between 1979 and the present is much more complete than for any previous period because a high quality seismograph network of approximately 53 stations has been operated in support of the Nevada Nuclear Waste Storage Investigations program since 1979. This network has a radius of about 150 km centered at the Nevada Test Site.

Historical Seismicity before 1979

Historical seismicity is shown on Figures 41 and 42. Figure 41 shows all known earthquakes occurring within approximately 400 km of the Site through 1974 having Modified Mercalli intensity (MM) greater than or equal to V and (or) $M \geq 4.0$. [All magnitudes reported herein are either surface wave, Richter, or equivalent to Richter magnitude. See Richter (1958) for description of Mercalli and Richter scales.] A list of the earthquakes shown on Figure 41 and the sources of data are given by Rogers and others (1976). None of the epicenters are located with a standard error of less than 7 km, and most of the non-instrumental locations probably have larger standard errors.

Figure 42, showing earthquakes of $M > 3$ in the Candidate Area, has been supplemented by data from the U.S. Department of Commerce (1976) catalog and Rogers and others (1977b). The epicenter locations in these addenda to the catalog have lower standard errors, in some cases, than the earlier portion of the catalog.

Earthquakes beyond 150 km generally do not produce ground motions that are damaging to structures with short natural periods (less than about 0.5s), but such earthquakes can produce ground motions having the potential to affect structures with long natural periods (greater than 0.5s). These effects can be more severe if a structure is underlain by deep alluvium or a deep sedimentary rock basin (Rogers and others, 1983a).

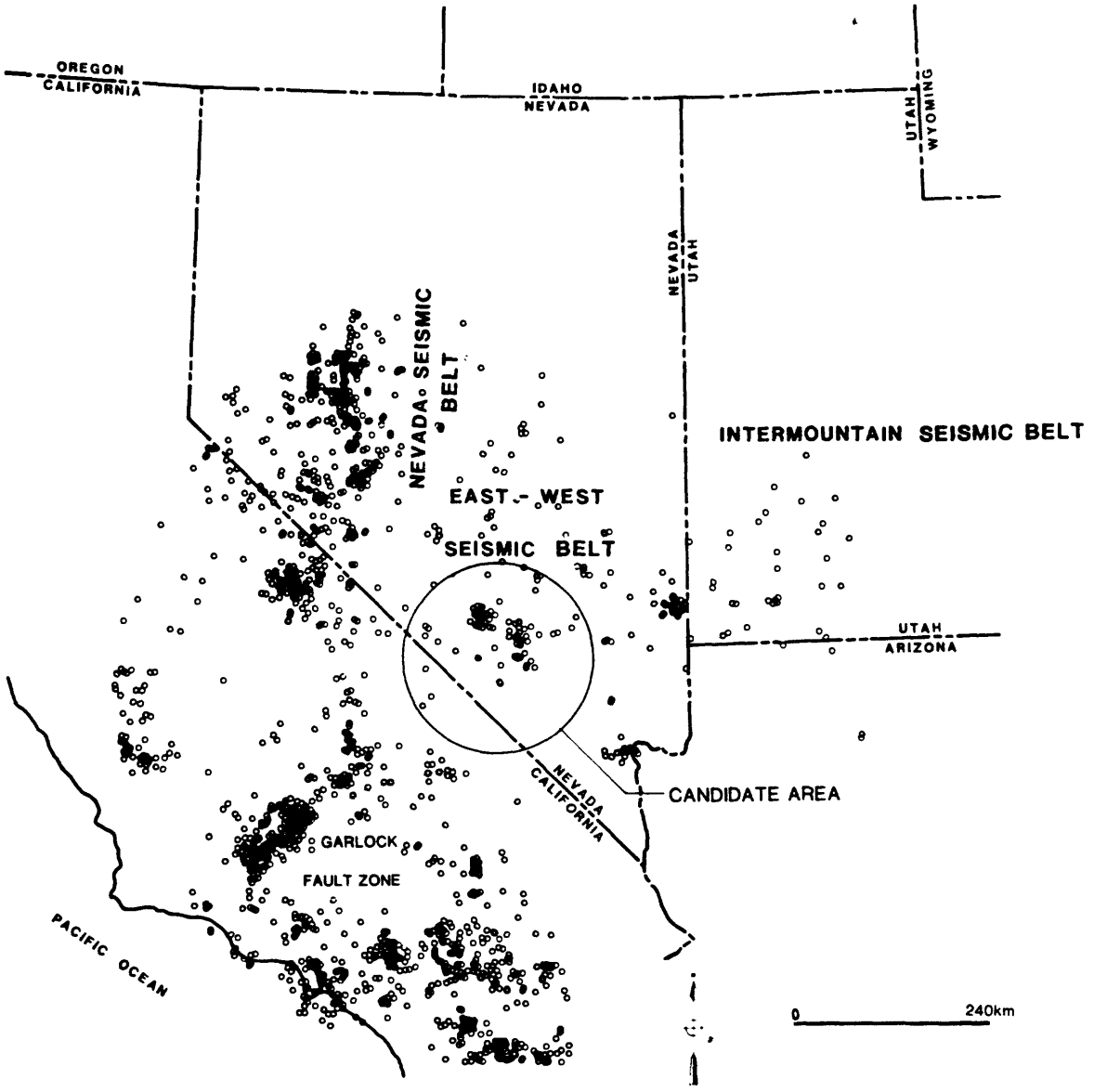

FIGURE 41

HISTORIC EARTHQUAKES OF MERCALLI INTENSITY ≥ V OR MAGNITUDE ≥ 4.0 WITHIN 400 KM OF THE CANDIDATE AREA THROUGH 1974

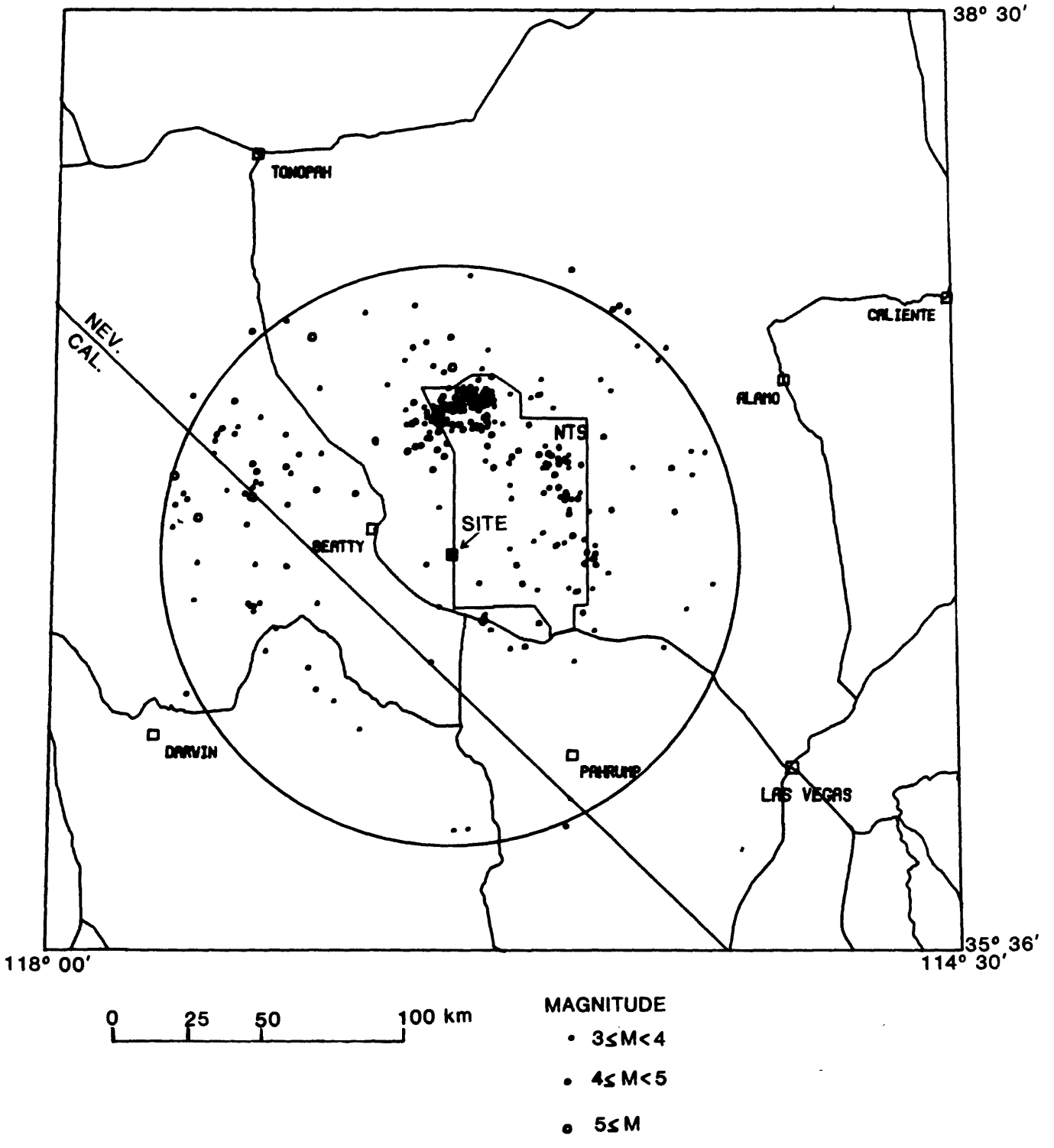

FIGURE 42 ALL KNOWN EARTHQUAKES OF MAGNITUDE >3.0 WITHIN APPROXIMATELY 100 KM OF THE SITE THROUGH JULY 1978.

The location of the Candidate Area with respect to the larger historical earthquakes and the most significant fault zones and seismic belts in the region is shown on figure 41. The Nevada seismic belt, approximately 125 km west of the Site, extends northward along the east side of the Sierra Nevada and then north-northeastward into western Nevada. It connects southward with a southwest-trending seismic belt parallel to and north of the Garlock fault zone. East of the Candidate Area is the Intermountain seismic belt, which generally parallels the Wasatch Front in Utah. Epicenters shown on Figure 41 probably do not adequately represent this belt in southern Utah because the area is sparsely populated and has not been closely monitored by seismic networks. The diffuse belt of seismicity connecting the Nevada seismic belt and the Intermountain seismic belt is referred to as the East-West seismic belt. A prong of this belt extends southward through the Nevada Test Site.

The Nevada seismic belt has been the location of several M 7 to 8 earthquakes (Table 6). Maximum accelerations produced by these events at locations underlain by rock in the Site Vicinity are likely to have been less than 0.1 g (Rogers and others, 1977a). Nevertheless, their occurrence indicates a potential for large magnitude earthquakes in the Great Basin.

A group of 600 earthquakes, referred to as the Clover Mountain earthquakes, occurred in the East-West seismic belt near the Nevada-Utah border in 1966 and 1967 (Figure 41) (Beck, 1970); the largest event of this series had a magnitude of M=6.1 (von Hake and Cloud, 1966) and was located about 210 km east of the Site. The relocation of the main shock and selected aftershocks in this series (Rogers and others, 1983b) using a joint epicenter method indicates that the earthquakes occurred along a north-northeast-trending zone. This result is in agreement with the findings of Smith and Lindh (1978) and Wallace and others (1983) that the main shock focal mechanism is nearly pure strike slip on either a vertical north-trending fault (producing right lateral slip) or a vertical east-trending fault (producing left-lateral slip). Another swarm of earthquakes in this region of eastern Nevada occurred 100 km northeast of the Site in the southern part of the northern Pahroc Range in 1971; the largest earthquake in this series was M=4.8 (Bayer and others, 1972).

An earthquake of about M=6 is reported to have occurred in the Death Valley region in 1908 (Lat. 36.0 N, Long. 117.0 W, MM intensity VII-VIII; Richter, 1958; Real and others, 1978). The assigned location of this earthquake, which is uncertain, is about 110 km southwest of the Site.

TABLE 6

MAJOR EARTHQUAKES (M>6.5) WITHIN 350 KILOMETERS OF THE SITE

Date	Name	Location	Magnitude (M)	Epicentral Intensity (MM)	Closest Distance to Site (km)
1857	Fort Tejon	35.0°N 119.0°W[a]	8 1/4[b]	IX[b]	300
1872	Owens Valley	36.5°N 118.0°W[a]	8 1/4[c]	XI[a]	147
1932	Cedar Mountain	38.7°N 117.8°W[d]	7.3[d]	X[d]	202
1952	Kern County	35.0°N 119.0°W[e]	7.7[e]	XI[e]	267
1954	Rainbow Mountain	39.4°N 118.5°W[d]	6.8[f]	IX[f]	331
1954	Rainbow Mountain	39.4°N 118.5°W[d]	6.8[f]	VIII[f]	331
1954	Fairview Peak	39.3°N 118.2°W[d]	7.2[d]	X[e]	276
1954	Dixie Valley	39.8°N 118.1°W[g]	6.9[f]	X[a]	323

[a]Coffman and von Hake (1973)

[b]Agnew and Sieh (1978)

[c]Oakeshott and others (1972)

[d]Slemmons and others (1965)

[e]Richter (1958)

[f]Ryall and Priestly (1975)

[g]Romney, C. (1957)

Figure 42 shows all earthquakes with magnitude greater than or equal to 3.0 occurring within approximately 100 km of the Site through July, 1978. The largest earthquakes recorded within this region are M=5+ (Hamilton and others, 1971; Rogers and others, 1977a,b). Much of the seismicity on Pahute Mesa and on Yucca Flat, approximately 50 km north and northeast of the Site, respectively, has been induced by nuclear explosions. Therefore, it is difficult to determine the natural earthquake activity of these areas. Earthquakes have also been induced in southern Nevada along the Colorado River southeast of Las Vegas by the creation of Lake Mead (Carder, 1970; Rogers and Lee, 1976). The largest induced earthquakes in that area are approximately M=5.

Several notable natural earthquakes of magnitude 4^+ have occurred in the Candidate Area. In the following list of those events, only earthquakes occurring south of the 37th parallel are included because events to the north, on Pahute Mesa and Yucca Flat, are likely to be related to nuclear tests. In chronological order (including the distance and direction from the Site to the earthquake), the list is: (1) 1948, M=4.0, 41 km southeast; (2) 1959, M=4.0, 23 km east; (3) 1960, M=4.9, 50 km east-southeast; (4) 1961, M=4.4, 27 km east-southeast; (5) 1969, M=4.1, 39 km northwest; (6) 1970, M=4.0, 39 km southwest; (7) 1971, M=4.3, 42 km east-northeast; (8) 1973, M=4.1, M=3.5, and M=4.0, 46 km east; (9) 1974, M=4.0 and M=4.1, 49 km east (Ranger Mountain area); (10) 1976, M=4.0, M=4.1, and M=4.2, 26 km southeast (Rogers and others, 1977b); and (11) 1977, M=4.0, 50 km east (Ranger Mountain area). Event (7), which was felt at the Nevada Test Site (Bayer and others, 1972), was called the Massachusetts Mountain earthquake and received special study by Tendall (1971), King and others (1971), and Fisher and others (1972). Earthquakes of event (8), referred to as the Ranger Mountain earthquake series (Bayer, 1973b) also were felt at the Nevada Test Site and occurred with two comparably sized aftershocks of M=3.9 and M=4.1. Several smaller earthquakes were located near the Site prior to August 1978, but the location of these events may have large errors because they were located using data from distant stations.

The near absence of seismicity at approximately the $M \geq 4$ level in some parts of the Candidate Area could be significant (Figure 41). The Site is quiescent at this level, as are nearby major structural features such as the southern part of the Death Valley-Furnace Creek fault zone and the Las Vegas Valley shear zone. Few earthquakes in this magnitude range have been recorded over large areas of the Desert Game Range approximately 100 km east of the

Site, the Spring Mountains 100 km to the southeast, the southern part of the Timber Mountain caldera immediately north of the Site, and the area northwest of the Site between Gold Flat and Tonopah (Figure 42). Several of these quiescent areas are also areas of little or no Quaternary faulting. Those areas that have no Quaternary faulting and are inactive seismically could be considered to have relatively low seismic hazard, but the hazard is more difficult to assess for areas having either Quaternary faulting and (or) seismicity.

Seismicity from 1979 to Present

A 47-station seismic network (Figure 43) was installed within a 160-km radius of the Site in 1978 and 1979 to locate and study earthquakes. This network was designed to study those tectonic features of greatest significance relative to seismic hazard assessment for the Site, including (1) the Fish Lake Valley and Death Valley-Furnace Creek fault zones, (2) the East-West seismic belt, and (3) the NTS paleoseismic belt of Carr (1974) (Figure 44). Some of the major tectonic features that could be important in seismic hazard assessment for the Site or for an understanding of regional tectonics are included on figures 43 and 44. A 6-station supplemental mini-net was deployed on Yucca Mountain in May 1981, to lower the detection threshold and improve location accuracy for earthquakes at the Site.

Initially the data from this network were recorded on film (Rogers and others, 1981); after October 1, 1981, however, the network data were digitally recorded. The digital data are analyzed using a DEC PDP 11-70 computer that is an existing part of the U.S. Geological Survey computer facility. This method of data recording and analysis is a significant improvement over the old method employing 16 mm film recorders and requiring reader scanning of three 24-hour film records. The computer system continually scans the incoming real-time signals and saves data only when a triggering algorithm indicates that an earthquake has been detected. The reader is required to separate false triggers from earthquake triggers, display the digital traces on an oscilloscope screen, and take readings from the screen electronically that are saved in the computer memory. This technique has not only resulted in at least a doubling of the number of earthquakes that it is possible to detect and read, but has increased the accuracy of the process by eliminating errors

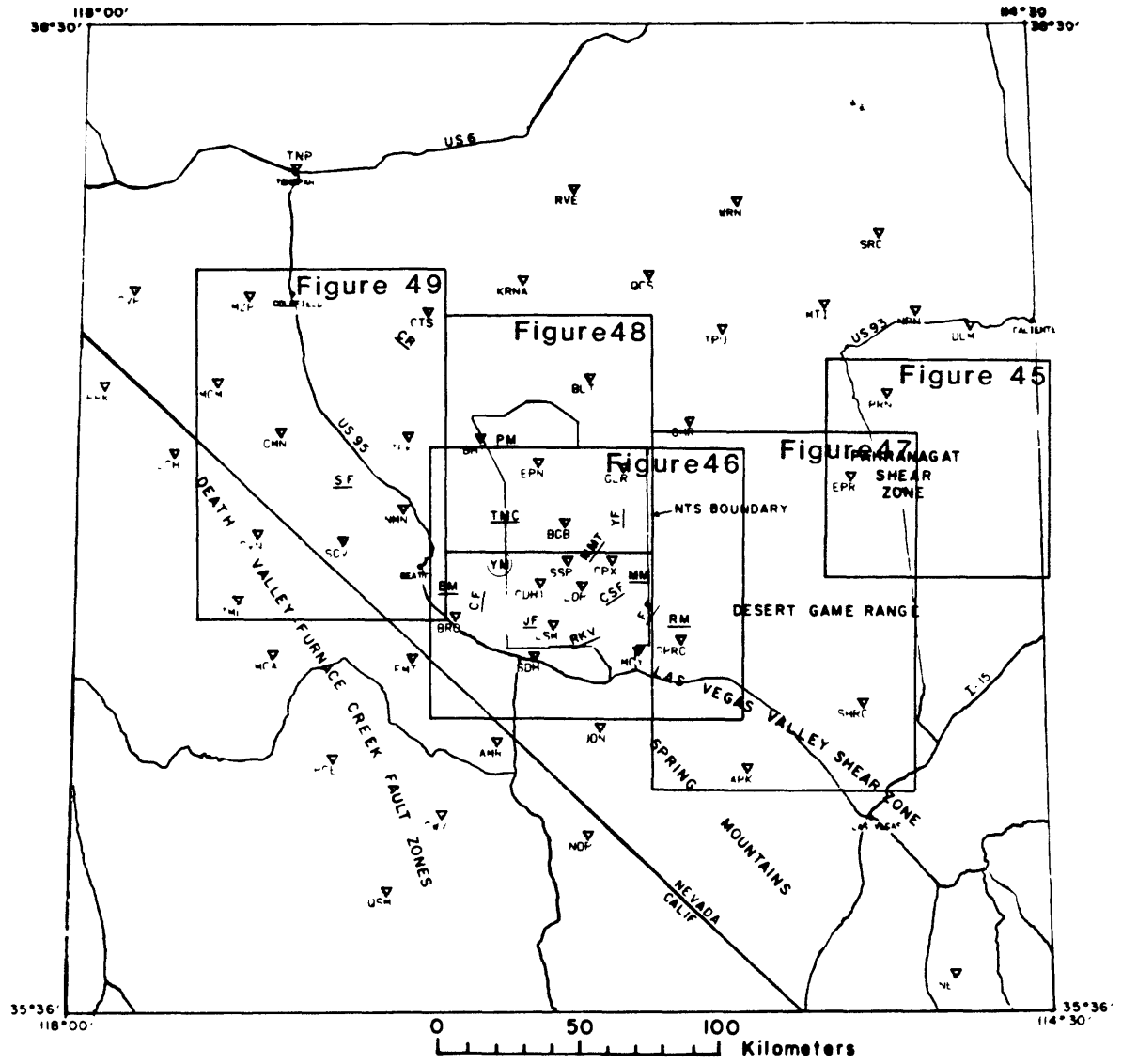

FIGURE 43

SEISMOGRAPH STATION LOCATIONS FOR THE CURRENT NETWORK AND LOCATIONS OF DETAILED SEISMICITY MAPS.

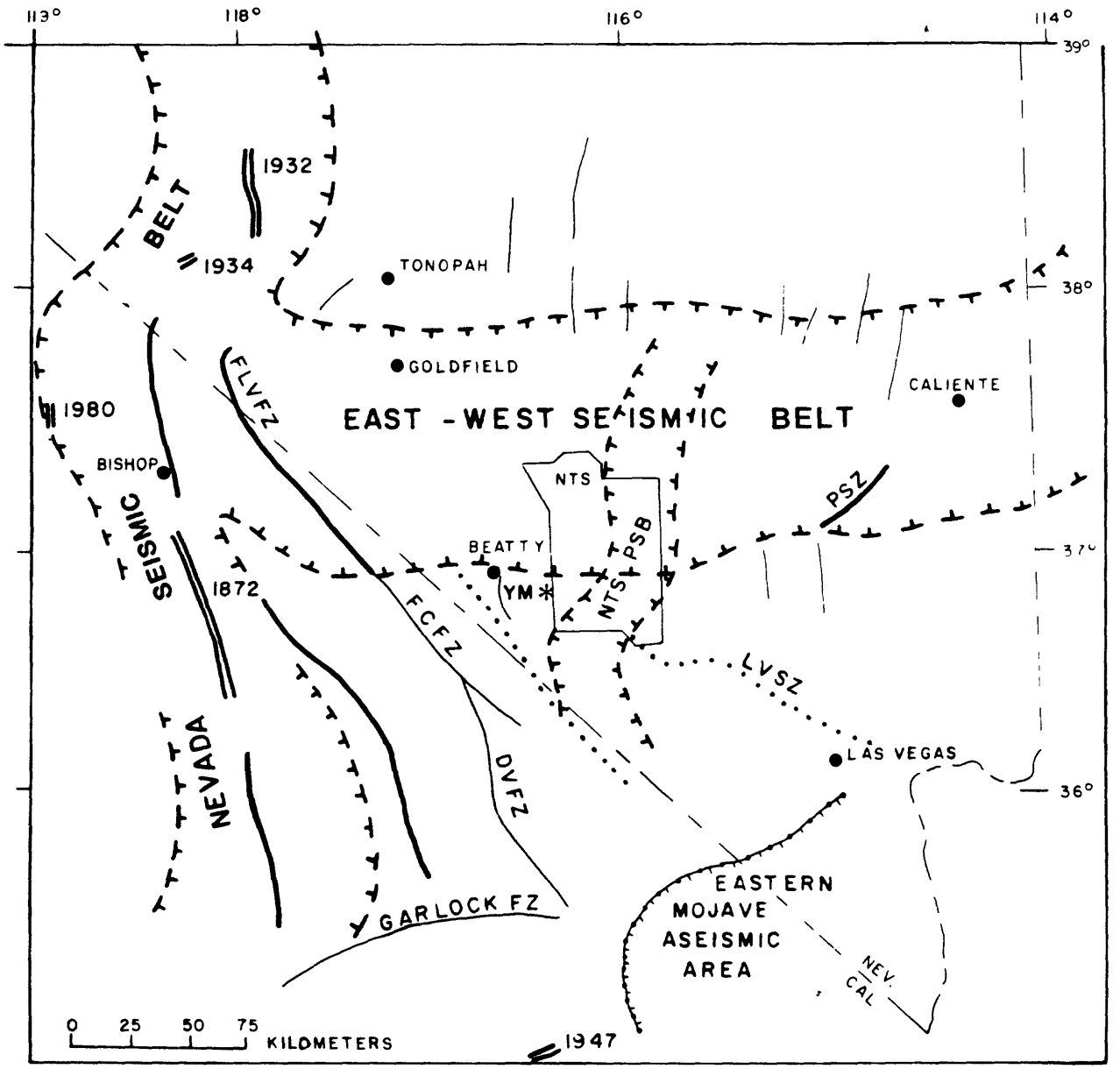

EXPLANATION

1872 Historic rupture, year

Seismically active **Quaternary Fault Zone**

Seismically inactive **Quaternary Fault Zone**

Seismically inactive **pre- Quaternary Fault Zone**

Eastern Mojave aseismic area

* YM Yucca Mountain

FLVFZ - Fish Lake Valley fault zone

FCFZ - Furnace Creek fault zone

DVFZ - Death Valley fault zone

LVSZ - Las Vegas Valley Shear zone

PSZ - Pahranagat Shear zone

NTSPSB - Nevada Test Site Paleoseismic Belt

- Outline of Major Seismic Zone

FIGURE 44

GENERALIZED TECTONIC MAP OF THE SOUTHERN GREAT BASIN SHOWING MAJOR SEISMIC BELT AND FAULT ZONES

caused by misreading times, incorrect association of a reading with the proper station, transcription errors, and key punching errors. The film records, however, continue to serve as a backup during periods when the computer fails.

The data collected by this network from 1978 through 1981 are discussed by Rogers and others (1983b) (some stations began operating in August 1978, and the network was fully operational in August 1979). Whereas most epicenter locations determined before 1979 had standard errors of ±7 km or more and unknown focal depths (with the exception of earthquakes from several detailed studies), earthquake locations from the present network have a modal horizontal standard error of ±0.5 km and a modal depth standard error of ±1.0 km (Rogers and others, 1981; Rogers and others, 1977a). We estimate that all earthquakes that occur within this network with $M \geq 2.0$ to 2.5 and numerous smaller events are detected and located. This threshold can be contrasted to previous periods when only earthquakes of M>4 were located consistently. It is probable, although difficult to evaluate precisely, that all earthquakes at Yucca Mountain of M>0 can be detected and all earthquakes of about M>1.0 can be located using the current seismic network. We infer on the basis of data from two earthquakes and several blasts located at or near Yucca Mountain that the epicenter location errors for events of about M>1.0 should generally be in the range of 0.2 to 0.5 km horizontally and 0.6 to 1.0 km vertically. The actual errors will depend on the size of the earthquake, the number of stations recording the event, the earthquake depth, and the degree to which the crustal model used approximates the velocity structure beneath Yucca Mountain [see Rogers and others (1981) and Rogers and others (1983b) for details about the location procedures].

Earthquakes are widespread throughout the region, although there are quiescent or nearly quiescent areas roughly corresponding to those noted in the historical record [Figures 41, 42, and Plate 1 of Rogers and others (1983b)]. No earthquakes with M>4.3 have been detected during the current monitoring period. Most earthquakes occur in the upper crust with less than five percent of the events at depths greater than 10 km. The typical pattern is one of widespread diffuse seismicity punctuated by tight clusters of earthquakes. Each cluster of events generally contains one or more of the largest events recorded to date (M 4 to 4.3). Fewer earthquakes occur near the northern and southern margins of the network giving the appearance of a seismic bridge connecting the Intermountain seismic belt with the Nevada seismic

belt. This band of earthquakes, the East-West seismic belt first noted by Smith (1978) before the establishment of the current seismic network, is more evident on regional seismicity maps. Evaluation of data from the current network indicates that the East-West seismic belt is broader and more active than previously recognized. The tectonic significance of seismicity in this belt is not known.

Although the nuclear events at the Nevada Test Site have been removed from our catalogs and maps, earthquakes induced by nuclear explosions continue to occur at Pahute Mesa and Yucca Flat as shown in Figures 41 and 42. Research by Hamilton and others (1971) and Rogers and others (1977b) suggested that underground nuclear explosion aftershocks were restricted to within 6 to 14 km from ground zero. The number of aftershocks appears to decrease to the background level within less than 15 days after the detonation. However, no clear way of removing these aftershocks from the catalog has been devised. Furthermore, the aftershocks could represent release of tectonic stress that would have occurred eventually, but over a longer time period. A more detailed evaluation of this problem is planned and will be presented in a future report.

Except for aftershock activity, the most seismically active areas in the region are the Pahranagat shear zone, the Mine Mountain, Cane Spring, Rock Valley, Frenchman Flat fault systems, the Thirsty Canyon, Sarcobatus Flat, and western Gold Flat areas, and an area along the California-Nevada border near Gold Mountain [Figures 41, 42, and Plate 1 of Rogers and others (1983b)]. The Pahranagat shear zone, the Mine Mountain, Cane Spring, Rock Valley, and Frenchman Flat fault systems, and the Gold Mountain area are geologically and seismologically similar, because in each of these areas, a large percentage of the regional earthquakes are localized along major northeast-trending, left-lateral Tertiary faults. In the Pahranagat shear zone, the majority of epicenters appear to be associated with short north- to north-northeast-trending fault segments located between the major northeast-striking shear zones (Figure 45). These epicenter locations, together with the two focal mechanisms in the Pahranagat Range area, suggest that the mode of faulting is right-lateral strike slip on north-trending faults. No surface faulting of Holocene age and probably none of late Quaternary age is known in the Pahranagat Range area (Ekren and others, 1977). However, the linear topography appears to be controlled by faulting, which could have occurred by many small incremental displacements that formed no distinct fault scarp.

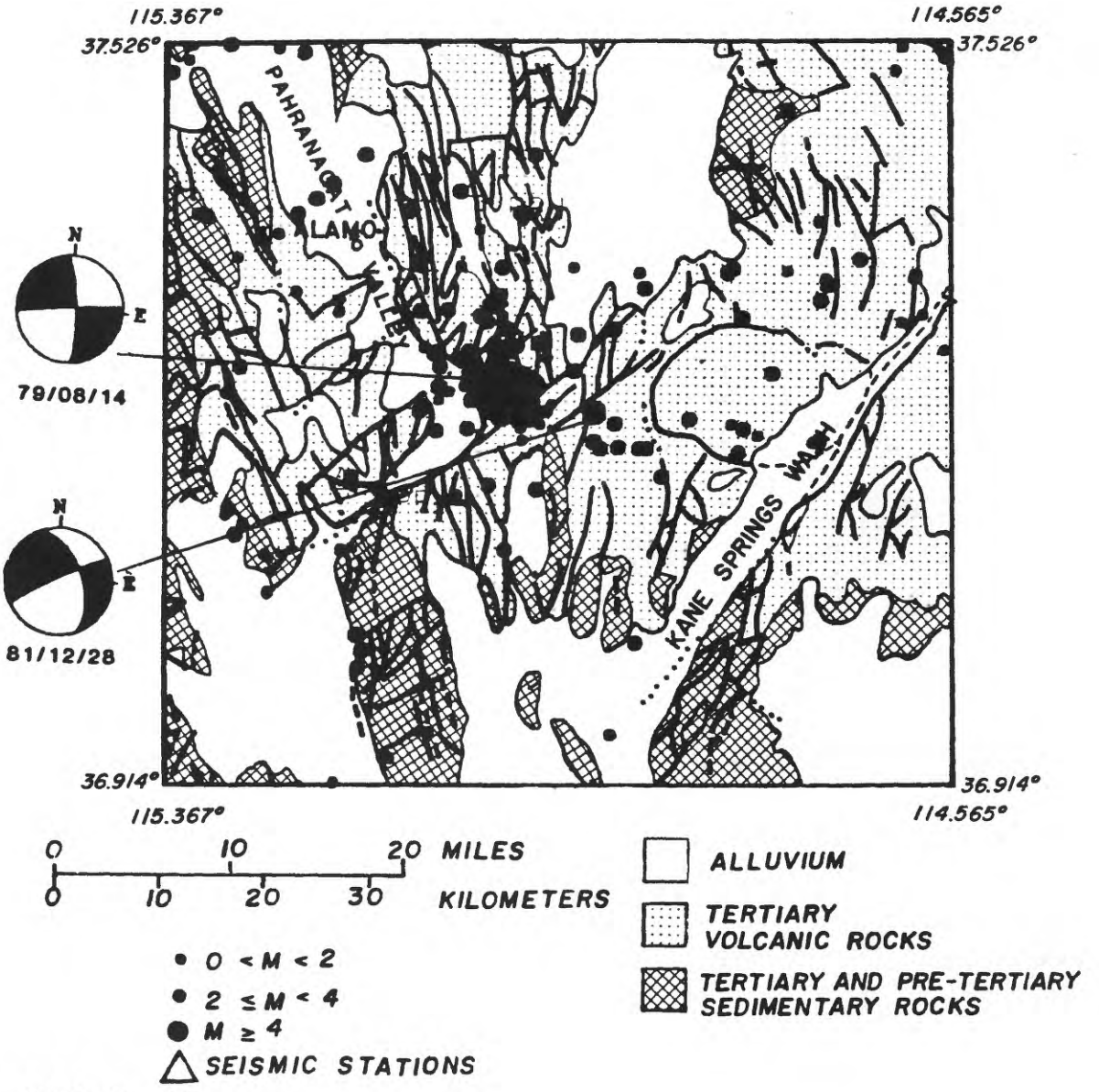

FIGURE 45

EARTHQUAKE EPICENTERS AND FOCAL MECHANISMS IN THE PAHRANAGAT SHEAR ZONE FROM AUGUST 1978 THROUGH 1982

Epicenters for seismic events occurring at the Nevada Test Site and in immediately surrounding areas are depicted in Figure 46. An earthquake for which a strike-slip focal mechanism was determined occurred beneath Frenchman Flat (B on Figure 46). The northwest-trending Yucca-Frenchman shear zone, a zone characterized by the right-lateral bending of structural trends in the area, passes about 2 km to the northeast of the epicenter of this event. Faults on the north side of the Yucca-Frenchman shear zone trend northerly and faults on the south side of the shear zone trend northeasterly. The north-trending focal mechanism fault plane for earthquake B on figure 46 coincides with the structural grain of mapped faults on the north side of the Yucca-Frenchman shear zone. The east-northeast-trending plane agrees with the structural grain to the south of the shear zone. Because alluvium covers the area around the epicenter, it is not possible to select unequivocally the correct fault plane solution in this case, but displacement was strike slip. Strike-slip focal mechanisms with fault plane solutions similar to those determined for the Frenchman Flat event described above, were also determined for two historical earthquakes in the area surrounding Frenchman Flat, the 1971 Massachusetts Mountain earthquake and the 1973 Ranger Mountain event (both M=4). Carr (1974) favored an east-northeast striking fault plane solution for the 1971 earthquake, which occurred approximately 4 km north of earthquake B on Figure 46. A preferred focal plane could not be chosen for the 1973 earthquake (Carr, 1974).

The focal mechanism determined for an earthquake with an epicenter located in Jackass Flats, near the projection of the surface trace of the Mine Mountain fault, (C on Figure 46) also indicates strike-slip. However, neither nodal plane is compatible with movement on the Mine Mountain fault in spite of the proximity of the epicenter and the fault. The lack of definition in hypocenters (not shown) precludes selection of the fault plane from the two nodal planes.

A strike-slip focal mechanism was determined for an earthquake near Lookout Peak (A on Figure 46) that could be associated with right-lateral motion on one of several mapped north-trending faults. Some earthquakes south of Little Skull Mountain and events northwest of Mercury occur on or near the trace of the Rock Valley fault and near the projected intersection of the Cane Spring and Rock Valley faults, suggesting association with those structures. The occurrence of earthquakes in the Rock Valley and Cane Spring shear zones,

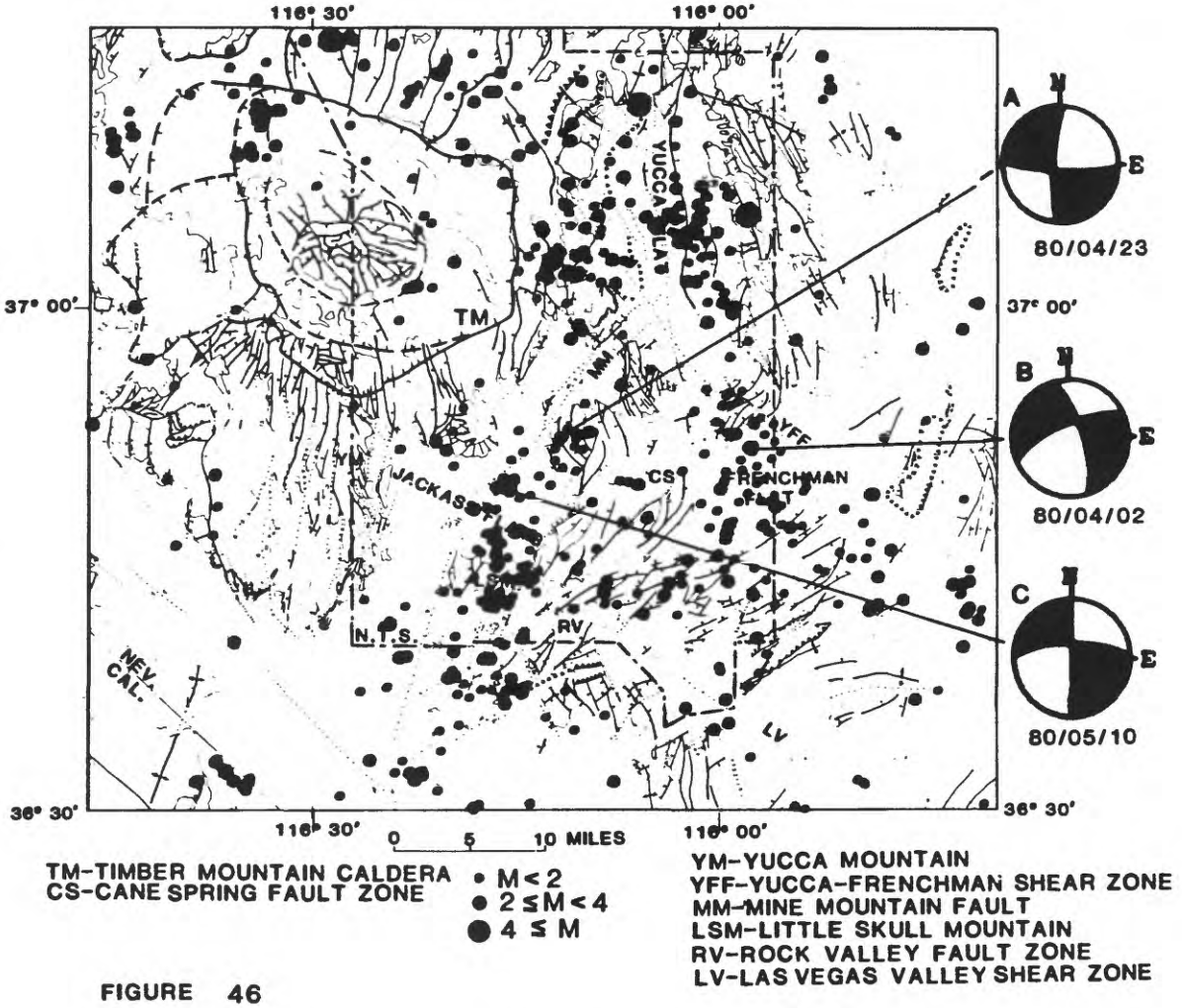

FIGURE 46

EARTHQUAKE EPICENTERS AND FOCAL MECHANISMS IN THE YUCCA MOUNTAIN, JACKASS FLATS,FRENCH FLAT,AND YUCCA FLAT AREAS FROM AUGUST,1978 THROUGH DECEMBER 1982.

however, provides only modest evidence that the main faults are active in these zones. Focal mechanisms with nodal plane orientations matching the strike of the mapped faults would provide the most convincing evidence. However, few focal mechanisms have been possible for the earthquakes of the southern Nevada Test Site area because of the prevalence of small magnitude earthquakes there. It is generally known from studies of Quaternary fault scarps that earthquakes do occur on northeast-trending fault zones in the southern Great Basin. Examples of normal fault earthquakes on northeast-trending faults were observed on Pahute Mesa (Hamilton and others, 1971) and at Lake Mead (Rogers and Lee, 1976).

Fault plane orientations were determined on the basis of seismic data from Indian Springs Valley (Figure 47), Thirsty Canyon (Figure 48), and Sarcobotus Flat (B, C, and D on Figure 49). In these areas, north-striking nodal planes and earthquake epicenter alignments are interpreted as indicating right-lateral strike-slip on north-striking faults. Earthquake epicenters in the Thirsty Canyon area are close to a mapped north-trending fault trace.

A focal mechanism determined for a M=4.0 earthquake at Gold Mountain (A on Figure 49) indicates strike slip with a small normal component. The epicenter lies in an area of east- to northeast-striking faults, therefore the northeast-striking nodal plane with left-lateral strike slip is preferred.

Fault orientation appears to be more important than age in microearthquake occurrence in the Nevada portion of the southern Great Basin (Rogers and others, 1983b). Most northwest-trending faults are inactive, including the Las Vegas Valley shear zone and the La Madre fault zone bordering the Spring Mountains. Many faults or fault zones of north to northeast orientation, such as the Yucca fault, the faults flanking Bare Mountain, Rock Valley and Mine Mountain, the Pahranagat shear zone, and faults southwest of Gold Mountain, are active. The youngest surface displacement on these faults ranges in age from pre-Quaternary to Holocene.

Earthquake Depths

As noted previously (Rogers and others, 1981), earthquake focal depths in the southern Great Basin appear to have a bimodal distribution (Figure 50), with peaks in the number of earthquakes occurring at about 2 km and 5 km below sea level. Very few well-located earthquakes have depths greater than

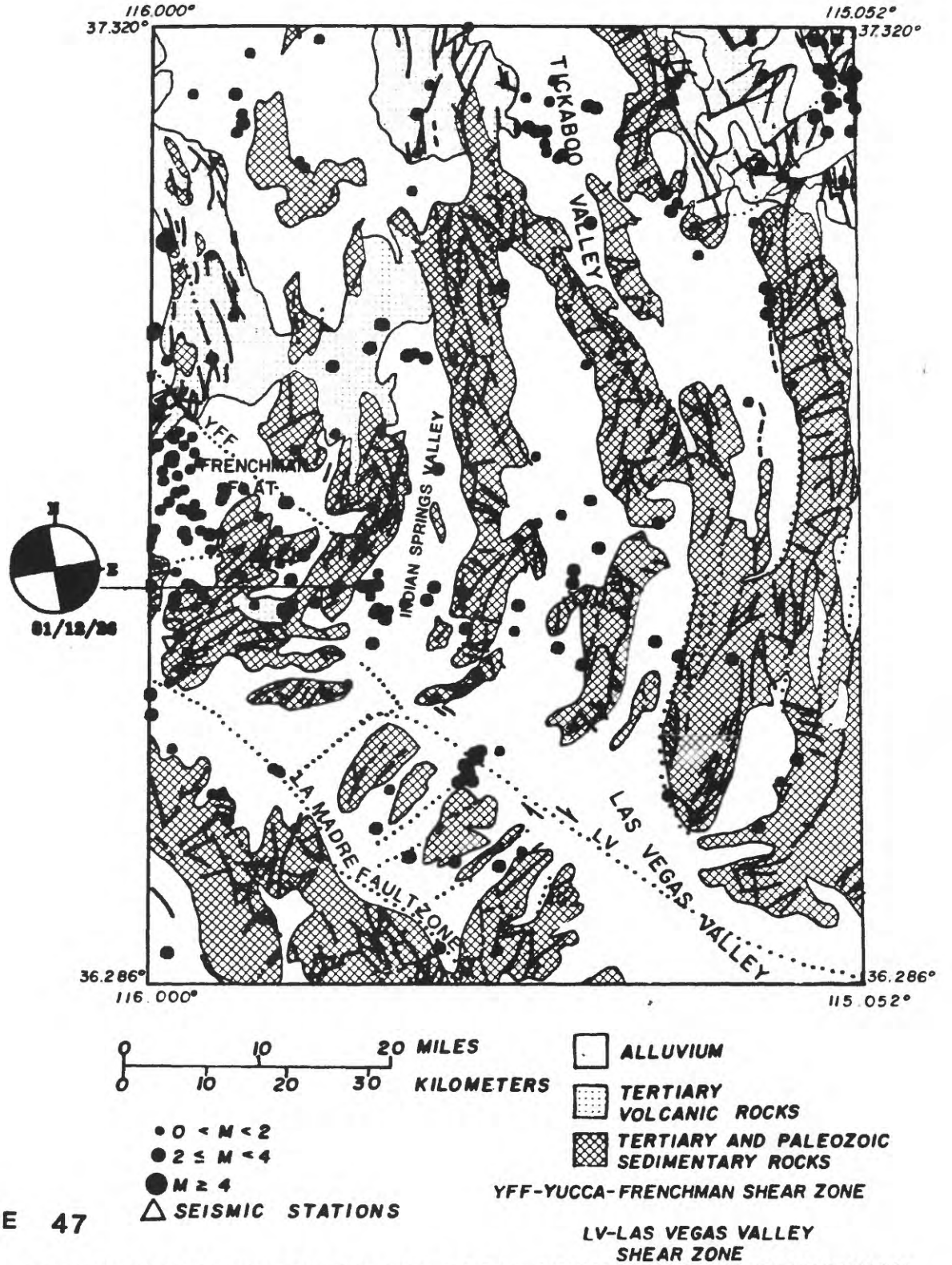

FIGURE 47

EARTHQUAKE EPICENTERS AND FOCAL MECHANISMS IN FRENCHMAN FLAT, INDIAN SPRINGS VALLEY, AND NORTHWESTERN LAS VEGAS VALLEY FROM AUGUST, 1978 THROUGH DECEMBER, 1982.

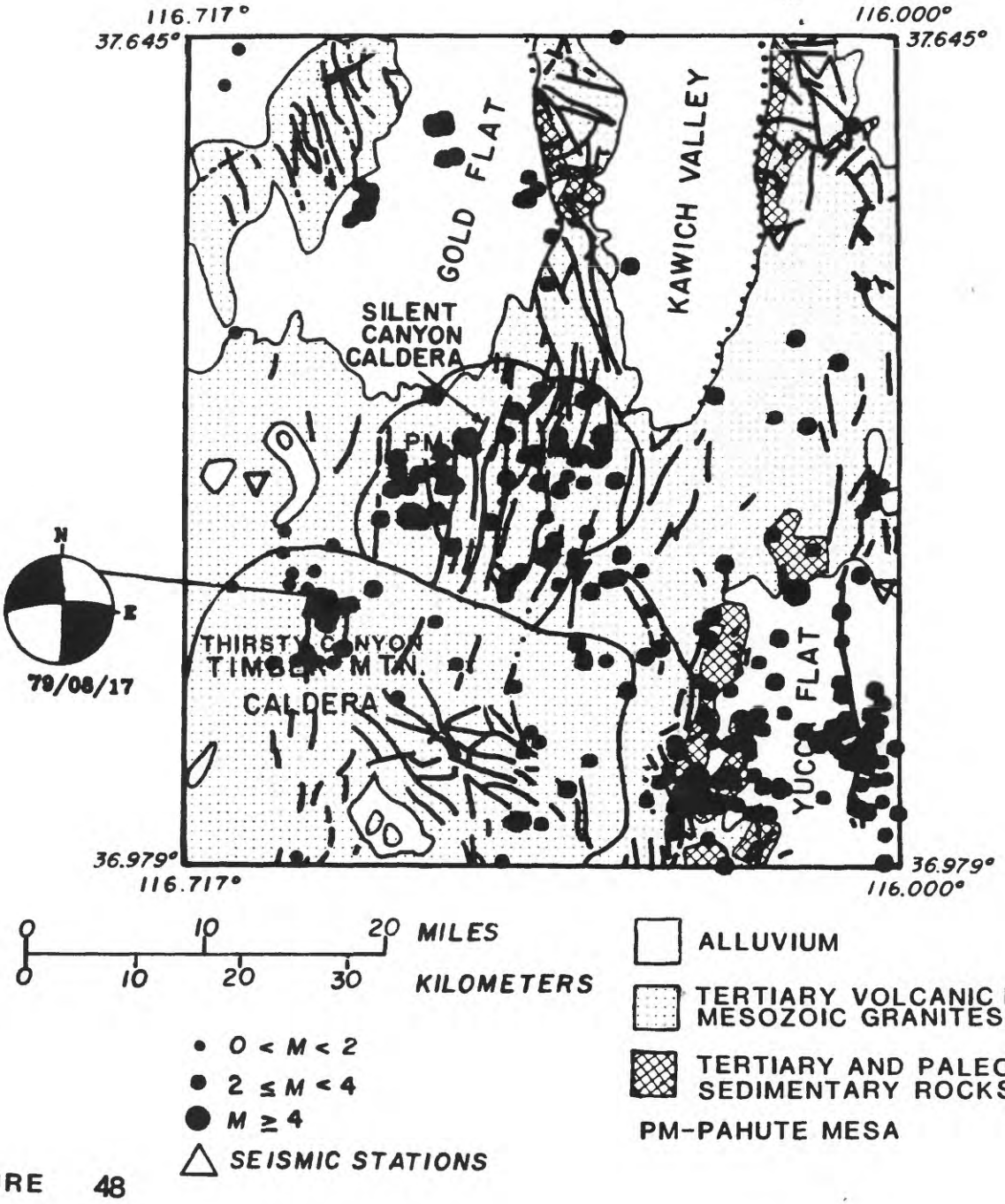

FIGURE 48

EARTHQUAKE EPICENTERS AND FOCAL MECHANISMS IN THE GOLD FLAT, KAWICH VALLEY, AND TIMBER MOUNTAIN AREAS FROM AUGUST, 1978 THROUGH DECEMBER, 1982

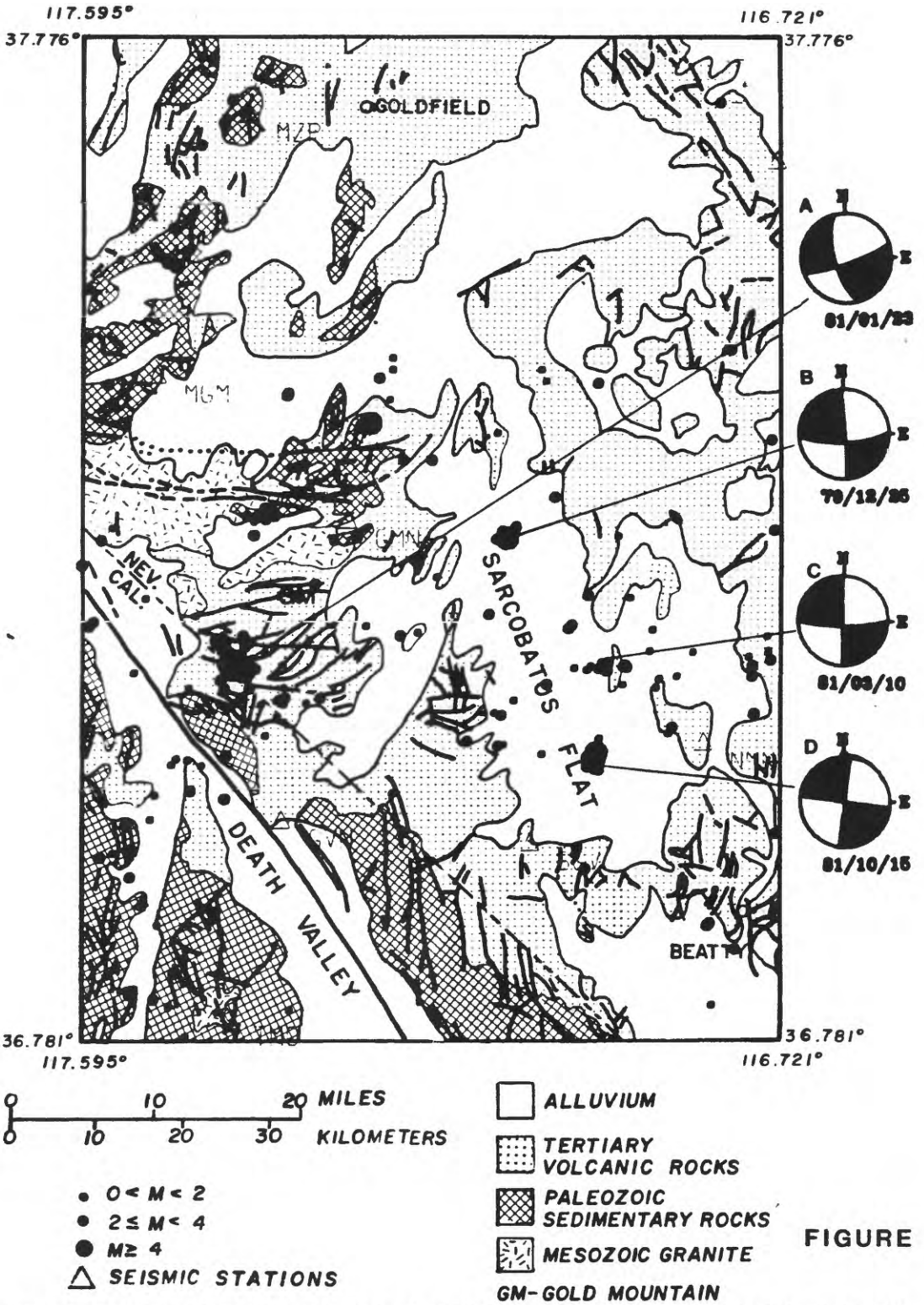

FIGURE 49

EARTHQUAKE EPICENTERS AND FOCAL MECHANISMS IN THE SARCOBATUS FLAT AND NORTHERN DEATH VALLEY AREA FROM AUGUST, 1978 THROUGH DECEMBER, 1982.

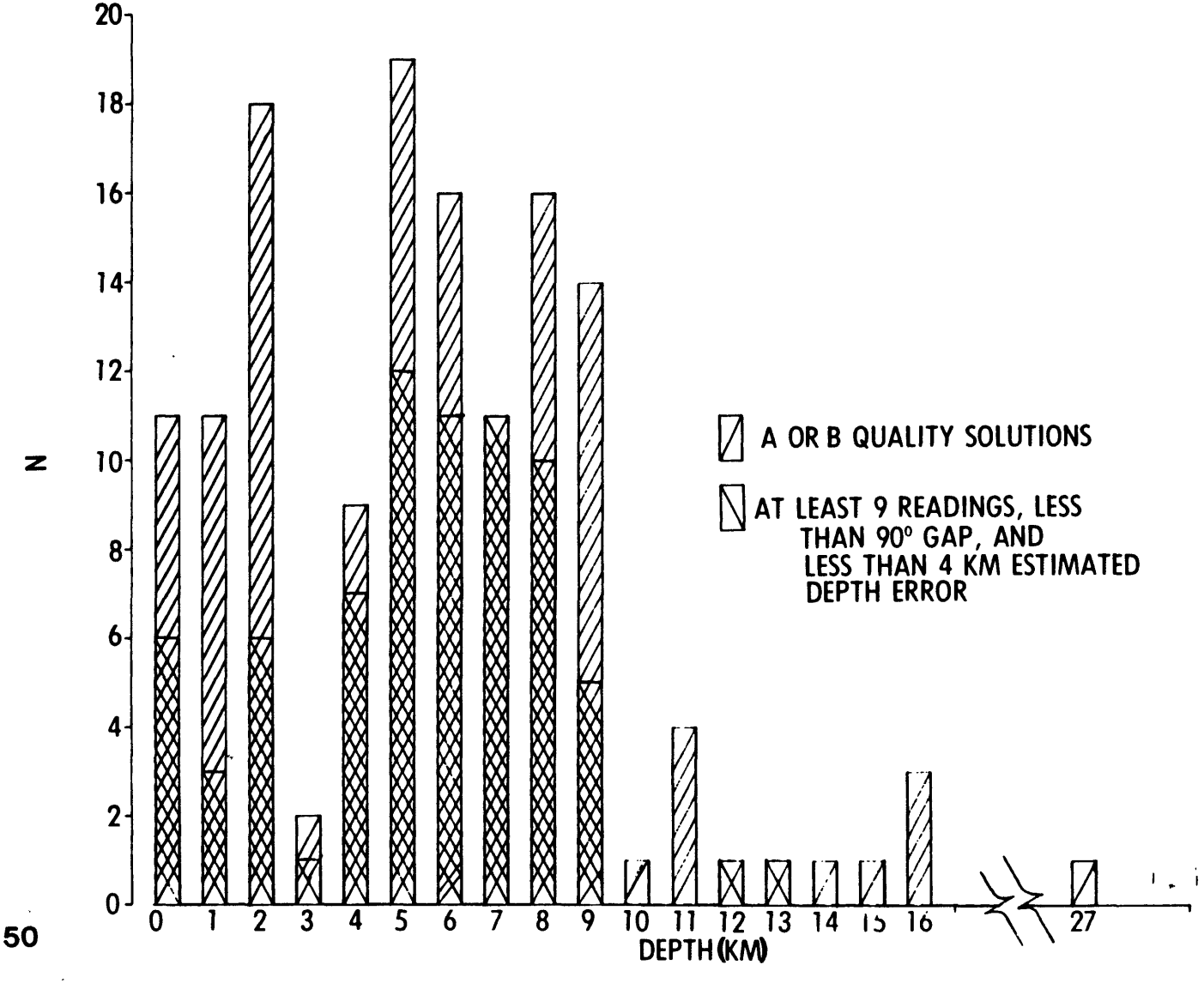

FIGURE 50

DISTRIBUTION OF FOCAL DEPTHS (relative to mean sea level) FOR STATISTICALLY WELL-LOCATED EARTHQUAKES IN THE SOUTHERN GREAT BASIN. BARS ARE SPACED APART FOR CLARITY, ALTHOUGH DEPTH INTERVALS ARE CONTINUOUS.

10 km. This pattern is persistent even though different crustal models have been employed and station delays are now incorporated into the location procedures. Some events within the shallower zone may be artifically constrained because of a layer boundary within that zone and the location procedure, but it is unlikely that this effect is important for all the earthquakes in that depth range because the peaks in the distribution do not occur at a layer boundary.

Most of the strike-slip mechanisms discussed above were determined for earthquakes occurring in the deeper active zone (4-9 km). Only two of the single event mechanisms have depths less than 5 km. The Thirsty Canyon and Sarcobatus Flat composite focal mechanisms are derived from earthquakes spanning both depth ranges. On the basis of this small sample, strike-slip faulting does not appear to be depth limited as was found for western Nevada (Vetter and Ryall, 1983).

Comparison of Seismic and Geologic Evidence for Active Faulting

The presence of seismicity along some fault zones with no recognized Quaternary displacement and the absence of seismicity in some areas of known Quaternary faulting show that the history of most recent surface displacements alone is not a reliable basis for evaluating potential seismic activity on a fault zone (Rogers and others, 1983b). Bedrock is exposed in many parts of the Candidate Area, and the Quaternary history of a fault cutting bedrock generally cannot be determined. Reconnaissance studies of faults cutting Quaternary deposits in the Site Vicinity have been completed (Swadley and Hoover, 1983; Swadley and others, 1984) and detailed studies of such faults are in progress, but at present the history of the most recent movement on most faults in the Candidate Area is not known. Seismic activity, therefore, remains as one of the best available indicators of active faulting even though high quality seismic data for the region only cover the past few years, and some areas that currently are seismically quiet are known to contain capable faults. Even in tectonically active regions, however, areas exist that have been stable for hundreds of thousands of years, as observed by Wallace (1978) in studies of young faulting in the northern Great Basin. Yucca Mountain and the areas to the west and south have been seismically quiet relative to some other parts of the Candidate Area throughout the historical record (Rogers and others, 1983b).

The current lack of small earthquakes on the northwest-trending Death Valley-Furnace Creek fault zone (Figures 41, 49; and Rogers and others, 1983b) is a paradox in that quiescence would be predicted there on the basis of the current stress orientation in the southern Great Basin, but the presence of numerous Holocene scarps along the fault zone indicates active faulting (Hunt and Mabey, 1966; Reynolds, 1969; Brogan, 1979). The geologic evidence for active faulting suggests that the stress orientation in the Death Valley region may be rotated in such a fashion as to be more favorable to faulting. A stress orientation more nearly like that in the region of the San Andreas fault than that in the southern Great Basin is required, possibly suggesting that the Death Valley-Furnace Creek fault zone is quiet because of relatively recent stress relief. The fault zone could be analogous to a section of the San Andreas fault zone that ruptured in 1857, but is presently quiescent.-

Zoback and Zoback (1980) concluded that a stress field with the least principal stress oriented more east-west than in the southern Greath Basin was likely in the Death Valley area; however, they placed the border of the area having such a stress orientation farther to the west. Walter and Weaver (1980) suggested that a change in the stress field orientation occurs between the San Andreas fault and Nevada Test Site on the basis of their study of the Coso volcanic field, 80 km west of Death Valley. Earthquakes in the Coso field were interpreted as occurring by right-lateral strike-slip on northwest-striking faults and normal faulting on north-striking faults. Because the geologic evidence suggests that the area characterized by an easterly trending least principal stress may extend to the Death Valley-Furnace Creek area, a stress rotation should occur between Death Valley and the Site, where the orientation of the least principal stress appears to be more northwesterly.

Seismic data for the southern Great Basin suggest that north to northeast-striking faults are more seismically active than faults of other orientations (Rogers and others, 1983b). Focal mechanisms indicate that strike-slip faulting on north- or east-trending faults is common throughout much of the southern Great Basin, although normal faulting occurs on some northeast-striking faults. Both types of focal mechanisms indicate least principal stresses that are consistent with the regional tectonic stress field inferred from other data. These relationships suggest that fault orientation is important in assessing seismic hazard. The block-bounding faults at Yucca Mountain have a northerly strike, which is a favorable orientation for movement in the present stress field.

The potential for significant future seismic activity on faults near Yucca Mountain cannot be precisely determined. Stress measurements at Yucca Mountain indicate a possibility that certain faults may be near failure (Healy and others, 1982). Stress measurements at Yucca Mountain, however, provide data for only a few locations at shallow depths compared to the range of depth over which faults potentially could rupture. The stresses are calculated under assumptions that may or may not be realistic; for instance, earth homogeneity is assumed, and topographic effects are generally ignored. The coefficient of friction and the pore pressure used in stress calculations are both theoretical quantities.

Faults having orientation and style similar to those at Yucca Mountain exist on Pahute Mesa, where large nuclear tests have resulted in stress release on faults [see Wallace and others (1983) for a discussion]. Although movement on the faults at Pahute Mesa was induced by nuclear explosions, the length of rupture (as much as 10 km), the amount of fault displacements (in some cases exceeding 1 m), and the magnitude and depths of accompanying aftershocks indicate that these faults were stressed tectonically near the failure point, and slip was triggered by stress changes produced by the explosions.

Each seismically active area in the southern Great Basin generally displays seismicity over a full range of depths (up to about 10 km) for the statistically best located events. Earthquakes apparently are occurring on faults of significant vertical dimension, suggesting the potential for the occurrence of a large earthquake. There is no evidence that earthquakes in this region are occurring on listric faults, which might reduce the potential maximum magnitude of earthquakes and (or) change the ground motion hazard in some manner (Anderson and others, 1983). Historically, two M=6 earthquakes have occurred in the East-West seismic belt, and one of these events occurred as a strike-slip earthquake on a north-trending fault.

Although none of this information is conclusive, the combination of data, including the stress data, the historic seismicity of the region, the depths of earthquakes, and the indication from current seismicity that fault activity depends more on fault orientation than fault age, suggests that a potential exists for renewed movement on faults in the Yucca Mountain vicinity. If shear stress approaching that required for failure were to occur over a large area of a fault zone, resulting in significant displacement at the time of

failure, a large earthquake could be generated. Stresses also can be released aseismically by fault creep or as a series of small incramental movements. Scarps in the Great Basin, however, are produced by large earthquakes, not creep according to Bucknam and others (1980) and Crone (1983); there is little evidence that creep is a significant mode of stress release in the Great Basin (R. C. Bucknam, oral commun., 1983). Some Basin and Range scarps are known to have resulted from historic earthquakes approaching M=8. Significant creep on any of the numerous faults that are crossed by cultural features should be easily noted.

Seismicity of the Site

The north-striking faults that transect Yucca Mountain are considered to have the potential for slip in the current stress field on the basis of the data presented above, together with the strong association between earthquakes and faults of north to northeast strike. However, only two earthquakes (M=1.7, 1981; M=1.5, 1982; Figure 46) have been recorded during monitoring with the current seismic network (through December, 1982). These events have been identified as earthquakes (rather than dynamite blasts) on the basis of their depths (4 and 9 km) and the observation of dilatational first motions at some stations.

Natural Seismic Hazard

Assessment of the deterministic or probabilistic seismic hazard at Yucca Mountain due to earthquakes requires knowledge of one or more of the following: the sources of earthquakes, the recurrence rates of earthquakes in each source zone, the peak ground motion values generated at the source, the rate of decay of ground motion with distance from the source, and the effects of heterogeneous ground conditions at the Site on ground motion. More sophisticated design analyses might also require knowledge of ground motion time histories at the Site, i.e., a record of ground acceleration versus time; however, only the peak horizontal acceleration on rock is considered as the hazard parameter of interest in the following discussion.

Seismic hazard analysis for the Candidate Area is difficult because many requirements necessary for evaluation of the seismic hazard are ill-defined or

unknown. The natural background rates of seismicity cannot be unequivocally established because of the heterogeneity of the seismic record in space and time. Acknowledging these constraints, Rogers and others (1977a) computed a preliminary seismic hazard analysis by considering several hypotheses about seismic rates that were estimated to bound the true rate. While this is a viable approach, acceptance of the most extreme hypothesis could lead to unnecessarily conservative design accelerations to attain an acceptable level of risk. The two principal hypotheses assessed by Rogers and others (1977a) were (A) that all earthquakes within 400 km of the Nevada Test Site can be used to establish the rate per unit area at each magnitude level (after corrections for incompleteness of the catalog); and (B) that earthquakes in the Great Basin exclusive of the Nevada seismic belt should be used to establish seismic rates in the Candidate Area. Hypothesis A may be an upper bound because it includes earthquakes of the Nevada seismic belt as well as other active areas of California and also events in southern Utah. These seismic rates are moderated somewhat by the fact that they are averaged over areas, such as the eastern Mojave Desert and northeastern Nevada, that are likely to be less active than the Candidate Area. Hypothesis B may underestimate seismic rates in the Candidate Area because the Candidate Area may be generally more active than the Great Basin on the average (exclusive of the Nevada seismic belt) because it probably lies within the East-West seismic belt.

In the following, we deterministically estimate the maximum horizontal peak surface acceleration expected at a Yucca Mountain site underlain by rock and then, under alternative probabilistic hypotheses, we estimate the seismic hazard (defined as the probability of exceeding a stated acceleration in a given exposure period) associated with this peak acceleration. These estimates are based on the work of Rogers and others (1977a). Table 7 lists faults that are thought to present the greatest hazard to the Site. The most likely maximum magnitude for earthquakes expected on those faults are calculated using the relationship

$$M = 5.56 + \log_{10}(L)$$

where L = rupture length in kilometers (Mark and Bonilla, 1977), assuming conservatively, that the full mapped length of the fault will rupture. Peak accelerations at the Site due to each hypothesized event were calculated using the Schnabel and Seed (1973) attenuation curves and the shortest distance from

TABLE 7

DETERMINISTICALLY COMPUTED PEAK ACCELERATIONS AT THE SITE FOR EARTHQUAKES ON POTENTIALLY ACTIVE FAULTS IN OR NEAR THE CANDIDATE AREA

Fault Name	Shortest Distance to Site (km)	Length (km)	Magnitude (M)	Maximum Expected Peak Acceleration at Site (g)
Bare Mountain	14	17	6.8	0.4
Mine Mountain	20	10	6.6	0.3
Wahmonie	23	10	6.6	0.2
Beatty	24	17	6.8	0.2
Rock Valley #1	26	15	6.7	0.2
Rock Valley #2	31	10	6.6	0.2
Rock Valley #3	42	10	6.6	0.1
Amargosa Valley	33	12	6.6	0.2
Carpetbag	38	12	6.6	0.1
Yucca and Boundary	40	38	7.1	0.2
Keane Wonder	43	25	6.9	0.1
Furnace Creek	51	42	7.2	0.1
Death Valley - Fish Lake Valley	51	175	7.9	0.2
South Death Valley				
East Side	51	120	7.6	0.2
West Side	75	100	7.5	0.1
Kawich Valley	59	33	7.1	0.1
Pahrump	60	38	7.1	0.1
Emigrant Wash	63	20	6.9	0.08
Resting Spring	75	10	6.6	0.05
Ubehebe - Emigrant Wash	80	70	7.4	0.08

TABLE 7 (Continued)

DETERMINISTICALLY COMPUTED PEAK ACCELERATIONS AT THE SITE FOR EARTHQUAKES ON POTENTIALLY ACTIVE FAULTS IN OR NEAR THE CANDIDATE AREA

Fault Name	Shortest Distance to Site (km)	Length (km)	Magnitude (M)	Maximum Expected Peak Acceleration at Site (g)
Panamint Valley				
East Side	95	100	7.5	0.07
West Side	104	40	7.2	0.04
Stonewall Mountain	93	10	6.6	0.03
Saline Valley	101	50	7.2	0.05
Sand Spring Valley	103	25	6.9	0.04
Pahroc	130	32	7.1	0.03
Sheep Range	113	35	7.1	0.03

the fault to the Site. The largest values of the most likely maximum magnitudes determined in this manner are M 7 to 8, and the resulting largest value of the most likely peak acceleration at the Site is approximately 0.4 g, which is produced by an M 6.8 earthquake on the Bare Mountain fault. Should active faults of the length of the Bare Mountain, Rock Valley, or Mine Mountain faults be discovered closer than about 15 km from the site or should the potential for damaging earthquakes exist at the Site, considerably larger accelerations are possible.

Figure 51 shows the computed acceleration return periods and acceleration hazard for a 30-year exposure time (Rogers and others, 1977a). These curves are based on the alternative probabilistic hypotheses (as outlined above; hypotheses A and B) that uniformily apply the observed historical rates of seismicity (corrected for incompleteness) over the region, including Yucca Mountain. The result of these computations shows that the peak deterministic acceleration of 0.4 g has a return period between 900 (Hypothesis A) and 30,000 (Hypothesis B) years. In a 30-year period, the probability that 0.4 g will be exceeded is between 3.3×10^{-2} (Hypothesis A) and 1.0×10^{-3} (Hypothesis B).

Improvement in the accuracy of the seismic hazard estimates can be made in conjunction with improved estimates of the extent of tectonically active areas and faults and their seismic rates. The assumption by Rogers and others (1977a) that seismic rates should be distributed over a region of 503,000 km^2 spanning several tectonic zones is less desirable than the specification of distinctive tectonic zones, faults, and associated seismicity because it is not known whether generalized models actually do bound the seismic hazard. An updated hazard map will be produced for the Candidate Area that will incorporate revised tectonic zone boundaries on the basis of (1) current models of deformation; (2) incorporation of active fault zones; (3) reevaluation of seismic rates by comparision of current seismicity with historic rates and rates inferred from study of Quaternary faults; and (4) modified acceleration attenuation laws. These improvements will be possible largely because of the expanded data base provided by ongoing seismic network studies.

The following conclusions can be drawn about seismicity and seismic hazard in the Candidate Area:

1. Over 2,100 earthquakes have been located within the network from 1979 through 1982; magnitudes ranged between 0 and about 4. The occurrence of

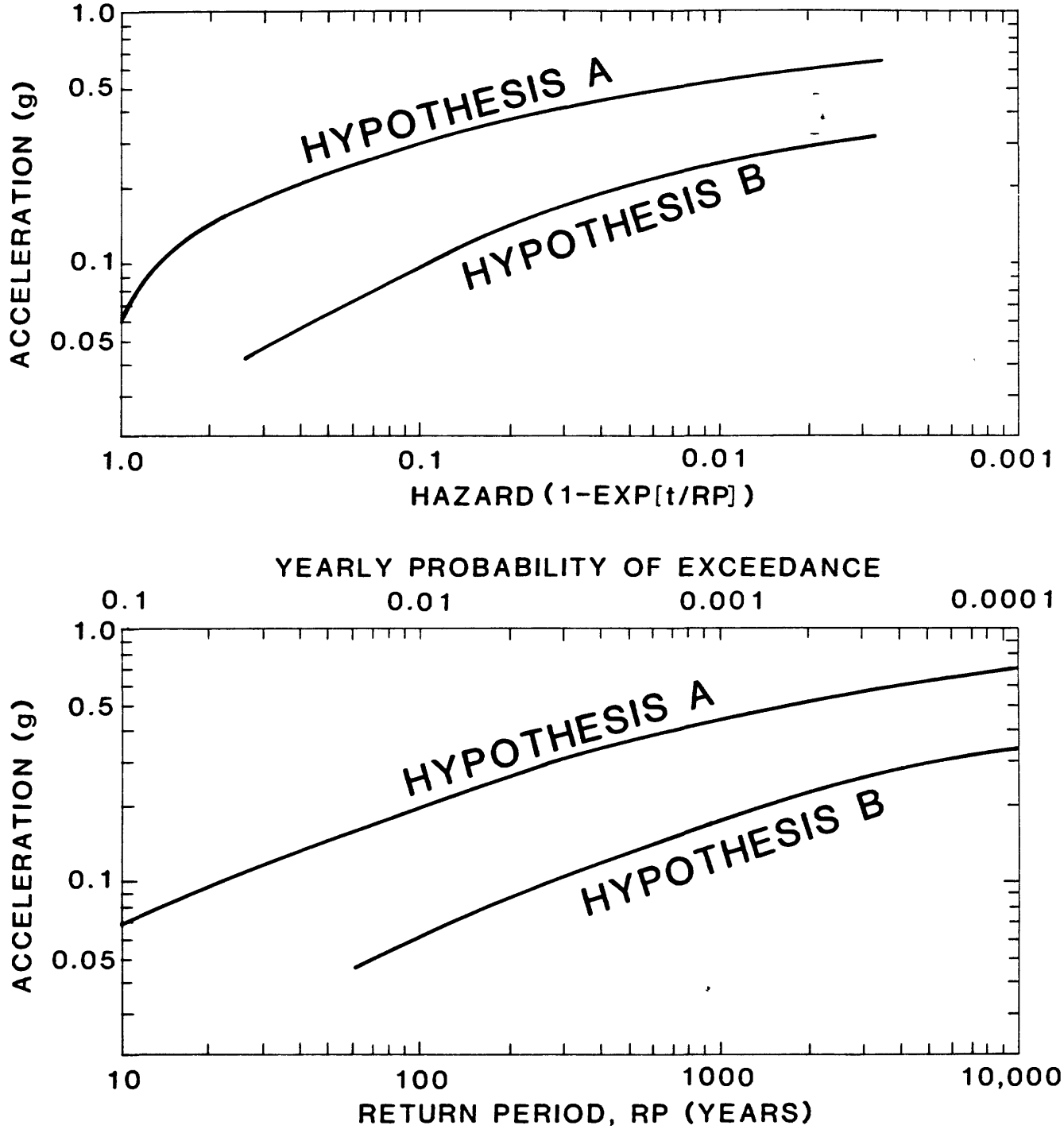

FIGURE 51
PEAK ACCELERATION VERSUS HAZARD AND RETURN PERIOD VERSUS ACCELERATION FOR HYPOTHESES A AND B (from Rogers and others, 1977a)

earthquakes is widespread in the southern Great Basin confirming the existence of the East-West seismic belt, first noted in the historical record, connecting the Intermountain and Nevada seismic belts.

2. The pattern of seismicity is characterized by a diffuse background level of earthquakes, punctuated by several areas of more compact and intense activity. Some of these concentrations of earthquakes have occurred as foreshock-main shock-aftershock series (M_L=4 main shocks), and others have had no distinguishing event.
3. The most seismically active areas occur in regions of major Tertiary northeast-trending left-lateral shear. Three important areas in this catagory are the Pahranagat, southern Nevada Test Site, and Gold Mountain shear zones. Although some earthquakes are probably occurring on the northeast-trending faults, the larger earthquakes in these areas, for which focal mechanisms are available, have occurred on shorter intervening fault segments with a north strike.
4. Seismicity also occurs in some north-trending fault zones. These earthquakes occur on or near segments of north-trending faults such as the Thirsty Canyon, Yucca, and Pahute Mesa faults (north-northeast trending) or are visible as north-trending epicenter lineations such as at Indian Springs Valley and Sarcobatus Flat.
5. Yucca Mountain lies within a broad area of low-level seismicity extending on the west to the Funeral Mountains, on the south to the Black Mountains and Nopah Range. Another region of relative quiescence extends from near Gold Flat to Tonapah.
6. Focal mechanisms, epicenter lineations, and epicenter-fault associations indicate that earthquakes occur principally as right-lateral strike-slip events on north-trending faults. A focal mechanism for an M=6 earthquake near the Nevada-Utah border in 1966 also indicated strike slip on a north-northeast-trending fault. Two M=4 earthquakes in 1971 and 1973 in the southeast Nevada Test Site were strike slip. Artifically induced earthquakes at Pahute Mesa and Lake Mead are either strike slip on north-trending faults or normal faulting on northeast-striking faults, indicating the likelihood that the northeast-trending faults are also active or potentially active.
7. A least principal stress with northwest orientation, and a greatest and intermediate principal stress of about equal magnitude are implied by the

results to date. With this stress configuration, faults of northwest orientation are less likely to produce earthquakes, a result that is supported by the current and historic seismicity, and by scarcity of northwest-striking Quaternary fault scarps east of Death Valley. The Death Valley-Furnace Creek, La Madre, and Las Vegas Valley shear zones are not presently producing earthquakes, although the presence of Holocene scarps on the Death Valley-Furnace Creek fault zone suggest that present quiescence there may be due to causes other than fault orientation.

8. From the historical seismicity of the southern Great Basin (two earthquakes of M=6) and length of active faults, a maximum magnitude of M 7-8 is inferred for earthquakes in the Yucca Mountain region. Earthquake depths range between 0 and about 10 km; very few well-located events are deeper than 10 km. The wide range of focal depths suggests that faults in the southern Great Basin have large surface areas and extend to considerable depth, which would make them capable of producing large earthquakes.

9. Only two earthquakes have been located at Yucca Mountain in about two and one half years of intensive monitoring. Some faults at Yucca Mountain are oriented such that slip, similar to that resulting from historic and present seismicity on other north- to northeast-trending faults in the southern Great Basin, is possible in the present stress field.

10. The most probable peak acceleration at the Site calculated under deterministic assumptions is 0.4 g assuming that faults at the Site area are inactive, and is based on the full-length fault rupture (M=6.8) of the Bare Mountain fault, which is 14 km west of the Site.

11. Using seismic rates believed to be an upper bound on rates for the Yucca Mountain region (Hypothesis A) and assuming a uniform distribution of seismicity, the deterministically estimated most likely acceleration at Yucca Mountain (0.4 g) has less than a four percent probability of being exceeded during a 30-year period.

LONG-TERM REGIONAL STABILITY WITH RESPECT TO TECTONIC AND GEOLOGICAL PROCESSES

Predictions of long-term stability at the Site are hampered by incompleteness of data. Most studies of the tectonic and geologic processes that might affect future stability are still in progress; however, volcanic hazard studies are nearly complete.

Seismically, the Site itself has been relatively quiet, but seismic activity in this part of the Great Basin has been carefully monitored for only a few years. Probability calculations of long-term seismic activity are limited by the incompleteness and inaccurancy of data and by the uncertainty in interpreting limited data. The Site is surrounded by several belts characterized by relatively high rates of seismic activity, and the region as a whole must be regarded as seismically active.

Studies of the spatial and temporal patterns of faulting, on which predictions of future tectonism must be based, are also incomplete. Landforms in the Site Vicinity suggest relatively youthful tectonism. Some faults at the Site have demonstrable Quaternary offset. Although Holocene displacement has not been demonstrated for any of the faults at the Site, neither can the absence of Holocene movement be demonstrated for all of the faults. Faults having possible Holocene surface displacement occur as close as 15 km west of the Site, and faults with known Holocene movement occur in Death Valley and Yucca Flat. Several faults with no evidence of Holocene surface rupture in the Site Vicinity and Candidate Area are the sites of present-day seismic activity. Lack of surface rupture is not sufficient evidence to discount active faulting. Northerly striking faults in the Site may be susceptible to movement in the current regional stress regime, but further study is necessary to understand the significance and implications of the limited hydraulic fracture and stress field data from the Site, especially with regard to tectonic stability and to hydrologic and mining conditions. Predicted accelerations at the Site from hypothetical maximum magnitude earthquakes on known faults in the Candidate Area do not appear to be great; however this assumes that faults at the Site would not move in response to such an event.

Volcanic Hazard

The perceived hazard of volcanism is based on the history of widespread and voluminous silicic and basaltic volcanism in the south-central Great Basin during Tertiary time and continued basaltic volcanism during the Quaternary. If ascending magma were to directly intersect a repository at the Site, there would be the possibility of local or regional dispersal of minor to significant quantities of radioactive waste elements by surface eruptions. Deposition of volcanic debris on top of the Site could make a repository at least temporarily inaccessible, make monitoring difficult, and could alter surface drainage. Injection of magma within the immediate vicinity of a repository could alter the geologic and hydrologic setting and change transport pathways of waste elements. The exact nature of future volcanic hazards would be dependent on (1) magma composition, (2) the presence or absence and depth of groundwater, (3) the geometry of magma at its intersection with the waste repository, and (4) the timing of the volcanic event with respect to decay time of waste in a repository. These factors have been discussed for volcanism in general by Crowe (1980) and Logan and others (1981) and are discussed briefly with respect to the Candidate Area by Crowe and Carr (1980).

Volcanic hazard assessment of the Candidate Area required an evaluation of: (1) future potential for hazards of silicic volcanism and (2) future hazards of basaltic volcanism. Crowe and Sargent (1979) examined the stratigraphy and geochemistry of the youngest (8 to 9 m.y. old) major volcanic center in the Candidate Area, the Black Mountain volcanic center located 50 km north of the Site. They noted that volcanism associated with this center represented a distinct episode of renewed silicic activity following cessation of the Timber Mountain-Oasis Valley magmatic cycle. This renewed activity suggests a finite, although probably very small, likelihood of recurrence of silicic volcanism, for a number of reasons:

(1) There has been no silicic volcanism within the Candidate Area for at least the last 6 m.y.

(2) There has been a regional decrease and in most areas a cessation of silicic volcanism within the central and southern parts of the Great Basin during the last 10 m.y.

(3) Silicic volcanic activity during Quaternary time has been restricted entirely to the margins of the Great Basin. Regionally dispersed airfall tuff from future eruptions of silicic centers in the western Great Basin could be deposited on the Candidate Area. However, such deposits would pose no recognized hazard to a repository.

Velocity structure of the crust and upper mantle was explored by teleseismic residual studies (Monfort and Evans, 1982). This method has proven useful in the detection of low-velocity magma chambers in the crust in other areas of young volcanism (Iyer and other, 1981). However, the station spacing and distribution of the southern Great Basin seismic network are not ideally suited for such work. Tentative conclusions for the Candidate Area are that (1) there is a low-velocity zone in the upper crust extending north-northeastward from Death Valley to the northern part of the Candidate Area, and (2) there is a general westward decrease in station delays across the central part of the Candidate Area, suggesting an eastward decrease in mantle velocity (Monfort and Evans, 1982). No major low velocity body, such as a magma chamber, was detected.

The Candidate Area contains a few low-temperature (50°C) thermal springs but no high temperature springs (Muffler, 1979, Map 1). Several heat flow measurements within the Candidate Area indicate low heat flow in comparison with surrounding regions. Much of the Candidate Area is within the Eureka Low, which has a heat flow of less than 1.5 heat flow units (Lachenbruch and Sass, 1977) compared to regional values. Absence of major high-temperature springs and generally low heat flow also suggest an absence of shallow magma bodies in the Candidate Area, a conclusion reached earlier by Blackwell (1978, Figure 8-4).

It is more difficult to define and assess the hazards of future basaltic volcanism. First, the nature of volcanic activity leads to extreme uncertainty in forecasting future rates. Forecasting rates of volcanism is based on projection of past rates (Crowe and others, 1982), but here the past is not the whole key to the future, for future volcanism may be influenced by changes in episodic processes that may not have affected past activity, such as changing rates or directions of plate motion. Second, the Candidate Area has had such a low rate of volcanic activity during Quaternary time that the Quaternary record may be a statistically insufficient guide to future activ-

ity. Third, the usability of data from pre-Quaternary volcanic activity is dependent on the degree of preservation and exposure of deposits and on the precision of techniques of age determinations. In these circumstances, a number of forecasting methods were used, combining procedures of hazard and risk assessment, and the results from each were compared for consistency. Assumptions were varied for each approach to examine the range of effects and provide conservatism. Research topics to date include:

Geology and geochronology
Tectonic setting
Eruptive history
Geochemistry and petrology
Probability calculations
Consequence analyses (including scenario development and radiation release calculations).

The first four topics are used to determine the history of volcanism and forecast future rates. Results from this work have been presented in earlier sections of this report. The last two topics are standard approaches for risk assessment.

Probabilities have been calculated for the likelihood of disruption of a repository at the Site by basaltic activity. The mathematical model used for the calculations is:

$$Pt = \exp^{-\text{lambda}(tp)}$$

Where Pt is the probability of no disruptive event before time t; lambda is the rate of volcanic events; and p is the probability of repository disruption, given an event. The parameter p is estimated as a/A, in which a is the area of the repository and A is some minimal area that encloses the repository and the area of occurrence of the volcanic events. A computer program finds either the minimum area circle or minimum area ellipse (defined as A) that contains the volcanic centers of interest and the repository site. This allows lambda to accommodate tectonic controls for the localization of volcanic centers, and attempts to constrain lambda to be uniform within the area of the circles or ellipses.

The rate of volcanic activity was calculated in two ways. The first was through determinations of the annual rate of magma production for the Candidate Area, through field studies and map measurements; examples are shown in Table 8. The second was through counts of volcanic cones similar to the procedure of Crowe and Carr (1980), but using refined age data. A significant finding from the studies of magma rate production (Vaniman and Crowe, 1981) is an apparent decline in the rate of magma production (surface eruptive products calculated as magmatic volume equivalents) for the Candidate Area during the last 4.0 m.y. This is consistent with a decrease in the rate of volcanic activity responsible for basaltic volcanism (Crowe and others, 1982). The average rate of magma production for the pertinent portion of the Candidate Area during the last 4.0 m.y. is 430 m^3yr^{-1} calculated as the average rate per year. A more reasonable rate based on a linear regression calculation that accounts for the decrease in rates of magma production is 210 m^3yr^{-1}. For comparison, the average rate of magma production for the island of Hawaii is about 108 m^3yr^{-1} (Shaw, 1980), and the rate of production of basalt during the previous 0.5 m.y. in the Coso Volcanic Field just west of the western edge of the Candidate Area is 2.8×10^3 m^3yr^{-1}.

Resulting probability values using the refined mathematical model were calculated for times of 1 year and 10,000 years. The annual probability of volcanic disruption of a waste repository located at Yucca Mountain falls in the range of 4.7×10^{-8} to 3.3×10^{-10}. These numbers can be used for probability bounds where the worst- and best-case approaches are defined by the extremes of the probability range. Collectively, the calculations indicate that the probability of volcanic disruption is very low, approximately one chance in 20 million to 3 billion per year.

Crowe and Carr (1980), Crowe and others (1983b) and Logan and others (1981) have investigated the consequences of volcanic activity should future basaltic magma intrude the Candidate Area and erupt at the surface. The major conclusions from these works are:

(1) Alkalic basalt has been the predominant product of volcanic activity in the Candidate Area during the last 8 to 9 m.y. and is likely to be the future product.

(2) Magmatic volumes of eruptions during this period were generally small (less than 0.1 km^3) and the eruptions were of short duration. Small

TABLE 8

DIMENSIONS OF THE QUATERNARY BASALTIC CENTERS OF THE NTS REGION

Volcanic Center	Height (m)	Width (m)	Cone Volume (m^3)	Flow Volume (m^3)	Vents (Number)	Total Magmatic Volume (m^3)*
Lathrop Wells	140	690	1.7×10^7	1.6×10^7	3	5.7×10^7
Little Cone No. 1	43	360	1.5×10^6	3.0×10^6	1	6.2×10^6
Little Cone No. 2	27	220	3.4×10^5	**	1	7.8×10^5
Red Cone	73	435	3.7×10^6	1.9×10^7	6	2.6×10^7
Black Cone	121	525	2.7×10^7	4.4×10^7	3	1.0×10^8
Sleeping Cone No. 1	63	240	2.7×10^6	4.9×10^6	1	1.1×10^7
Sleeping Cone No. 2	70	562	5.8×10^6	8.1×10^6	1	2.1×10^7

*Magmatic volume is equal to the volume of the cone, plus the volume of an inferred ash-fall scoria sheet, plus the lava volume corrected for magmatic density.

**Indicates no data.

volume basalt cycles of the Candidate Area reflect the low magma flux in this region during late Cenozoic time.

(3) Understanding of triggering mechanisms or of the specific conditions leading to generation of basalt magma is insufficient to predict future rates of basaltic activity.

(4) Basalt magma ascends rapidly through the upper mantle and crust (tens of centimeter per second) and mantle-derived basalt melts are likely to be trapped temporarily and to fractionate at the base of the crust. Magma rising directly from 35 km to the surface would require travel times ranging from 4 days to less than 1 day.

(5) Surface basalt centers are fed through narrow linear dikes with aspect ratios on the order of 10^{-2} to 10^{-3}. Two or three dikes are commonly associated with each basalt center. At some centers, shallow sill-like intrusions may form at shallow depths (200-300 m). The emplacement of intrusions beneath basalt centers may be favored by volatile-poor magma, by the presence of low-density tuff, and by the stress conditions associated with active extensional faulting.

(6) Basalt centers in the Candidate Area were predominantly formed by Strombolian eruptions. Major products are moderate-size scoria cones and relatively short lava flows (<2 km). Scoria fall sheets associated with the cones but removed by erosion probably extended for distances of 5 to 12 km.

(7) Phreatomagmatic eruptions have occurred at four basalt centers in the Candidate Area. Such eruptions are less likely at Yucca Mountain due to the combination of deep groundwater, the apprent lack of perched groundwater or local surface water, and the low flux of moisture in the unsaturated zone (Crowe and others, 1983b). The principle condition that could lead to increased concern about future phreatomagmatic activity could be the recognition of future development of perched groundwater.

(8) Waste incorporated in magmas would be dispersed by surface eruptions; the major pathway of contaminants would be through the pyroclastic component. Magma pathways can be approximated assuming that waste dispersal follows the dispersal patterns of lithic fragments studied in cone scoria. Thus, the greatest volume of dispersed waste would be in the scoria sheet, with lesser amounts dispersed with fine-grained (<65 microns) wind-borne particles and in a scoria cone.

(9) Potential doses of radiation to maximally exposed individuals, hypothetically living near the eruption or in houses built of scoria, would be a few millirems for eruptions 100 years after waste emplacement and less for later eruptions.

The combination of the low probability of repository disruption and the limited release consequences suggest that the risk of volcanism is low. The tectonic setting of basaltic volcanism in the Candidate Area, however, is not well understood and requires further study.

Faulting and Vertical Movements

Evidence of Quaternary and Holocene faulting in the region around Yucca Mountain, present-day seismicity, and an active extensional stress field require that the effects of renewed faulting at Yucca Mountain be carefully considered. The Site has been seismically quiescent over the brief monitoring period, and there is no unequivicol evidence for Holocene surface rupture at the Site itself. It is difficult, however, to assess the implications of these conditions in terms of future stability, because the Site is in a region of active faulting and little is known about the recurrence intervals for movement events on faults in the southern Great Basin. (For discussion of recurrence intervals for faults elsehwere in the Basin-and-Range Province, see, for example, Bell, 1981 and Wallace, 1979b). Holocene tectonic and seismic activity observed in the region surrounding the Site seems certain to continue, but predictions of the level of that activity and its effect on waste isolation at the Site must await completion of ongoing studies.

The potential for fault disruption of engineered barriers cannot be evaluated until the nature of such barriers is better defined. At this stage, it can only be said that ways to accommodate small fault displacements (1 m or less) and retard the propagation of fracture through waste containers should be included in barrier design.

Modification of the hydrologic system at and near the Site by renewed faulting within the required isolation period is another possiblity that must be evaluated. A preliminary assessment that future faulting probably would not seriously change the waste isolation capability of geologic barriers at the Site is based on the following qualitative observations:

1. The ambient stress field indicates that new or reactivated movement would be on north-northeast-striking, steeply-dipping normal faults, which are the most prominent existing faults. Until detailed studies of existing faults and fractures are complete, however, it would be fruitless to speculate on the new faults or fractures that might form and their effect on groundwater flow.
2. The permeability due to the present system of faults and fractures is aleady dominant over interstitial or matrix permeability in the saturated zone. The role of fracture permeability in the unsaturated zone remains to be fully understood, and studies are in progress.

SUBSURFACE DRILLING AND MINING

Before 1978, only two drill holes existed in the area of the Site: water wells J-13, 7 km east-southeast of the Site, and J-12, approximately 15 km southeast (Figure 3). In the period 1978-1981; 17 exploratory drill holes were completed at and near the Site to investigate the geologic, hydrologic, and geophysical characteristics of the subsurface rocks (Figure 22). Information concerning the construction of drill holes at the Site is maintained by the U.S. Department of Energy Nevada Operations Office.

Drill holes within the Site extend to depths ranging from 148.5 to 1,830 m; none has been sealed. Most of these holes were intended to be vertical, but drill holes UE25a-7 and USW-GA1 were intentionally inclined approximately 26° from vertical and directed S51°W and 90°W, respectively.

Holes drilled primarily for geologic information were continuously cored. To maximize core recovery and maintain hole stability, a polymer-based drilling fluid was used as a lubricant. The fractured nature of the rock did not permit circulation of the fluid to the surface, and considerable amounts of fluid were lost. On the average, 20,000 to 30,000 barrels of fluid were used to complete a hole 1,800 m deep.

In holes drilled mainly for hydrologic information, air-foam was used as a circulating medium to minimize the introduction of excessive amounts of drilling fluid that would alter hydraulic and geochemical properties. Fluid loss while drilling the hydrologic drill holes ranged from 4,000 to 30,000 barrels.

The Site is within an area of government-controlled lands, most of which have been restricted since the early 1950's to prevent public access, and the entire area has been mapped geologically and topographically by the U.S. Geological Survey. Consequently, there is little likelihood that other wells or boreholes than those listed or excavations other than shallow prospect pits exist at the Site.

REFERENCES

Agnew, D. D. and Sieh, K. E., 1978, A documentary study of the felt effects of the great California earthquake, 1857: Seismological Society of America Bulletin, v. 68, p. 1717-1730.

Albers, J. P., 1967, Belt of sigmoidal bending and right-lateral faulting in the western Great Basin: Geological Society of America Bulletin, v. 78, p. 143-156.

Anderson, R. E., Longwell, C. R., Armstrong, R. L., and Marvin, R. F., 1972, Significance of K-Ar ages of Tertiary rocks from the Lake Mead region, Nevada-Arizona: Geological Society of America Bulletin, v. 83, p. 273-287.

Anderson, R. E. Zoback, M. L., and Thompson, G. A., 1983, Implications of selected subsurface data on the structural form and evolution of some basins in the northern Basin and Range province, Nevada and Utah: Geological Society of America Bulletin, v. 94, p. 1055-1072.

Armstrong, R. L., and Suppe, John, 1973, Potassium-argon geochronometry of Mesozoic igneous rocks in Nevada: Geological Society of America Bulletin, v. 84, p. 1375-1392.

Armstrong, R. L., Ekren, E. B., McKee, E. H., and Noble, D. C., 1969, Space-time relations of Cenozoic volcanism in the Great Basin of the western United States: American Journal of Science, v. 267, p. 478-490.

Atwater, Tanya, 1970, Implications of plate tectonics for the Cenozoic tectonic evolution of western North America: Geological Society of America Bulletin, v. 81, no. 12, p. 3513-3535.

Baldwin, M. J., and Jahren, C. E., 1982, Magnetic properties of drill core and surface samples from the Calico Hills area, Nye County, Nevada: U. S. Geological Survey Open-File Report 82-536, 27 p.

Barnes, Harley, Cristiansen, R. L., and Byers, F. M., Jr., 1965, Geologic map of the Jangle Ridge quadrangle, Nye and Lincoln Counties, Nevada: U. S. Geological Survey Geologic Quadrangle Map GQ-363, scale 1:24,000.

Bath, G. D., Jahren, C. E., Rosenbaum, J. G., and Baldwin, M. J., 1983, Magnetic investigations: in Geologic and geophysical investigations of Climax stock intrusive, Nevada: U. S. Geological Survey Open-File Report 83-77, p. 40-77.

Bath, G. D., and Jahren, C. E., 1984, Interpretations of magnetic anomalies at repository site proposed for Yucca Mountain area, Nevada Test Site: U. S. Geological Survey Open-File Report, 84-120, 40 p.

Bayer, K. C., Mallis, R. R., and King, K. W., 1972, Earthquakes recorded by a seismograph network located in the southern Nevada region, January 1 to December 22, 1971: U. S. Department of Commerce Publication, National Oceanic and Atmospheric Administration, Technical Memorandum TM-ERL-ESL-16, 13 p.

Bayer, K. C., 1972, A preliminary seismicity study of the southern Nevada region for the month of July 1972: U. S. Department of Commerce, National Oceanic and Atmospheric Administration, Earth Sciences Laboratories, Report prepared for U. S. Atomic Energy Commission, NVO-746-4, Contract AT(29-2)-746, 9 p.

Bayer, K. C., 1973a, Seismic data report southern Nevada region December 22, 1971-December 31, 1972: U. S. Department of Commerce, National Oceanic and Atmospheric Administration, Technical Memorandum TM-ERL-ESL-24, 7 p.

Bayer, K. C., 1973b, A preliminary seismicity study of the Southern Nevada Region Quarterly Report January-March 1973: U. S. Department of Commerce, National Oceanic and Atmospheric Administration, Earth Sciences Laboratories, Report prepared for the U. S. Atomic Energy Commission, NVO-746-12, Contract AT (29-2)-746, 19 p.

Bayer, K. C., 1974, A preliminary study of the Southern Nevada Region Quarterly Report April-June 1973, U. S. Geological Survey Report NVO-474-1, Report prepared for the U. S. Atomic Energy Commission, 29 p.

Beck, P. J., 1970, The southern Nevada-Utah border earthquakes, August to December, 1966: M. S. thesis, University of Utah, Department of Geophysics, 62 p.

Bell, J. W., 1981, Map of young fault scarps in the Reno 1x2° Quadrangle: U. S. Geological Survey Open-File Report of 81-982 scale 1:250,000.

Blackwell, D. D., 1978, Heat flow and energy loss in the western Cordillera: Geological Society of America Memoir 152, p. 175-208.

Bol, A. J., Snyder, D. B., Healey, D. L., and Saltus, R. W., 1983, Principal facts, occurrances, sources, and base station description for 3662 gravity stations in the Tonopah and Lund quadrangles, Nevada: U. S. Geological Survey Report, NTIS - PB 83-202671.

Bracken, R. E., and Kane, M. F., 1983, Complete Bouguer gravity map of Nevada, Kingman sheet: Nevada Bureau of Mines and Technology, scale 1:250,000.

Brogan, G. E., 1979, Late Quaternary faulting along the Death Valley-Furnace Creek fault system, California and Nevada: U. S. Geological Survey Contract Report, Contract No. 14-08-0001-17801, scale 1:24,000.

Bucknam, R. C., Algermissen, S. T. and Andersen, R. E., 1980, Patterns of late Quaternary faulting in western Utah and an application in earthquake hazard evaluation: U. S. Geological Survey Open-file Report 80-801, 15 p.

Burchfiel, B. C. and Davis, G. A., 1975, Nature and controls of Cordilleran orogenesis, western United States: Extensions of an earlier snythesis: American Journal of Science, v. 275-A, p. 363-396.

Burchfiel, B. C., and Stewart, J. H., 1966, "Pull-apart" origin of the central segment of Death Valley, California: Geological Society of America Bulletin, v. 77, p. 439-442.

Burchfiel, B. C., Fleck, R. J., Secor, D. T., Vincelette, R. R., and Davis, G. A., 1974, Geology of the Spring Mountains, Nevada: Geological Society of America Bulletin, v. 85, p. 1013-1022.

Burchfiel, B. C., Hamill, G. S. IV, and Wilhelms, D. E., 1983, Structural geology of the Montgomery Mountains and the northern half of the Nopah and Resting Srpings Ranges, Nevada and California: Geological Society of America Bulletin, v. 94, no. 11, p. 1359-1376.

Burchfiel, B. C., Hamill, G. S. IV, and Wilhelms, D. E., 1982, Stratigraphy of the Montgomery Mountains and the northrn half of the Nopah and Resting Spring Ranges, Nevada and California: The Geological Society of America Map and Chart Series MC-44.

Byerlee, J. D., 1978, Friction of rocks: Pure and Applied Geophysics, v. 116, p. 615-626.

Byers, F. M., Jr., and Harley Barnes, 1967, Geologic Map of the Paiute Ridge quadrangle, Nye and Lincoln Counties, Nevada: U. S. Geological Survey Geologic Quadrangle Map GQ-577, scale 1:24,000.

Byers, F. M., Jr., Carr, W. J., Orkild, P. P., Quinlivan, W. D., and Sargent, K. A., 1976, Volcanic suites and related cauldrons of Timber Mountain-Oasis Valley caldera complex, Southern Nevada: U. S. Geological Survey Professional Paper 919, 70 p.

Carder, D. S., 1970, Reservoir loading and local earthquakes, in Engineering Seismology—The Works of Man: Geological Society of America Engineering Geology, Case Histories 8, p. 51-61.

Carr, W. J., 1974, Summary of tectonic and structural evidence for stress orientation at the Nevada Test Site: U. S. Geological Survey Open-File Report 74-176, 83 p.

_____, 1982a, Volcano-tectonic history of Crater Flat, Southwestern Nevada, as suggested by new evidence from drill hole USW-VH-1 and vicinity, U. S. Geological Survey Open-File Report 82-457, 23 p.

_____, 1982b, Structural setting and rate of tectonic activity in the Yucca Mountain region, southwestern Great Basin, Nevada and California: EOS, v. 63, no. 45.

Carr, W. J., Byers, F. M., Jr., and Orkild,P. P., 1984, Stratigraphic and volcano-tectonic relations of Crater Flat Tuff and some older volcanic units, Nye County, Nevada: U. S. Geological Survey Open-file Report 84-114, 42 p.

Chapman, R. H., Healey, d. L., and Troxel, B. W., 1973, Bouguer gravity map of California, Death Valley sheet: California Division of Mines and Geology, scale 1:250,000.

Christiansen, R. L. and Lipman, P. W., 1965, Geologic map of the Topopah Spring NW Quadrangle, Nye County, Nevada: U. S. Geological Survey Geologic Quadrangle Map GQ-444, scale 1:24,000.

Christensen, R. L. and Lipman P. W., 1972, Cenozoic volcanism and plate tectonics evolution of the western United states; Part II, Late Cenozoic: Philosophical Transactions of the Royal Society of London, ser. A, v. 271, p. 249-284.

Christiansen, R. L., Lipman, P. W., Orkild, P. O., and Byers, F. M., Jr., 1965, Structure of the Timber Mountain Caldera, Southern Nevada, and its relation to basin-range structure: U. S. Geological Survey Professional Paper 525-B, p. B43-B48.

Christiansen, R. L., Lipman, P. W., Carr, W. J., Byers, F. M., Jr., Orkild, P. P., and Sargent, K. A., 1977, Timber Mountain-Oasis Valley caldera complex of southern Nevada: Geological Society of America Bulletin, v. 88, p. 943-959.

Christiansen, R. L. and McKee, E. H., 1978, Late Cenozic volcanic and tectonic evolution of the Great Basin and Columbia intermontane regions: in Smith, R. B. and Eaton, G. P., eds., Cenzoic Tectonics and Regional Geophysics of the Western Cordillera: Geological Society of America Memoir 152, p. 283-311.

Coffman, J. L. and von Hake, C. A., 1973, Earthquake history of the United State: U. S. Department of Commerce Publication No. 41-1, 208 p.

Cornwall, H. R. and Kleinhampl, F. J., 1961, Geology of the Bare Mountain quadrangle, Nevada: U. S. Geological Survey Geological Quadrangle Map GQ-157, scale 1:62,500.

Cornwall, H. R. and Kleinhampl, F. J., 1964, Geology of the Bullfrog quadrangle and ore deposits related to the Bullfrog Hills caldera, Nye County, Nevada and Inyo County, California: U. S. Geological Survey Professional Paper 454-J, 25 p.

Crittenden, M. S. Jr., Coney, P. J., Davis, G. H., eds., 1980, Cordilleran metamorphic core complexes: Geological Society of America Memoir 153, 430 p.

Crone, A. J., 1983, Amount of displacement and estimated age of a Holocene surface faulting event, eastern Great Basin, Millard County, Utah, in Gurgel, K. D., ed., Geologic excursions in neotectonics and engineering geology in Utah: Utah Geological and Mineralogical Survey Special Studies 62, p. 49-55.

Cross, T. A., and Pilger, R. H., Jr., 1978, Constraints on absolute motion and plate interaction inferred from Cenozoic igneous activity in the western United States: American Journal of Science, v. 278, p. 865-902.

Crowe B. M., 1978, Cenozoic volcanic geology and probable age of inception of basin-range faulting in the south easternmost Chocolate Mountain, California: Geological Society of America Bulletin, v. 89, no. 2, p. 251-264.

Crowe, B. M., 1980, Disruptive event analysis: Volcanism and igneous intrusion, Battelle Pacific Northwest Laboratory Report PNL-2822, 28 p.

Crowe, B. M., and Carr, W. J., 1980, Preliminary assessment of the risk of volcanism at a proposed nuclear waste repository in the southern Great Basin: U. S. Geological Survey Open-File Report 80-357, 15 p.

Crowe, B. M., Johnson, M. E., and Beckman, R. J., 1982, Calculation of probablility of volcanic disruption of a high-level radioactive waste repository within southern Nevada, USA: Radioactive Waste Management and the Nuclear Fuel Cycle, v. 3, p. 167-190.

Crowe, B. M. and Sargent, K. A., 1979, Major-element geochemistry of the Silent Canyon-Black Mountain peralkaline volcanic centers, northwestern Nevada Test Site: Applications to an assessment of renewed volcanism, U. S. Geological Survey Open-File Report 79-926, 25 p.

Crowe, B. M., Self, S., and Amos, R. C., 1981, Strombolian Eruptive Sequences: Transactions American Geophysical Union v. 82, no. 45, p. 1084.

Crowe, B. M., Self, S., Vaniman, D., Amos, R. C., and Perry, F., 1983a m.s., Aspects of potential magmatic disruption of a high-level radioactive waste repository in southern Nevada: Journal of Geology, (in press).

Crowe, B. M., Vaniman, D. J., and Carr, W. J., 1983b, Status of volcanic hazard studies for the Nevada nuclear waste storage investigations: Los Alamos National Laboratory Report LA-9325-MS.

Davis, G. A., and Burchfiel, B. C., 1973, Garlock fault: an intra-continental transform structure, southern California: Geological Society of America Bulletin, v. 84, p. 1407-1422.

Davis, G. A., Monger, J. W. H., and Burchfiel, B. C., 1978, Mesozoic construction of the Cordilleran "collage", central British Columbia to central California, in Howell, D. G., and McDougall, K. A., eds., Mesozoic Paleogeography of the Western United States: Pacific Section: Society of Economic Paleontologists and Mineralogists, Pacific Coast Paleogeography Symposium 2, p. 1-32.

Dickinson, W. R., 1981, Plate tectonics and the continental margin of California, in Ernst, W. G., ed., The Geotectonic Development of California, Rubey volume I: New Jersey, Prentice-Hall, 1981, p. 29-49.

Dickinson, W. R., and Snyder, W. S., 1979, Geometry of triple junctions related to the San Andreas transform: Journal of Geophysics Research, v. 84, p. 561-572.

Diment, W. H., Healey, D. L., and Roller, J. C., 1960, Gravity and seismic exploration at the Nevada Test Site: U. S. Geological Survey Professional Paper 400B, 156 p.

Diment, W. H., Stewart, S. W., and Roller, J. C., 1961, Crustal structure from the Nevada Test Site to Kingman, Arizona, from seismic and gravity observations: Journal of Geophysical Research, v. 66, p. 201-204.

Eaton, G. P., Wahl, R. R., Prostka, H. J., Mabey, D. R., and Kleinkopf, M. D., 1978, Regional gravity and tectonic patterns: Their relation to late Cenozoic epeirogeny and lateral spreading in the western cordillera: in Cenozoic Tectonics and Regional Geophysics of the western Cordillera: Geological Society of America Memoir 152, p. 51-91.

Eckel, E. B., ed., 1968, Nevada Test Site: Geological Society of America Memoir 110, 290 p.

Ekren, E. B., Anderson, R. E., Rogers, C. L., and Nobel, D. C., 1971, Geology of northern Nellis Air Force Base Bombing and Gunnery Range, Nye County, Nevada: U. S. Geological Survey Professional Paper 651, 91 p.

Ekren, E. B., Bath, G. D., Dixon, G. L., Healey, D. L., and Quinlivan, W. D., 1974, Tertiary history of Little Fish Lake Valley, Nye County, Nevada, and implications as to the origin of the Great Basin: U. S. Geological Survey Journal Research v. 2, p. 105-118.

Ekren, E. B., Orkild, P. P., Sargent, K. A., and Dixon, G. L., 1977, Geologic map of Tertiary rocks, Lincoln County, Nevada: U. S. Geological Survey Miscellaneous Investigations Map I-1041, scale 1:24,000.

Ekren, E. B. and Byers, F. M. Jr., 1976, Ash-flow fissure vent in west-central Nevada: Geological Society of America, Geology, v. 4, no. 4, p. 247-251.

Ekren, E. B., Quinlivan, W. D., Snyder, R. P., and Kleinhampel, F. J., 1974b, Stratigraphy, structure, and geologic history of the Lunar Lake caldera of Northern Nye County, Nevada, U. S. Geological Survey Journal of Research, v. 2, no. 5, p. 599-608.

Ekren, E. B., Rogers, C. L., Anderson, R. E., and Orkild, P. P., 1968, Age of Basin and Range normal faults in Nevada Test Site and Nellis Air Force Range Nevada in Eckel, E. B., ed., Nevada Test Site: Geological Society of America Memoir 110, p. 247-250.

Ekren, E. B. and Sargent, K. A., 1965, Geologic map of the Skull Mountain Quadrangle, Nye County, Nevada: U. S. Geological Survey Geologic Quadrangle Map GQ-387.

Fisher, F. G., Papanek, P. J., and Hamilton, R. M., 1972, Massachusetts Mountain earthquake of 5 August 1971 and its aftershocks, Nevada Test Site: U. S. Geological Survey Report USGS-474-149, 20 p.; available only from U. S. Department of Commerce, National Technical Information Service, Springfield, VA 22161.

Fleck, R. J., 1970, Tectonic style, magnitude, and age of deformation in the Sevier orogenic belt in southern Nevada and eastern California: Geological Society of America Bulletin, v. 81, p. 1705-1720.

Fouty, Suzanne, C. 1984, Index to published geologic maps in the region around the potential Yucca Mountain nuclear waste repository site, southern Nye county, Nevada: U. S. Geological Survey Open-file Report 84-524, 31 p.

Greensfelder, R. W., Kintzer, F. C. and Somerville, M. R., 1980, Seismotectonic regionalization of the Great Basin and comparison of moment rates computed from Holocene strain and historic seismicity: Geological Society of America Bulletin, v. 91, no. 9, p.1518-1523.

Guth, P. L., 1981, Tertiary extension north of the Las Vegas Valley shear zone, Sheep and Desert ranges, Clark County, Nevada: Geological Society of America Bulletin, Part I, v. 92, p. 763-771.

Hamilton, W. B., 1969, Mesozoic California and the underflow of Pacific mantle: Geological Society of America Bulletin, v. 80, p. 2409-2430.

Hamilton, W. B., 1978, Mesozoic tectonics of the western United States: in Howell, D. G., and McDougall, K. A., eds., Mesozoic paleogeography of the western United States: Pacific Section, Society of Economic Paleontologists and Mineralogists, Pacific Coast Paleogeography Symposium 2, p. 33-70.

Hamilton, W. B., 1982, Structural evolution of the Big Maria Mountains, northeastern Riverside County, southeastern California: in Frost, E. G., and Matrin, D. L., eds., Mesozoic-Cenozoic Tectonic Evolution of the Colorado River Region, California, Arizona, and Nevada: San Diego, Cordilleran Publishers, p. 1-27.

Hamilton, W. B. and Myers, W. B., 1966, Cenozoic tectonics of the western United States: in The World Rift System--International Upper Mantle Committee, Symposium, Ottawa, 1965: Reviews of Geophysics and Space Physics, v. 4, no. 4, p. 509-549.

Hamilton, R. M., Smith, B. E., Fisher, F. G., and Papanek, P. J., 1971, Seismicity of the Pahute Mesa area, Nevada Test Site (8 December 1968 through 31 December 1970): U. S. Geological Survey Report USGS-474-138, 169 p.; available only from U. S. Department of Commerce, National Technical Information Service, Springfield, VA 22161

Hanna, W. F., Oliver, H. W., Sikora, R. F., and Robbins, S. L., 1975, Bouguer gravity map of California, Bakersfield sheet: California Division of Mines and Geology, scale 1:250,000.

Healey, D. L., 1968, Application of gravity data to geological problems at the Nevada Test Site, in Eckel, E. B., ed., Nevada Test Site: Geological Society of America Memoir 110, p. 147-156

Healey, D. L., and Miller, C. H., 1962, Gravity survey of the Nevada Test Site and vicinity, Nye, Lincoln, and Clark counties, Nevada--interim report: U. S. Geological Survey Trace Elements Investigations Report TEI-827, 36p.

Healey, D. L., Snyder, D. B., and Wahl, R. R., 1981, Complete Bouguer gravity map of Nevada, Tonopah sheet: Nevada Bureau of Mines and Geology Map 73, scale 1:250,000.

Healy, J. H., Hickman, S. H., and Zoback, M. D., 1982, Deep borehole stress measurements at the Nevada Test Site [abs.]: American Geophysical Union Transactions, v. 63, p. 1099-1100.

Hinrichs, E. N., 1968, Geologic structure of Yucca Flats area in Eckel, E. B., ed., Nevada Test Site: Geological Society of America Memoir 110, p. 239-246.

Hoffman, L. R. and Mooney, W. D., 1983, A seismic study of Yucca Mountain and vicinity, southern Nevada: Data report of preliminary results: U. S. Geological Survey Open-file Report 83-588, 50 p.

Hoover, D. L. and Morrison, J. N., 1980, Geology of the Syncline Ridge area related to nuclear waste disposal, Nevada Test Site, Nye County, Nevada: U. S. Geological Survey Open-File Report 80-942, 70 p.

Hoover, D. L., Swadley, W. C., and Gordon, A. J., 1981, Correlation characteristics of surficial deposits with a description of stratigraphy in the Nevada Test Site Region: U. S. Geological Survey Open-File Report 81-512, 27 p.

Hunt, C. B. and Mabey, D. R., 1966, Stratigraphy and structure of Death Valley, California: U. S. Geological Survey Professional Paper 494-A, 162 p.

Iyer, H. M., Evans, J. R., Zandt, G., Stewart, R. M., Coakley, J. M., and Roloff, J., 1981, A deep magma body under the Yellowstone caldera: delineation using teleseismic P-wave residuals and tectonic interpretations: Geological Society of America Bulletin, v. 92, p. 1471-1646.

Izett, G. A., 1982, The Bishop ash bed and some older compositionally similar ash beds in California, Nevada, and Utah: U. S. Geological Survey Open-File Report 82-582, 44 p.

Jennings, C. W., 1977, Geologic Map of California: California Division of Mines and Geology, California Geologic Data Map Series, scale 1:750,000.

Kane, M. F., Healey, D. L., Peterson, D. L., Kaufmann, H. E., and Reidy, D., 1979, Bouguer gravity map of Nevada, Las Vegas sheet: Nevada Bureau of Mines and Geology Map 61, scale 1:250,000.

Kane, M. F., and Bracken, R. E., 1983, Aeromagnetic map of Yucca Mountain and surrounding regions, southwest Nevada: U. S. Geological Survey Open-File Report 83-616, scale 1:48,000, 19 p.

King, K. W., Bayer, K. C., and Brockman, S. R., 1971, Earthquakes on and around the Nevada Test Site, 1950-1971: U. S. Department of Commerce Publication CGS-746-12, 32 p.

Kistler, R. W. and Peterman, Z. E., 1978, Reconstruction of crustal blocks of California on the basis of initial strontium isotopic compositions of Mesozoic Granitic Rocks: U. S. Geological Survey Professional Paper 1071, 17 p.

Lachenbruch, A. H. and Sass, J. H., 1977, Heat flow in the United States and the thermal regime of the crust, in Heacock, J. G., ed., The Structure and Physical Properties of the Earth's Crust: American Geophysical Union Monograph 14, 348 p.

Lipman, P. W. and Christiansen, R. L., 1964, Zonal features of an ash-flow sheet in the Piapi Canyon formation, southern Nevada: U. S. Geological Survey Professional Paper 501-B, p. B74-B78.

Lipman, P. W., Christiansen, R. L., and O'Connor, J. T., 1966, A compositionally zoned ash-flow sheet in southern Nevada: U. S. Geological Survey Professional Paper 524-F, p. F1-F47.

Lipman, W. W. and McKay, E. J., 1965, Geologic map of the Topopah Spring SW quadrangle: U. S. Geological Survey Geologic Quadrangle Map GQ-439, scale 1:24,000.

Lipman, P. W., Prostka, H. J., and Christiansen, R. L., 1972, Cenozoic volcanism and plate tectonic evolution of the western United States (1) early and middle Cenozoic: Royal Society of London, Philosophical Transactions, Series A., v. 271, p. 217-248.

Locke, Augustus, Billingsley, P. R., and Mayo, E. B., 1940, Sierra Nevada tectonic patterns: Geological Society of America Bulletin, v. 51, p. 513-540.

Logan, S. E., Link, R. L., Ng, H. S., Rockenbach, A., and Hong, K. J., 1981, Parametrical studies of radiological consequences of basaltic volcanism: Sandia National Laboratories International Report SAND81-2375, 219 p.

Longwell, C. R., 1960, Possible explanation of diverse structural patterns in southern Nevada: American Journal of Science, v. 258-A, p. 192-203.

Luedke, R. G. and Smith, R. L., 1981, Map showing distribution, composition, and age of late Cenozoic volcanic centers in California and Nevada: U. S. Geological Survey Miscellaneous Investigation Series, I-1091-C, 2 sheets.

Mabey, D. R., 1960, Gravity survey of the western Mojave Desert, California: U. S. Geological Survey Professional Paper 316-D, 73 p.

Maldonado, Florian, 1977a, Summary of the geology and physical properties of the Climax Stock, Nevada Test Site: U. S. Geological Survey Open-File Report 77-356, 25 p.

_____, 1981, Geology of the Twinridge pluton area, Nevada Test Site, Nevada: U. S. Geological Survey Open-File Report 81-156, 13 p.

Maldonado, Florian and Koether, S. L., 1983, Stratigraphy, structure, and some petrographic features of Tertiary volcanic rocks at the USW G-2 drill hole, Yucca Mountain, Nye County, Nevada: U. S. Geological Survey Open-file Report 83-732, 83 p.

Maldonado, Florian, Muller, D. C., and Morrison, J. N., 1979, Preliminary geologic and geophysical data of the Ue25a-3 exploratory drill hole, Nevada Test Site, Nevada: U. S. Geological Survey Report, USGS-1543-6, 47 p.; available only form U. S. Department of Commerce, National Technical Information Service, Springfield, VA 22161.

Mark, R. K. and Bonilla, M. G., 1977, Regression analysis of earthquake magnitude and surface fault length using the 1970 data of Bonilla and Buchanan: U. S. Geological Survey Open-File Report 77-614, 3 p.

McGovern, T. F. and Turner, D. W., 1983, Evaluation of seismic reflection studies in the Yucca Mountain area, Nevada Test site, with an introduction by L. W. Pankratz and H. D. Ackerman: U. S. Geological Survey Open File 83-912.

McKay, E. J. and Williams, W. P., 1964, Geology of the Jackass Flats quadrangle, Nye County, Nevada: U. S. Geological Survey Geologic Quadrangle Map GQ-368, scale 1:24,000.

Monfort, M. E., and Evans, J. R., 1982, Three-dimensional modeling of the Nevada Test Site and vicinity from teleseismic p-wave residuals: U. S. Geological Survey Open-File Report 82-409.

Muffler, L. J. P., ed., 1979, Assessment of geothermal resources of the United States--1978: U. S. Geological Survey Circular 790, 163 p. and maps, scale 1,1,000,000 and 1:5,000,000

Naeser, C. W. and Maldonado, Florian, 1981, Fission-track dating of the climax and Gold Meadows stocks, Nye County, Nevada, in Short contributions of Geochronology: U. S. Geological Survey Professional Paper 1199-E, p. 45-47.

Nilsen, T. H., and Chapman, R. H., 1974, Bouguer gravity map of California, Trona sheet: California Division of Mines and Geology, scale 1:250,000.

Oakeshott, G. B., Greensfelder, R. W., and Kahle, J. E., 1972, One-hundred years later, California Geology: California Division of Mines and Geology, v. 25, no. 3, p. 61.

Oliver, H. W., Chapman, R. H., Biehler, Shawn, Robbins, S. L., Hanna, W. F., Griscom, Andrew, Beyer, Larry, and Silver, E. A., 1980, Gravity map of California and its continental margin: California Division of Mines and Geology, scale 1:750,000.

Oliver, H. W., and Robbins, S. L., 1982a, Bouguer gravity map of California, Mariposa sheet: California Division of Mines and Geology, scale 1:250,000.

Oliver, H. W., and Robbins, S. L., 1982b, Bouguer gravity map of California, Fresno sheet: California Division of Mines and Geology, scale 1:250,000, 15 p.

Orkild, P. P., 1965, Paintbrush Tuff and Timber Mountain Tuff of Nye County, Nevada: U. S. Geological Survey Bulletin 1224-A, p. A44-A51.

Peterson, F. F., 1981, Landforms of the Basin and Range province defined for soil survey: Nevada Agricultural Experiment Station Technical Bulletin 28, 52 p.

Plouff, Donald, 1983, Bouguer gravity map of Nevada, Walker Lake sheet: Nevada Bureau of Mines and Geology, scale 1:250,000.

Ponce, D. A., 1981, Preliminary Gravity Investigations of the Wahmonie Site, Nevada Test Site, Nye County, Nevada: U. S. Geological Survey Open-File Report 81-522, 64 p.

Poole, F. G., 1974, Flysch deposits of Antler foreland basin, western United States: in Dickinson, W. R., ed., Tectonics and Sedimentation: Society of Economic Paleontologists and Mineralogists Special Publications, no. 22, p. 58-82.

Poole, F. G., Carr, W. J., and Elston, D. P., 1965, Salyer and Wahmonie Formations of southeastern Nye County, Nevada: U. S. Geological Survey Bulletin 1224-A, p. A44-A51.

Real, C. R., Toppozada, T. R., and Parke, D. L., 1978, Earthquake catalog of California; January 1, 1900-December 31, 1984: California Division of Mines and Geology, Special Publication No. 52, 15 p.

Reynolds, M. W., 1969, Stratigraphy and structural geology of the Titus and Titanothere Canyons area, Death Valley, California: Ph.D. dissertation, University of California at Berkeley, 310 p.

Reynolds, M. W., 1974a, Geology of the Grapevine Mountains, Death Valley, California: a summary: in Guidebook: Death Valley region, California and Nevada: 70th annual meeting Cordilleran section, Geological Society of America Field Trip no. 1, p. 91-97.

Reynolds, M. W., 1974b, Recurrent middle and late Cenozoic deformation, northeastern Death Valley, California-Nevada (abs.): Geological Society of America Abstracts with Programs (Cordilleran Section), v. 3, no.2, p. 182-183.

Richter, C. F., 1958, Elementary Seismology: W. H. Freeman and Co., San Francisco, Calif., 768 p.

Rogers, A. M., and Lee, W. H. K., 1976, Seismic study of earthquakes in the Lake Mead, Nevada-Arizona Region: Bulletin of the Seismological Society of America, v. 66, p. 1657-1681.

Rogers, A. M., Harmsen, S. C., and Carr, W. J., 1981, Southern Great Basin Seismological Data Report for 1980, and Preliminary Analysis: U. S. Geological Survey Open-File Report 81-1086, 148 p.

Rogers, A. M., Perkins, D. M., and McKeown, F. A., 1976, A catalog of seismicity within 400 kilometers of the Nevada Test Site: U. S. Geological Survey Open-File Report 76-832, 44 p.

Rogers, A. M., Perkins, D. M., and McKeown, 1977a , A preliminary assessment of the seismic hazard of the Nevada Test Site region: Seismological Society of America Bulletin, v. 67, no. 6, p. 1587-1606.

Rogers, A. M., Wuollet, G. M., and Covington, P. A., 1977b, Seismicity of the Pahute Mesa Area, Nevada Test Site (8 October 1975 to 30 June 1976): from U. S. Department of Commerce, National Technical Information Service, Springfield, VA 22161.

Rogers, A. M., Tinsley, J. C., and Hays, W. W., 1983a, The issues surrounding the effects of geologic conditions on the intensity of ground shaking, in W. W. Hays, ed., Proceedings of Conference XXII: U. S. Geological Survey Open-File Report 83-845, p. 32-67.

Rogers, A. M., Harmsen, S. C., and Carr, W. J., 1983b, Southern Great Basin seismological data report for 1981 and preliminary data analysis: U. S. Geological Survey Open-File Report 83-669, 240 p.

Rosholt, J. N., 1980, Uranium-trend dating of Quaternary sediments: U. S. Geological Survey Open-file Report 80-1087, 34 p.

Romney, C., 1957, Seismic waves from the Dixie Valley-Fairview Peak earthquakes of December 16, 1954: Seismological Society of America Bulletin, v. 47, p. 301-320.

Rush, F. E., Thordason, William and Bruckheimer, Laura, 1983, Geohydrologic and drill-hole data for test well USW-H1, adjacent to Nevada Test Site, Nye County, Nevada: U. S. Geological Survey Open-File Report 83-141, 38 p.

Ryall, A. and Priestly, Keith, 1975, Seismicity, secular strain, and maximum magnitude in the Excelsior Mountains Area, western Nevada and eastern California: Geological Society of America Bulletin, v. 86, p. 1585-1592.

Schell, B. A., Farley, T., and Muir, S. G., 1981, Fault-rupture and earth hazards in east-central Nevada and west-central Utah: Association Engineering Geologists Meeting Programs with Abstracts, p. 52.

Schell, B. A., and Muir, S. G., 1982, Young faults and lineaments in the southern Great Basin of Nevada and Utah: Geological Society of America Meeting Programs with Abstracts, v. 14, p. 231.

Schnabel, D. B. and Seed, H. B., 1973, Accelerations in rock for earthquakes in the western United States: Seismological Society of America Bulletin, v. 63, p. 501-516.

Scott, R. B. and Bonk, Jerry, 1984, Preliminary geologic map of Yucca Mountain with geologic sections, Nye County, Nevada: U. S. Geological Survey Open-File Report 84-494, scale 1:12,000.

Scott, R. B. and Castellanos, Mayra, 1984, Stratigraphic and structural relations of volcanic rocks in drill holes USW GU-3 and USW G3, Yucca Mountain, Nye County, Nevada: U. S. Geological Survey Open-file Report 84-491, 94 p.

Scott, R. B., Nesbitt, R. W., Dasch E. Julius, 1971, A strontium isotope evolution model for Cenozoic magma genesis, Eastern Great Basin, USA: Bulletin Volcanologique, vol.35, no. 1, p. 1-26.

Scott, R. B., Spengler, R. W., Diehl, S., Lappin, A. R. and Chornack, M. P., 1983, Geologic character of tuffs in the unsatruated zone at Yucca Mountain, southern Nevada: in Mercer, J. M., Rao, P. C. and Marine, W., eds., Role of the unsaturated zone in radioactive and hazardous waste disposal: Ann Arbor Press, Ann Arbor, Michigan, p. 289-335.

Scott, R. B., Spengler, R. W., Lappin, A. R., and Chornack, M. P., 1982, Structure and intra-cooling unit zonation in welded tuffs of the unsaturated zone, Yucca Mountain, Nevada, a potential nuclear waste repository, abs.: EOS, v. 63, no. 18, p. 330.

Shaw, H. 1980, The fracture mechanism of magma transport from the Mantle to the Surface: in Hargraves, R. B., ed., Physics of Magmatic Transport: Princeton University Press, p. 201-264.

Simpson, H. E., Weir, J. E., Jr., and Woodward, L. A., 1979, Inventory of clay-rich bedrock and metamorphic derivatives in eastern Nevada, excluding the Nevada Test Site: U. S. Geological Survey Open-File Report 79-760, 147 p.

Slemmons, D. B., 1967, Pliocene and Quarternary crustal movements of the Basin and Range province, U.S.A.: in Sea level changes and crustal movements of the Pacific--11th Pacific Science Congress, Tokyo, 1966, Symposium 19: Osaka City University Journal Geosciences, v. 10, art. 1, p. 91-103.

Slemmons, D. B., Jonas, A. E., and Gimlett, J. I., 1965, Catalog of Nevada earthquakes, 1852-1960: Seismological Society of America Bulletin, v. 55, p. 519-566.

Smith, G. I., 1979, Subsurface stratigraphy and geochemistry of late Quaternary evaporites, Searles Lake, California: U. S. Geological Survey Professional Paper 1043, 130 p.

Smith, R. B., 1978, Seismicity, crustal structure, and intraplate tectonics of the interior of the western Cordillera: in Smith, R. B., and Eaton, G. P., eds., Cenozoic Tectonics and Regional Geophysics of the Western Cordillera: Geological Society of America Memoir 152, p. 111-145.

Smith, R. B., and Lindh, A. G., 1978, A compilation of fault plane solutions of the Western United States: in Smith, R. B., and Eaton, G. P., eds., Cenozoic tectonics and regional geophysics of the Western United States, Geological Society of America Memoir 152, p. 107-111.

Smith, R. L., 1960, Zones and zonal variations in welded ash flows: U. S. Geological Survey Professional Paper 354-F, p. F149-F159.

Snyder, D. B. and Carr, W. J., 1982, Preliminary results of gravity investigations at Yucca Mountain and vincinity, southern Nye County, Nevada: U. S. Geological Survey Open-File Report 82-701, 36 p.

Spaulding, W. G., 1983, Vegetation and climates of the last 45,000 years in the vicinity of the Nevada Test Site, south-central Nevada: U. S. Geological Survey Open-file Report 83-535, 199 p.

Spengler, R. W., Byers, F. M., Jr., and Warner, J. B., 1981, Stratigraphy and structure of volcanic rocks in drill hole USW-G1, Yucca Mountain, Nye County, Nevada: U. S. Geological Survey Open-File Report 82-1338, 36 p.

Spengler, R. W., Maldonado, Florian, Weir, J. E., Jr., and Dixon, G. L., 1979a, Inventory of granitic masses in the state of Nevada: U. S. Geological Survey Open-File Report 79-235, 264 p.

Spengler, R. W., Muller, D. C., and Livermore, R. B., 1979b, Preliminary report on the geology of drill hole Ue25a-1, Yucca Mountain, Nevada Test Site: U. S. Geological Survey Open-File Report 79-1244, 43 p.

Spengler, R. W. and Rosenbaum, J. G., 1980, Preliminary interpretations of results obtained from Boreholes Ue25a-4, -5, -6, -7, Yucca Mountain, Nevada Test Site: U. S. Geological Survey Open-File Report 80-929, 35 p.

Stewart, J. H., 1967, Possible large right-lateral displacement along fault and shear zones in the Death Valley-Las Vegas Area, California and Nevada: Geological Society of America Bulletin, v. 78, p. 131-142.

Stewart, J. H., 1971, Basin and range structure--a system of horsts and grabens produced by steep-sided extension: Geological Society of America Bulletin, v. 82, p. 1019-1044.

Stewart, J. H., 1978, Basin-range structure in North America: a review: in Smith, R. B., and Eaton, G. P., eds., Cenozoic tectonics and regional geophysics in the western Cordillera: Geological Society of America Memoir 152, p. 1-31.

Stewart, J. H., 1980, Geology of Nevada: Nevada Bureau of Mines Special Publication no. 4, 136 p.

Stewart, J. H., Albers, J. P., and Poole, F. G., 1968, Summary of regional evidence for right-lateral displacement in the western Great Basin: Geological Society of America Bulletin, v. 79, no. 10, p. 1407-1414.

Stewart, J. H. and Carlson, J. E., 1976, Cenozoic rocks of Nevada -- Four Maps and a brief description of distribution, lithology, age, and centers of volcanism: Nevada Bureau of Mines and Geology Map 52, scale 1:1,000,000.

Stewart, J. H. and Carlson, J. E., 1978, Geologic Map of Nevada: U. S. Geological Survey and Nevada Bureau of Mines and Geology, scale 1:500,000.

Stewart, J. H., Moore, W. J., and Zietz, Isidore, 1977, East-west pattern of Cenozoic igneous rocks, aeromagnetic anomalies, and mineral deposits in Nevada and Utah: Geological Society of America Bulletin, v. 88, p. 67-77.

Stewart, J. H. and Poole, F. G., 1974, Lower Paleozoic and uppermost Precambrian Cordilleran miogeocline, Great Basin, western United States: in Dickerson, W. R., ed., Tectonics and Sedimentation: Society of Economic Paleontalogists and Mineralogists Special Publication 22, p. 28-57.

Swadley, W. C. and Hoover, D. L., 1983, Geology of faults exposed in trenches, Nye County, Nevada: U. S. Geological Survey Open-File Report 83-608, 15 p.

Swadley, W. C., Hoover, D. L., and Rosholt, J. N., 1984, Preliminary report on Late Cenozoic faulting and stratigraphy in the vicinity of Yucca Mountain, Nye County, Nevada: U. S. Geological Survey Open-File Report (in press).

Tendall, D. M., 1971, Epicenter location of NTS earthquake on August 5, 1971: Sandia Laboratories Technical Memorandum SC-TM-710593, 18 p.

Thenhaus, P. C. (ed.), 1983, Summary of workshops concerning regional seismic source zones of parts of the conterminous United States, convened by the U. S. Geological Survey 1979-1980, Golden, Colorado: U. S. Geological Survey Circular 898, 36 p.

Trexler, D. T., Flynn, T., and Koen, F., 1979, Assessment of low to moderate temperature resources of Nevada: U. S. Department of Energy, Nevada Operations Office, NVO-156-I, Las Vegas, NV.

U. S. Department of Commerce, 1976, Earthquake Data File Summary, Key to Geophysical Records Documentation Series, KGRD No. 5, National Atmospheric Administration, Boulder, Colorado, 32 p.

U. S. Geological Survey, 1983, Preliminary determination of epicenters, National earthquake information service, monthly listing, prepared by National Ocean and Atmospheric Adminstration (NOAA).

Vaniman, D. T. and Crowe, B. M., 1981, Geology and petrology of the basalts of Crater Flat: Applications to Volcanic risk assessment for the Nevada nuclear waste storage investigations: Los Alamos National Laboratory Report, LA-8845-MS, 67 p.

Vaniman, D. T., Crowe, B. M., and Gladney, E. S., 1982, Petrology and geochemistry of Hawaiite lavas from Crater Flat, Nevada: Contributions to Mineralogy and Petrology, v. 80, p. 341-357.

Vetter, U. R. and Ryall, A. S., 1983, Systematic change of focal mechanism with depth in the western Great Basin: Journal of Geophysical Research, v. B 88, no. 10, p. 8237-8250.

von Hake, C. A. and Cloud, W. K., 1966, United States Earthquakes, 1966, U. S. Department of Commerce, 110 p.

Wallace, R. E., 1978, Pattern of faulting and seismic gaps in the Great Basin Province: in Evernden, J. ed., Proceedings of conference 6 on methodology of identifying gaps and soon-to-break gaps: U. S. Geological Survey Open-File 78-943, p. 858-868.

Wallace, R. E., 1979, Map of young fault scarps related to earthquakes in north-central Nevada: U. S. Geological Survey Open-File Report 79-1554. scale 1:125,000.

Wallace, T. C., Helmberger, D. V., Engen, G. R., 1983, Evidence of tectonic release from underground nuclear explosions in long-period P-waves: Bulletin of the Seismological Society of America 73, p. 593-613.

Walter, A. W., and Weaver, C. S., 1980, Seismicity of the Coso Range, California: Journal of Geophysical Research, v. 85, p. 2441-2458.

Wasserburg, G. J., Wetherill, G. W., and Wright, L. A., 1959, Ages in Precambrian terrain of Death Valley, California: Journal of Geology, v. 57, p. 702-708.

Wernicke, Brian, 1981, Low-angle normal faults in the Basin and Range province: nappe tectonics in an extending orogen: Nature, v. 291, p. 645-648.

Wernicke, Brian, and Burchfiel, B. C., 1982, Modes of extensional tectonics: Journal of Structural Geology, v. 4, no. 2, p. 105-115.

Wernicke, Brian, Spencer, J. E., Burchfiel, B. C., and Guth, P. L., 1982, Magnitude of crustal extension in the southern Great Basin: Geology, v. 10, no. 10, p. 499-502.

Willis, D. E., Taylor, R. W., Torfin, R. D., Tatar, P. J., Revock, K. L., Poetel, R. G., George, G. D., and Bufe, C. G., 1974, Explosion-induced ground motion, tidal and tectonic forces, and their relationship to natural seismicity: University of Wisconsin report to the U. S. Atomic Energy Commission under Contract no. AT(11-1)-2138, Report no. COO-2138-13, 269 p.; available from U. S. Department of Commerce, National Technical Information Service, Springfield, VA 22161.

Winograd, I. J. and Thordarson, William, 1975, Hydrogeologic and hydrochemical framework, south-central Great Basin, Nevada-California, with special reference to the Nevada Test Site: U. S. Geological Survey Professional Paper 712-C, p. C1-C126.

Wright, L. A., and Troxel, B. W., 1973, Shallow-fault interpretation of Basin and Range structure, southwestern Great Basin: in DeJong, K. A., and Scholten, R., eds., Gravity and Tectonics: New York, John Wiley & Sons, p. 397-407.

Zietz, Isodore, Gilhert, F. P., and Kirby, J. R., 1978, Aeromagnetic map of Nevada: color-coded intensites: U. S. Geological Survey Geophysical Investigations Map GP-922, scale 1:100,000.

Zoback, M. L. and Thompson, G. A., 1978, Basin and range rifting in northern Nevada: Clues from a mid-Miocene rift and its subsequent offsets: Geology 6, no. 2, 111-116.

Zoback, M. L. and Zoback, M. D., 1980, Faulting patterns in north-central Nevada and strength of crust: Journal of Geophysical Research, v. 85, p. 6113-6156.

Zoback, M. D., Healy, J. H., Roller, J. C., Gohn, G. S. and Higgins, B. B., 1978, Normal faulting and in situ stress in the South Carolina coastal plain near Charleston: Geology, v. 6, p. 147-152.

Zoback, M. L., Anderson, R. E., and Thompson, G. a., 1981, Cainozoic evolution of the state of stress and style of tectonism of the Basin and Range province of the United States: Philosphical Transactions of the Royal Society of London, v. A300, p. 407-434.

10-km-long scarp in alluvial deposits on the northwest side of Bare Mountain. A preliminary evaluation of surface exposures and one trench across the fault suggests that upper Pleistocene deposits are cut but Holocene deposits are not disturbed.

Several general observations regarding Holocene faulting can be made for the Site Vicinity. First, no unequivicol displacements of Holocene deposits have been discovered, and in areas where Holocene displacement cannot be ruled out, such displacements are not likely to exceed 3 m. Late Pleistocene movements have been documented on several faults in the Site Vicinity, and most faults should be considered capable of movement. Present-day earthquake activity is associated with some fault zones that show no evidence for Holocene surface rupture; thus the absence of surface rupture is not sufficient evidence on which to preclude active Holocene faulting.

Cenozoic Volcanism

There are no volcanic rocks of Paleocene or Eocene age in the Candidate Area. A hiatus in volcanic activity over most of the Great Basin between Cretaceous and middle Eocene time was noted by Cross and Pilger (1978) and Dickinson (1981). Cenozoic volcanism began in north-central Nevada during the late Eocene and progressively spread southward across Nevada along a generally east-trending arcuate front (Cross and Pilger, 1978).

Two important changes in Basin-and-Range volcanism occurred between 14 and 10 m.y. ago: (1) the southward spread of silicic volcanic activity ended at about the latitude of the Site. Subsequent volcanism progressively shifted toward the margins of the Great Basin (Christiansen and McKee, 1978). (2) Volcanism changed from dominantly silicic to both basaltic and bimodal rhyolitic-basaltic (Lipman and others, 1972; Christiansen and Lipman, 1972). This change in magma composition occurred between 11 and 8.5 m.y. ago in the central part of the Candidate Area (Crowe and others, 1983a). The origin of the spatial and temporal patterns of Basin-and-Range volcanism and the relationship between volcanism and extensional faulting are controversial. Opposing models have been postulated in which mantle upwelling and volcanism are considered alternatively as the causes or consequences of Cenozoic crustal extension. These models are discussed by Stewart and others, (1977), Cross and Pilger (1978) and Dickinson and Snyder (1979). There is general agreement